INFORMATION TO USERS

This manuscript has been reproduced from the microfilm master. UMI films the text directly from the original or copy submitted. Thus, some thesis and dissertation copies are in typewriter face, while others may be from any type of computer printer.

The quality of this reproduction is dependent upon the quality of the copy submitted. Broken or indistinct print, colored or poor quality illustrations and photographs, print bleedthrough, substandard margins, and improper alignment can adversely affect reproduction.

In the unlikely event that the author did not send UMI a complete manuscript and there are missing pages, these will be noted. Also, if unauthorized copyright material had to be removed, a note will indicate the deletion.

Oversize materials (e.g., maps, drawings, charts) are reproduced by sectioning the original, beginning at the upper left-hand corner and continuing from left to right in equal sections with small overlaps.

Photographs included in the original manuscript have been reproduced xerographically in this copy. Higher quality 6" x 9" black and white photographic prints are available for any photographs or illustrations appearing in this copy for an additional charge. Contact UMI directly to order.

Bell & Howell Information and Learning
300 North Zeeb Road, Ann Arbor, MI 48106-1346 USA

UMI®
800-521-0600

Boron and strontium isotope study of fluids situated in fractured and unfractured rock of the Lac du Bonnet Batholith, eastern Manitoba.

By

Richard M. McLaughlin, M.Sc.

A Thesis

Submitted to the School of Graduate Studies in Partial

Fulfilment of the Requirements for the Degree

Doctor of Philosophy

McMaster University

B and Sr Isotopes in Fluids of the Lac Du Bonnet Batholith.

DOCTOR OF PHILOSOPHY (Geology)

McMASTER UNIVERSITY
Hamilton, Ontario

TITLE: Boron and strontium isotope study of fluids situated in fractured and unfractured rock of the Lac du Bonnet Batholith, eastern Manitoba.

AUTHOR: Richard M. McLaughlin
B.Sc. (Queen's University, Kingston, Ontario)
M.Sc. (Lakehead University, ThunderBay, Ontario)

SUPERVISOR: Dr. R. H. McNutt

NUMBER OF PAGES: xiv, 147

Abstract

Groundwater from fractured and unfractured rock in the Lac du Bonnet Batholith, Manitoba, has been analyzed for B and Sr isotopes, and ion chemistry. Fluids from unfractured rock (pore fluids) have been sampled by several methods 1) direct sampling of undiluted pore fluids flowing into boreholes; 2) leaching of pore fluids into boreholes filled with distilled deionized water; 3) extraction of intercrystalline fluids from drill cores. Pore fluids can be very saline, up to 100 g/L total dissolved solids, and are chemically distinct from fracture waters. They are 1) enriched in radiogenic ^{87}Sr, exhibiting $^{87}Sr/^{86}Sr$ ratios as high as 0.801; 2) depleted in Sr with respect to Ca having Ca/Sr molar ratio > 918; 3) depleted in Na and Sr with respect to Cl (Na/Cl <0.18; Sr/Cl < 0.00085) ; and 4) have low $\delta^{11}B$-values (<13.5 ‰) and low boron concentrations (<0.27 μg/g). In contrast, fracture waters exhibit $^{87}Sr/^{86}Sr$ ratios between 0.713-0.734, have an average Ca/Sr molar ratio of 236, Na/Cl ratio of 0.55, and a Sr/Cl ratio of 0.0014. They are also enriched in ^{11}B up to a $\delta^{11}B$-value of 52.7 ‰ and have relatively high boron concentrations compared to the pore fluids; as high as 1.57 μg/g.

The dissimilarity in compositions between the two groundwater types indicate that two distinct chemical environments are present in the Lac du Bonnet Batholith. The fracture water chemistry is strongly controlled by the dissolution and alteration of minerals, in particular plagioclase. The dominance of plagioclase dissolution is seen in the Na/Ca molar ratios (5.60), Ca/Sr molar ratios, and Sr isotopic compositions similar to the granite's oligoclase. The fracture waters are interpreted as an open system where chemical equilibrium between groundwaters and rock has not been attained.

Boron isotopes in fracture waters exhibit marine-like compositions, however, due to boron's low concentration in the fracture waters relative to seawater and it's relationship to bromide and chloride concentrations in solution, the source of the boron is not considered to be marine in origin. A model is proposed where the exchange of boron between host rock and solution has resulted in boron concentrations and isotopic compositions of the fracture waters reaching a steady state.

In contrast, pore fluid chemistry is not controlled by plagioclase dissolution as evidenced by the absence of a plagioclase $^{87}Sr/^{86}Sr$ and Ca/Sr molar ratio signature, and low Na/Ca molar ratio. The high Ca/Sr and low Na/Ca ratios are attributed to the formation of albite. The similarity between the isotopic composition of pore fluids and granite indicate that these waters have reached isotopic and chemical equilibrium with the host rock. The pore fluids can, therefore, be considered a closed system.

The similarity in salinities of the most saline fluid inclusions (≈ 200g/L) and the predicted salinities of pore fluids below 1000 m depth in the Lac du Bonnet pluton may indicate a genetic link between pore fluids and fluid inclusions.

Acknowledgments

I am indebted to my supervisor Dr. Bob McNutt for his invaluable suggestions during all stages of research and writing of this thesis, and his generosity in funding this project.

I am grateful to all the technical staff on the fourth floor of the Arthur Bourne building - Jim McAndrew for instruction on the operation of the ICP-MS and standards, and Pam Collins for lending some much needed equipment. I am especially grateful to Catherina Jager for her help in the clean-lab and her ceaseless endeavors to insure my continuing humility. Additional instruction on the operation of the TIMS was provided by Dr. Alan Dickin, and Dr. Bob Bowins and was greatly appreciated.

Much frustration was avoided through helpful discussions with Dr. Denis Shaw and Dr. Minzghe Zhai on the complexities of boron chemistry and the difficulties associated with the isotopic analysis of boron.

I would like to extend my gratitude to all the staff of AECL in the Whiteshell Laboratories in Pinawa, Manitoba who provided samples and constructive suggestions; in particular Mel Gascoyne, without whose support this study could not have been done.

Just as important as those mentioned above who provided technical advise, are the graduate and undergraduate students at McMaster University who provided emotional support and camaraderie, especially Mark, Tim, Trevor, Jodie, Dave, Bronco, Joy and Nicole.

Last, but not least, are friends and family outside the McMaster community, who also provided much support during those rather long periods of frustration. Special gratitude is given to Sarah - you left much too soon.

TABLE OF CONTENTS

LIST OF FIGURES

LIST OF TABLES

CHAPTER ONE
INTRODUCTION

1.1 Purpose of this Study.

By the year 2000 there is expected to be an accumulation of 27,000 tonnes of high-level nuclear waste produced from the operation of Canada's nuclear reactors. Presently, used nuclear fuel is stored in water-filled pools or is placed in dry storage in above ground concrete canisters. It is recognized that this type of storage is only a temporary measure and that a permanent means of waste disposal is needed to insure long term isolation of wastes from the biosphere. Due to this need, the Government of Canada and the Government of Ontario launched the Nuclear Fuel Waste Management Program (CNFWMP) to develop technologies for the safe, and permanent disposal of Canada's nuclear wastes. Atomic Energy of Canada Limited (AECL) was given the responsibility of assessing the concept for the disposal of nuclear fuel wastes in the stable granitic rock formations of the Canadian Shield. Preliminary investigations into deep disposal in crystalline rocks involved hydrogeological and hydrogeochemical studies of mine workings in the Canadian Shield, and of non-mineralized plutons of East Bull Lake, Ont; Chalk River, Ont.; Eye-Dashwa Lakes pluton, Ont.; and the Lac du Bonnet batholith, Manitoba.

This research revealed large changes within individual rock units in hydrogeology and geochemistry of the groundwater with increasing depth. At shallow depths (less than 200 m), there exists active hydrogeological flow systems containing generally fresh waters (dissolved load <1000 mg/L); the waters occurring in highly connected fault and joint systems. With increasing depth the hydrologic interconnectivity appears to decrease. Although interconnectivity may diminish with depth, in some instances, meteoric water may infiltrate down to 1000 m into Shield rocks through large vertical or nearly vertical fracture systems which are hydraulically connected to the surface. At depths as great as 2000 m, large

horizontal or sub-horizontal faults have been encountered during drilling. These faults systems contain considerable volumes (100's of L/min of flow) of very concentrated Ca-Na-Cl brines (usually >250 g/L) (Frape and Fritz, 1987).

Several theories have been proposed for the origin of the groundwater salinity found in these deep structures and generally they can be grouped according to whether the salinity was initially derived from outside the present geological unit (ie. allochthonous origin) or was derived from processes occurring within the rock unit (autochthonous origin). Supporters of an allochthonous origin believe the saline groundwaters of the Canadian Shield are marine in origin, however, theories on time of emplacement into the Shield and chemical evolution vary (Frape and Fritz., 1981; Kelly et al., 1986; Guha and Kanwar, 1987, Bottemley, 1994). It has been suggested that the salinity is derived from, 1) Paleozoic seawater which once inundated large portions of the Canadian Shield and infiltrated deep into the Shield rocks through fracture systems; or 2) marine waters trapped and modified as sedimentary basin brines, prior to infiltration along marginal areas of the Shield (Gascoyne et al. 1989a); or connate brines from Paleozoic sediments that once covered the Shield but have subsequently been removed by erosion.

Alternately, the high salinities in crystalline rocks maybe autochthonous in origin, where the groundwater salinity is primarily a result of slow aluminosilicate-water reactions (Fritz and Frape, 1982; Frape et al. 1984; Kamineni, 1987, Edmunds et al., 1984, 1985, 1987). There is general agreement that at least the cation component in solution has been contributed to, and strongly influenced by, reactions with certain mineral phases susceptible to alteration, such as plagioclase or amphibole. This is supported by the correlation between shallow groundwater chemical composition and the composition of the host rock. Water associated with granitic rock is dominated by Na>Ca>Mg as the major cations, while water associated with mafic rocks is dominated by Ca>Mg>Na as the major cations (Frape and Fritz., 1987). Also it has been noted, that the Ca, Na, and Mg mole ratios in groundwaters are usually similar to the mole ratios of their host rocks (Garrels, 1967).

Another possible autochthonous source is the leaching of intracrystalline fluid inclusions (Nordstrom et al., 1985,1989; Nordstrom and Olssen,1987), or intercrystalline pore fluids (Grigsby et al., 1983; Richards et al., 1992). With regard to fluid inclusions, a mechanism is required to move the fluid inclusion's contents into the groundwater system. The transport process may either be diffusive, or direct release by breakage or pressure dissolution. Diffusion flow through solid mineral phases would be too slow to be effective, therefore the most plausible mode of release is leakage of inclusion contents through microcracks into the flow porosity and eventual migration to larger fractures. Typically, fluid inclusions and pore fluids are considered autochthonous sources of salinity, implying derivation from processes occurring within the rock. In plutonic rocks, it is assumed that fluid inclusions or pore fluids are deuteric or hydrothermal fluids trapped during the early cooling history of the rock mass. This is not necessarily true, as the rock matrix fluids may have a complex history where different generations of chemically distinct fluids may exist within the same rock mass or within the same crystal. It is conceivable that pore fluids may in fact, be marine in origin where seawater has been emplaced into intergranular pores.

Knowledge of the origin of these saline fluids and their compositions can aid in assessing the suitability of waste disposal in the Canadian Shield. The primary purpose of the geological barrier is to prevent or retard the migration of the radionuclides to the biosphere. Considering that the only conceivable mode of radionuclide migration is via advection or diffusion through groundwater, a full understanding of groundwater flow and its' chemistry is essential to properly evaluate deep disposal in crystalline rocks. It is therefore necessary to characterize and understand the local and regional flow regimes of groundwater in the rock unit over tens of thousands of years.

An obvious measure of a rock unit's potential as a barrier to radionuclide migration is the degree in which it is isolated from present-day and historical flow systems. In other words, the residence time of the solvent or solute component within the rock unit may give some indication of the unit's ability to prevent migration of radionuclides. Ideally, it would

be possible to determine the residence time by directly "dating" the groundwater; and in some instances, this can be done for post-bomb groundwaters of meteoric waters by analysing for tritium. Unfortunately, for the time scale of interest to nuclear waste disposal, there is no radiometric method available. Residence time, therefore, must be inferred by determining the origin of the solvent or solute component of the groundwater.

As indicated above, most groundwaters in crystalline rocks have been sampled from shallow active flow systems in fractures or from hydrogeologically inactive large structural features located at great depth. Using chemical and isotopic compositions of these groundwaters, researchers have tried to determine the origin of these brines. Little research has been done, however, on the chemical compositions of fluids found outside these large structural features, that is, in the less fractured and less permeable regions of the crystalline rock bodies. Information on fluids located in unfractured rock may help in explaining the origin of the salinity in the active groundwater systems. In addition, full understanding of the pore fluid properties is necessary for evaluating vault performance. Influx of bedrock pore fluids during vault operation, due to chemical diffusional gradients following reflooding of the vault, may cause a gradual change in the backfill possibly affecting its sorption capacities (Gascoyne et al, 1995).

A major component of AECL's disposal program has been the construction of the Underground Research Laboratory (URL) at the Lac du Bonnet batholith in eastern Manitoba. The laboratory consists of a shaft and a series of drifts excavated to approximately 450 m below surface. Data collected from research activities at the URL has been used to understand the processes that may significantly affect the performance of the disposal vault, and to develop a methodology for evaluating a plutonic rock mass for its suitability as a waste repository. As part of the ongoing research on groundwater chemistry at the laboratory, this thesis investigates the occurrence of saline pore fluids in the Lac du Bonnet Batholith. Major ion chemistry, strontium isotopes and boron isotopes are employed to determine the relationship between pore fluids and groundwaters from more fractured

regions of the pluton. Several methods have been used to sample intercrystalline fluids from unfractured rock specimens; these include direct sampling of undiluted pore fluids into boreholes, leaching of pore fluids into boreholes filled with distilled de-ionized water, and flushing of intercrystalline fluids from drill cores.

1.2 Geology of the Lac du Bonnet

The Lac du Bonnet batholith is located approximately 70 km northeast of Winnipeg and is part of the Winnipeg River batholithic belt of the English River subprovince (Fig 1.1). It is a east-northeasterly elongated body approximately 75 km by 25 km in surface extent. To its north it is in contact with metasediments and metavolcanic rocks of the Bird River Greenstone Belt. Ordovician sediments, sandstones of the Winnipeg Formation and limestone and dolostone of the Red River Formation, unconformably overlie the batholith in the west.

The pluton is a relatively undifferentiated body, with variation attributed to contamination by country rock assimilation (McCrank, 1985). Granite and granodiorite make up the bulk of the batholith. The URL site is 2.5 km north of the southern contact of the batholith and approximately 17 km north east of the Whiteshell Laboratories (Fig 1.2). The site is dominated by two major phases, a lower magnetite-bearing grey granite-granodiorite and a upper haematite-bearing pink granite. The boundary between the two types occur between 200 m to 250 m depth from the presently exposed surface. The grey granite, with almost unaltered microcline, plagioclase and biotite, represents the primary phase of granite while the pink granite, has been overprinted by hydrothermal alteration. The hydrothermal overprint is interpreted as an early feature formed from deuteric fluids produced during the cooling and crystallization of the magma. Epidote, chlorite, phengite and carbonate replace plagioclase and biotite; the leached iron from the biotite has lead to local deposition of iron oxide, giving rise to the pink colouration.

There are numerous near-vertical fractures and three major sub-horizontal fracture

Figure 1.1. The regional geology around the Lac du Bonnet batholith (modified from Brown and Davison, 1986).

Figure 1.2. Map showing the geological setting of the Lac du Bonnet batholith and surrounding country rock. Also shown are the locations of the Whiteshell Research Area and URL lease site (shaded black) (modified from Brown et al., 1989)

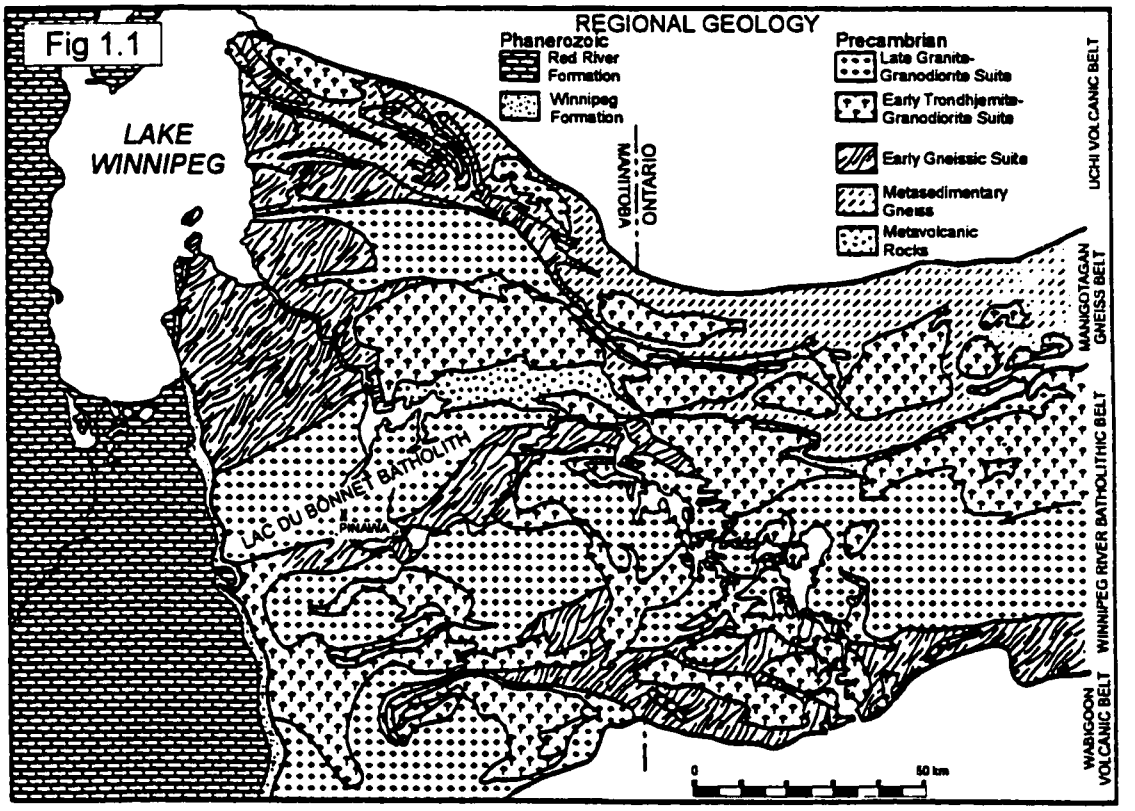
Fig 1.1
REGIONAL GEOLOGY
Phanerozoic
Red River Formation
Winnipeg Formation
Precambrian
Late Granite-Granodiorite Suite
Early Trondhjemite-Granodiorite Suite
Early Gneissic Suite
Metasedimentary Gneiss
Metavolcanic Rocks
LAKE WINNIPEG
MANITOBA
ONTARIO
LAC DU BONNET BATHOLITH
PINAWA
UCHI VOLCANIC BELT
MANIGOTAGAN GNEISS BELT
WINNIPEG RIVER BATHOLITHIC BELT
WABIGOON VOLCANIC BELT
0
50 km

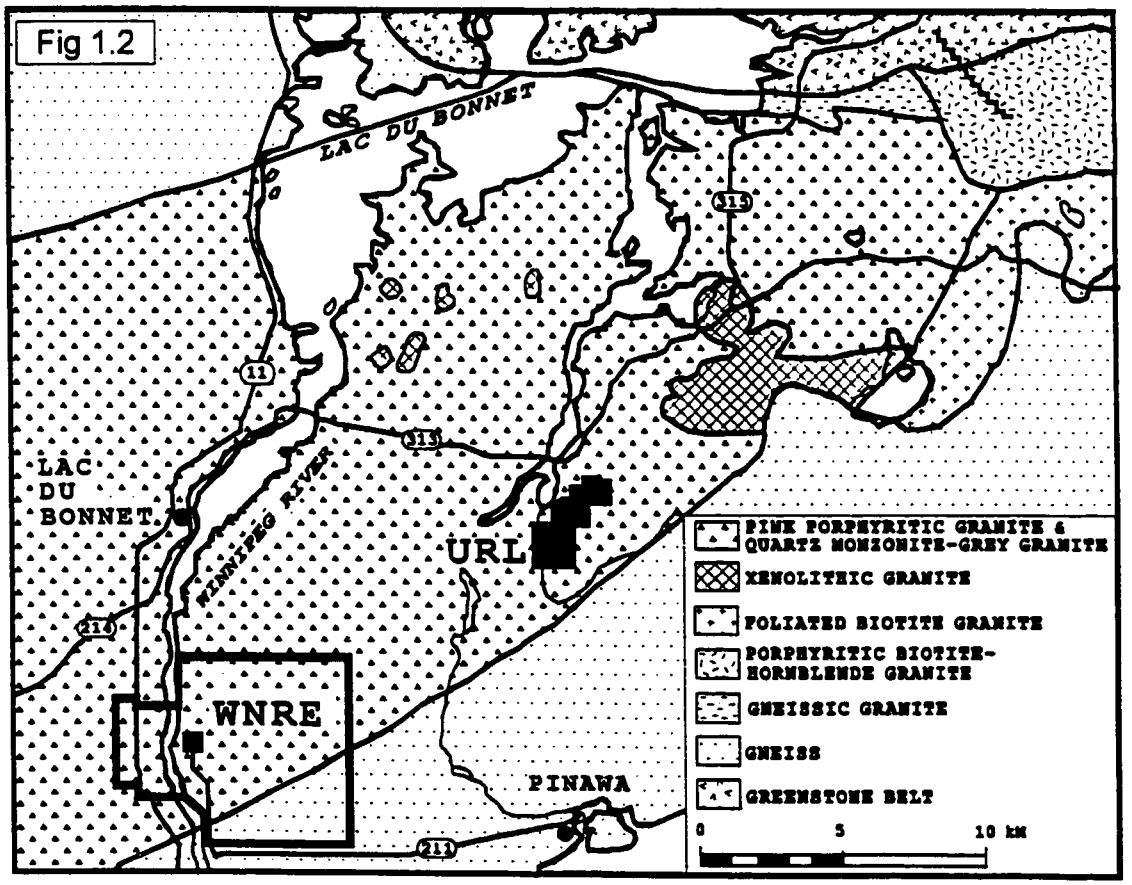
Fig 1.2
LAC DU BONNET
LAC DU BONNET
WINNIPEG RIVER
URL
WNRE
PINAWA
11
313
313
211
211
PINK PORPHYRITIC GRANITE & QUARTZ MONZONITE-GREY GRANITE
XENOLITHIC GRANITE
FOLIATED BIOTITE GRANITE
PORPHYRITIC BIOTITE-HORNBLENDE GRANITE
GNEISSIC GRANITE
GNEISS
GREENSTONE BELT
0
5
10 km

zones. The three fracture zones vary in thickness and dip to the south-east extending westward 15 km to the Whiteshell Research area (Fig 1.3). At the URL site, joints are commonly either subvertical, or dip 10°-30°; subhorizontal fractures disappear within a few metres of the surface except where associated with low-dipping fault zones (Brown and Davison, 1986). The fracture zones all dip in the same direction to the granite compositional layering in these regions; where the layering is locally strong in a different direction, a zone splay may also be found to dip in this direction. No evidence of post-crystallization tectonic events disturbing this batholith exists. Therefore, these fractures are believed to have formed under regional stress during the cooling of the magma and subsequent hydrothermal events.

The age of crystallization has been dated at 2665 ±20 Ma based on U-Pb isotope ratios in zircons (Krogh et al, 1976). After the initial crystallization of the magma, the batholith experienced an extend period (2000 Ma) of hydrothermal alteration (Gascoyne and Cramer, 1987). The circulation of high-temperature oxidizing fluids has created discrete zones of deep-red granite associated with major fracturing. The intensity of the pink colouration increases both toward individual fractures and also as the total number of fractures increases. Narrow zones of dark-red granite are concentrated in the pink granite, but discrete occurrences are found at deeper levels in the grey granite. In the dark-red granite, biotite is heavily altered to chlorite and vermiculite, plagioclase to sericite, with illite present interstially.

In specific fractures and immediately adjacent to the fractures, the deep-red granite grades into a bleached material composed of clay mixed with rock matrix, . Within the fractures themselves only clay minerals are present, these are illite, montmorillonite, mixed-layer montmorillonite, vermiculite, and nontronite (Brown et al, 1989). Oxygen isotope study of illite ($\delta^{18}O$ = 17.-20.9‰) indicates that the clays have formed under low temperature conditions (Kerrich and Kamenini, 1988). Low temperature kaolinite, Fe-oxyhydroxides, and vermiculite have also been identified in fractures at a depth of 1000 m in the grey granite (Griffault et al., 1993). The presence of Ordovician sedimentary rocks overlaying the

batholith in the west indicate that the batholith was at surface or near surface for at least 450 Ma; it is therefore believed, that the low temperature alteration by meteoric water has been occurring since the Ordovician.

1.3 Hydrogeology and Geochemistry of Groundwaters

Hydrological studies have shown that the 3 major fracture zones largely control the patterns of groundwater movement and groundwater chemistry within the rock mass at the URL site (Fig. 1.3). There is a complex spatial pattern of hydraulic conductivities within each of the fracture zones which strongly controls both the groundwater movement and chemistry within each zone. Low conductivity areas correlate with the narrower regions of the fracture zone, whereas areas of higher conductivity are correlatable to the intersections of small low dipping or subvertical fractures with the major fracture. Within Zone 2, there is a correlation between hydraulic conductivity variations and alteration zone thickness. The regions of high hydraulic conductivity ($K=10^{-6}$ - 10^{-8} m/s) have thick alteration haloes(>40m); the regions of low hydraulic conductivity ($K=10^{-10}$ - 10^{-12} m/s) have thin alteration haloes(<5m) . This relationship is indicator of the present, and past, groundwater flow variations within Fracture Zone 2 (Everitt et al., 1990).

In between the major fracture zones are domains of sparsely fractured pink and grey granite, which contain only microcracks along and within grain boundaries, and only sparsely-distributed single fractures (Stevenson et al., 1996b). The permeabilities of these zones range between 3×10^{-17} m^2 to 1×10^{-22} m^2, and are orders of magnitude lower than the permeabilities measured in the major fracture zones.

Significant variations in chemistry occur from shallow to deep regions in the Lac du Bonnet Batholith waters. At the URL site, groundwaters are classified as 6 different types and are related to different hydrogeological environments (Fig. 1.4). Shallow waters, such as those found in near surface vertical joints fractures and FZ-3 are typically low to

Figure 1.3. Schematic cross-section from NW to SE through the URL research area showing the 3 main fracture zones and their relative permeabilities. The fracture zones are numbered in descending order from 3 to 1 with increasing depth (modified from Gascoyne et al., 1987).

Figure 1.4 Schematic representation of groundwater compositions and flow paths in the fracture zones. Hydraulic head and density data obtained from numerous instrumented boreholes permit determination of flow direction and areas of recharge and discharge (modified from Gascoyne et al., 1987)

Fig. 1.3

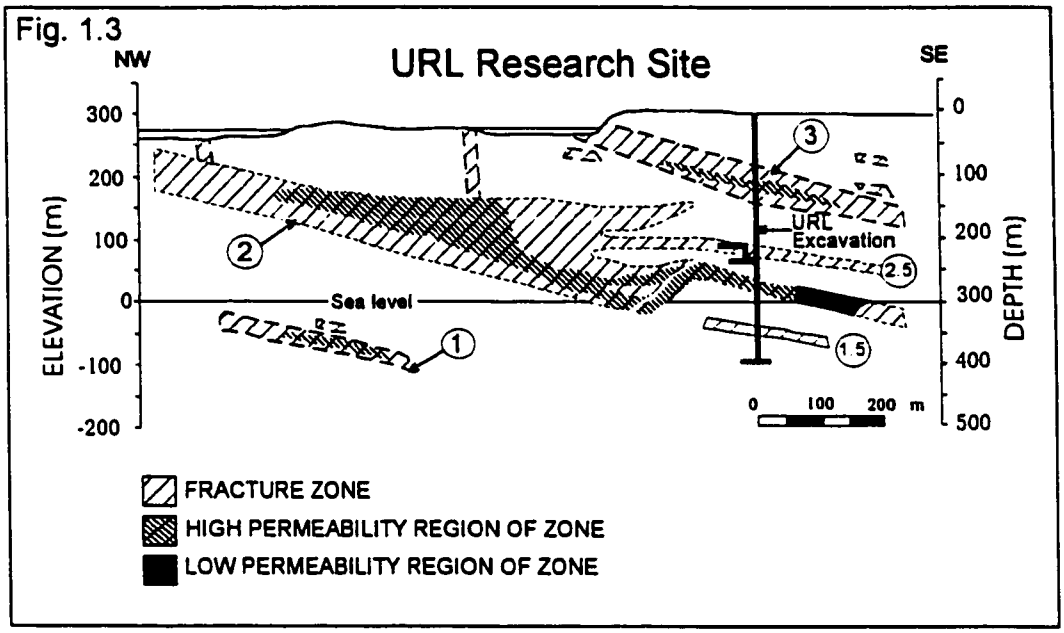
NW
URL Research Site
SE
ELEVATION (m)
DEPTH (m)
300
200
100
0
-100
-200
0
100
200
300
400
500
Sea level
URL
Excavation
1
1.5
2
2.5
3
0 100 200 m
FRACTURE ZONE
HIGH PERMEABILITY REGION OF ZONE
LOW PERMEABILITY REGION OF ZONE

Fig. 1.4

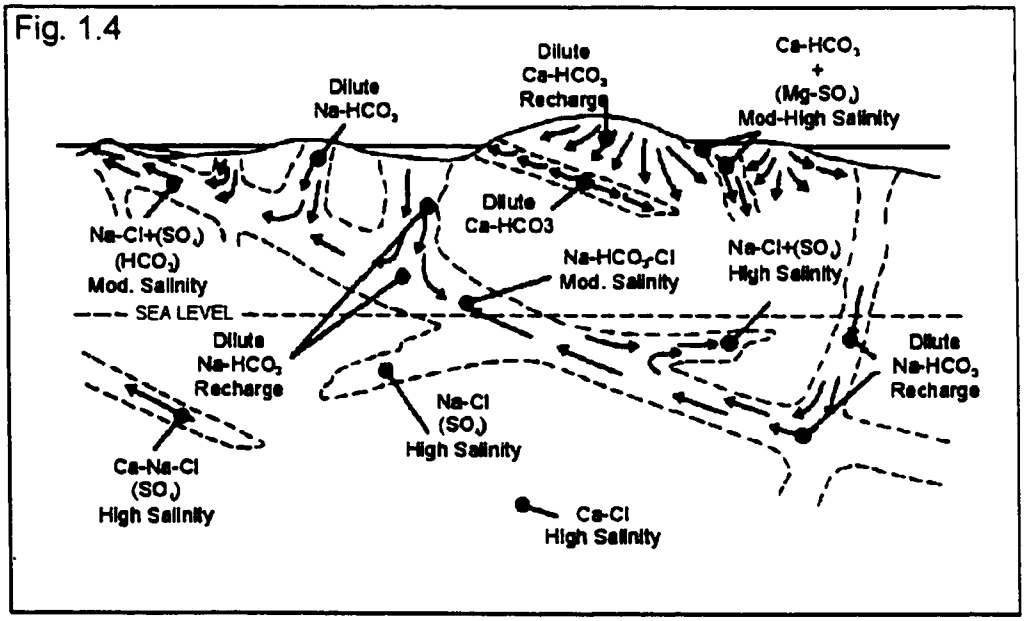
Dilute
Na-HCO3
Dilute
Ca-HCO3
Recharge
Ca-HCO3
+
(Mg-SO4)
Mod-High Salinity
Dilute
Ca-HCO3
Na-Cl+(SO4)
(HCO3)
Mod. Salinity
Na-HCO3-Cl
Mod. Salinity
Na-Cl+(SO4)
High Salinity
SEA LEVEL
Dilute
Na-HCO3
Recharge
Dilute
Na-HCO3
Recharge
Na-Cl
(SO4)
High Salinity
Ca-Na-Cl
(SO4)
High Salinity
Ca-Cl
High Salinity

moderately saline (TDS < 0.35 g/L) and are Ca-HCO_3 (Table 1.1). The dominance of bicarbonate in the shallow groundwaters is a result of the dissolution of carbonates in the overburden by slightly acidic, CO_2- and O_2-rich recharge waters (Gascoyne et al, 1987). With increasing depth the groundwaters evolve to Na-Cl-SO_4 composition. Salinity also increases with depth as evidenced by the TDS content of FZ-2 groundwaters ranging between 0.3 - 2 g/L. In Fracture Zone 1 groundwaters Ca becomes the dominant cation species and salinity increases to over 5.0 g/L.

The major trends in the transition in chemistry from shallow to deep groundwaters are decreasing HCO_3 and increasing Ca/Na. The loss of HCO_3 is possibly due to the precipitation of calcite induced by the increasing Ca concentration and the isolation of the deeper groundwaters from atmospheric CO_2. This is supported by the presence of calcite as a secondary fracture-infilling mineral and by the supersaturated nature of many URL groundwaters with respect to calcite. The increase in Ca is to be expected in a granitic environment, based on thermodynamic considerations. Albitization of plagioclase that is in contact with Na-rich groundwaters will remove Na from groundwaters and release Ca.

Based on the correlations between TDS, Ca, Sr, HCO_3, and SO_4, Li (1989) suggested that mixing was occurring between waters from FZ-3 and FZ-2, and between waters from FZ-2 and FZ-1, and that mixing between FZ-3 and FZ-1 was not significant. This is to be expected considering the higher permeability of the shallower rocks and the higher hydrological connectivity between FZ-2 and FZ-3 due to near surface subvertical jointing compared to the relative hydrological isolation of FZ-1.

1.4 Terminology and Samples

In this study, two water types are defined based on the nature of the rock from which they are sampled. The term "pore fluids" will be applied to those fluids extracted or derived from unfractured granite; this includes samples collected in the Borehole Leaching Test

Fracture Zone	Water Type	TDS	$^{87}Sr/^{86}Sr$
Zone 3	$CaNaHCO_3$	~ 0.3 g/L	0.714-0.719
Zone 2	$Na(Ca)HCO_3(Cl)$ -$NaCaClSO_4HCO_3$	0.4g/L - 2g/L	0.720-0.729
Zone 1	$CaNaClSO_4$	6g/L - 11g/L	0.729-0.737

Table 1.1 General chemical characteristics of groundwaters sampled from the the main fracture zones in the Lac du Bonnet Batholith (see Fig. 1.3). Chemical data is from Gascoyne et al. (1995). Sr isotopic data is from this study and Li, (1989).

experiment, salt removed from granite and granodiorite cores (Pore Salt Extraction Experiment), and from the seepage collected from unfractured granite. Some fluids sampled from sparsely fractured rock are isotopically and chemically similar to water from unfractured rock. Considering their chemical affinity, these fluids are classified as pore fluids as well. Ground water sampled from major fracture zones and from near surface fractures are called "fracture waters". The term "groundwater" in this study is used inclusively, referring to any fluid type in the Lac du Bonnet Batholith.

Groundwater samples were obtained from surface boreholes at the URL lease area and from the Whiteshell Laboratories, additional fracture waters were sampled from Underground boreholes within the URL. Rock samples were also collected from drill cores obtained from the URL. In some instances, the identification of samples have been abbreviated in tables and figures. Appendix 4 contains information on sample abbreviations, borehole name, and sample location.

CHAPTER TWO

BOREHOLE LEACHING TEST

To sample pore fluids or soluble salts located in the effective porosity of the unaltered grey granite of the Lac du Bonnet Batholith, an experiment was devised at AECL's Underground Research Laboratory (Gascoyne et al, 1995). The Borehole Leaching Test experiment (BLT) consists of 3 boreholes filled with distilled deionized water, which are used to accumulate in flowing pore fluids and leach any soluble salts located in the rock matrix adjacent to the boreholes.

2.1 Borehole Leaching Test - Design

At the 420 m level, in the Underground Research Laboratory, three 6 cm diameter boreholes were drilled into unfractured grey granite. The holes intersect granodiorite dykes and minor pegmatite intrusions and are divided into six zones of varying length using inflatable packers (Fig. 2.1). Each zone is situated in rock composed of different proportions of granite to granodiorite (Table 2.1). Distilled deionized water is introduced into the boreholes to leach any saline fluids or intergranular salts adjacent to the boreholes. To monitor the change in chemical composition of the Borehole Leach Test waters with time, water from each zone was periodically sampled over the duration of the experiment. To maintain a constant volume of water in the zones and to allow for continued sampling, water taken for chemical and isotopic analyses was replaced with fresh distilled deionized water.

The retrieved samples were analysed for ion chemistry at AECL Whiteshell Laboratories and Sr isotopes were analysed at McMaster University. The longest duration for sampling a zone was 1024 days. Whole rock and mineral samples were taken from drill cores removed in making the Leach Test boreholes and were also analysed for Sr isotopes.

The methodology and sample handling for both water and silicate samples is given in appendix 5.0.

Figure 2.1. A simplified drill core log of the three boreholes used in the BLT experiment. The boreholes were divided into six zones using inflatable packers. Each zone is in contact with grey granite and/or granodiorite. Granite and granodiorite are unfractured, with the exception of 403-014-MB2-Zone 2. (*based on Atomic Energy of Canada Ltd. drill core logs*)

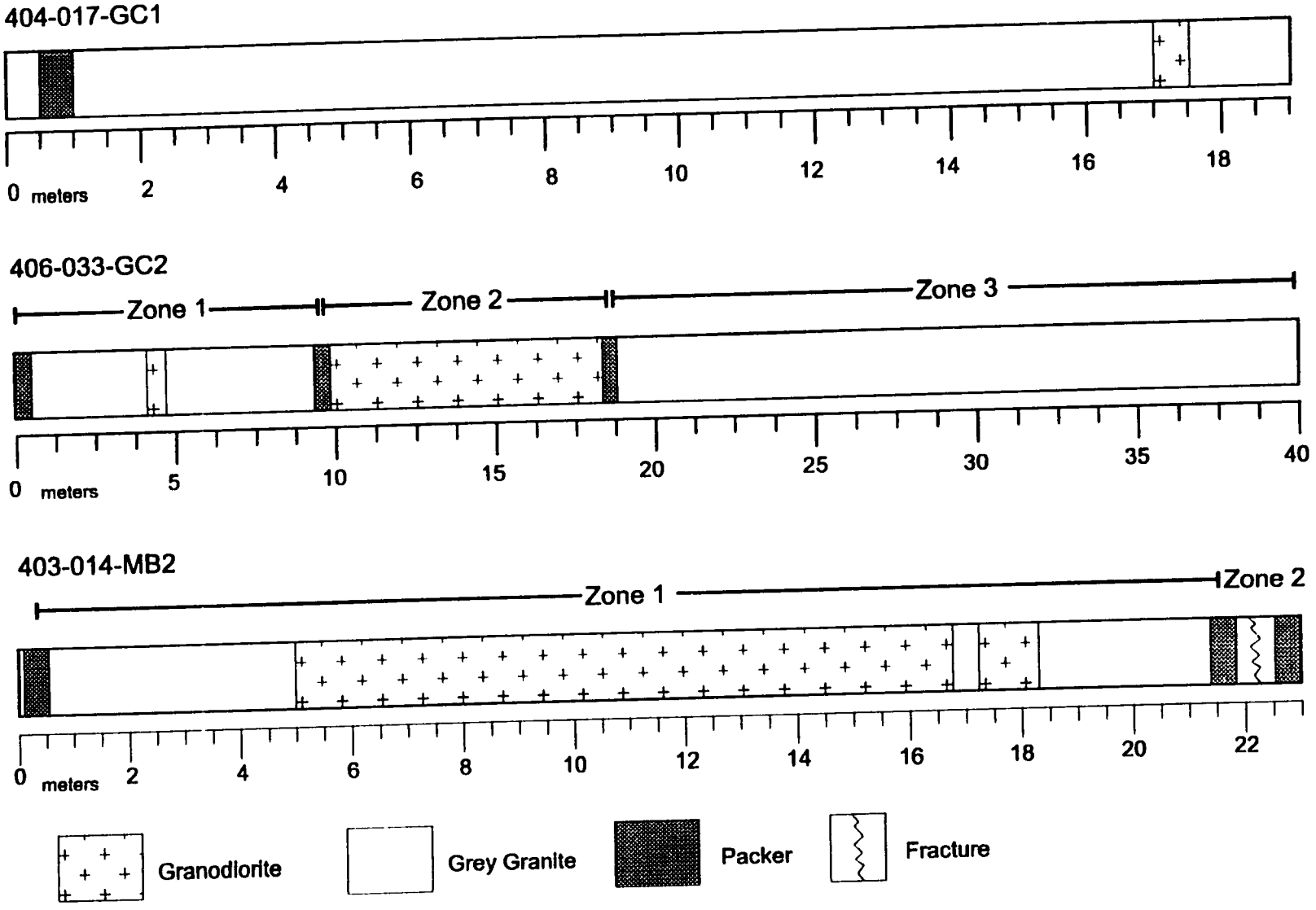
404-017-GC1
0 meters
2
4
6
8
10
12
14
16
18
406-033-GC2
Zone 1
Zone 2
Zone 3
0 meters
5
10
15
20
25
30
35
40
403-014-MB2
Zone 1
Zone 2
0 meters
2
4
6
8
10
12
14
16
18
20
22
Granodiorite
Grey Granite
Packer
Fracture

Hole/Zone	Length (m)	Lithology
403-014-MB2-Z1	21	39% / 61%
403-014-MB2-Z2	0.5	100% / 0%
404-017-GC1	19	97% / 3%
406-033-GC2-Z1	9	70% / 30%
406-033-GC2-Z2	8	0% / 100%
406-033-GC2-Z3	22	98% / 2%

Table 2.1 Percentage of granite and granodiorite in contact with zones of the BLT. Percentages were determined from Atomic Energy of Canada Ltd. drill core logs.

2.2 Borehole Leaching Test - Results.

2.2.1 Major Ion Chemistry.

In the BLT experiment, there was a rapid linear increase in salinity with time in all zones (Fig. 2.2). Such an increase in salinity, in particular the rapid rise in Cl content, cannot be explained by dissolution or leaching of mineral phases in the granite or granodiorite as a result of interactions with the distilled water. For example, in Zone 2 of 403-014-MB2, the chloride content after 500 days is more than 4500 mg/L. Biotite is the only abundant mineral phase in the Lac du Bonnet Batholith that can potentially contain significant amounts of Cl, typically 0.1 to 0.4 wt. % (Kamenini, 1987). If it is assumed that the biotite in the LDB contains 0.4 wt% Cl in its structure, then one thousand grams of biotite must dissolve to produce the observed concentration. Since the modal percentage of biotite in the granite is 5% this would entail the dissolution of biotite in 7.4 m^3 of rock and would require a volume of distilled water far in excess of the 5.5 liters introduced into the zone to penetrate into the adjacent rock matrix.

An alternative source of chloride is readily soluble salts present in the rock matrix. Intergranular salts contribute to salinity in circulating waters in the hot dry rock experiments in the Carnmellis granite (Richards et al., 1992) and saline pore fluids, having estimated Cl concentrations as high as 2.7 *M*, have been identified in the granite basement of Illinois (Couture et al., 1983, Couture and Sietz, 1986). At the Lac du Bonnet Batholith, the leaching of salts may contribute significantly to the chloride content of the groundwaters (Gascoyne et al., 1989b). Therefore, the rapid increase in chloride concentration and salinity in the BLT experiment probably is caused by the flow of pore fluids into the boreholes. The hydrostatic pressure in the intergranular cavities exceeds the one atm. pressure in the boreholes; the resulting hydraulic gradient leads to the injection of these fluids into the boreholes (Gascoyne et al., 1995). The increase in solute concentration in the BLT waters, therefore, can be

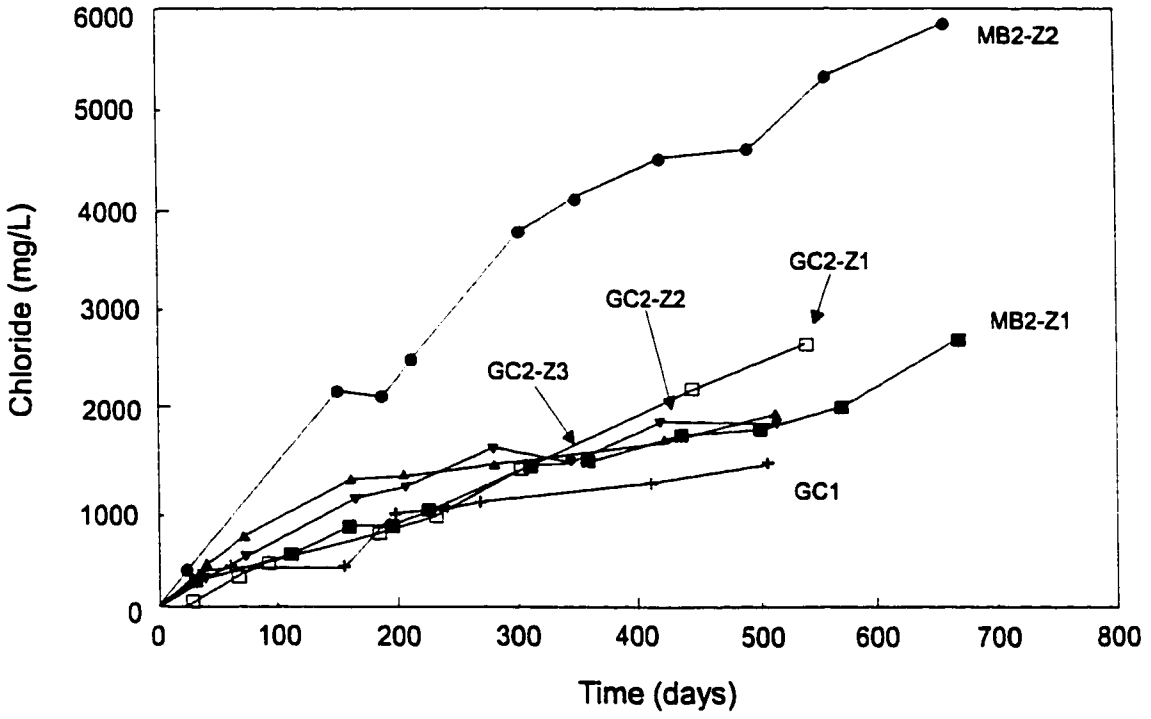

Figure 2.2. Change in chloride concentration with time in the water-filled zones of the Borehole Leaching Test experiment. Line labels indicate borehole and zone (refer to Table 2.1 and Figure 2.1). There is a rapid linear increase in chloride for all zones in the BLT experiment due to the influx of pore fluids (modified from Gascoyne et al. 1995).

considered a simple mixing trend between the initially pure distilled deionized water and the pore fluids. Although the absolute concentration of the pore fluid end member cannot be determined, information on the pore fluids' chemistry can be obtained by looking at ion ratios. This assumes that the chemistry of the pore fluids has not been altered by the dissolution or leaching of minerals in the granite and granodiorite, or the precipitation of secondary minerals within the boreholes. Evidence will be presented later that indicates mineral dissolutions, mainly plagioclase, has occurred in the boreholes, but contributes only minor amounts of Ca, Na, and Sr to the leach test waters compared to the pore fluids.

Figures 2.3 to 2.7 illustrate the differences in cation/Cl proportions between the Lac du Bonnet's fracture waters and BLT waters. In assessing the origin of the salt component, graphical comparisons can be made between different ions in solution and an ion such as chloride which is assumed to act in a conservative manner. These plots are useful in interpreting the interrelationship of cations and anions with the major anionic component of the saline waters. Comparisons between the molar ratios in the fracture waters, BLT water samples, are given in Table 2.2. Sodium, calcium, and strontium concentrations in the fracture water samples exhibit positive linear trends with respect to the chloride anion. In contrast potassium and magnesium exhibit poorly defined positive trends. Potassium is a major cationic component of rock forming minerals such as K-feldspar, micas and secondary fracture filling clays. It is easily dissolved from rocks during weathering, but it also tends to be easily removed from solution into secondary minerals such as the phyllosilicates . In this respect, the scatter of fracture water data in the Cl versus K plot may reflect the complex nature of potassium geochemistry in the fracture zones. The Cl versus K plot of the BLT waters shows a positive linear correlation between K and Cl up to 1500 mg/L Cl at which point, the increase in K concentration ceases, and remains relatively constant even though the chloride concentration continues to rise in the BLT zones. Potassium's constant concentration with continuing influx of pore fluids suggests that potassium is being removed from solution by secondary reactions within the boreholes. Therefore, the K/Cl ratios in the

Figures 2.3 to 2.7 Cation-Cl plots of the Lac du Bonnet's fracture waters and BLT waters. The two plots for each figure are the same data plotted at different ranges. Open squares (□) are fracture waters and open circles (O) are BLT water from the six zones. Solid line in Na, Ca, and Sr vs. Cl plots follow dilution trend of the sample waters. Four water samples from sparsely fractured and unfractured rock (SM7-28, URL13-9-1, URL13-11-1, URL2-PZ15) exhibit similar chemical characteristics to the BLT sample water. Dashed line represents dilution trend of present-day seawater. Data for fracture waters compiled from Gascoyne et al. (1987) and Li (1989) and this study.

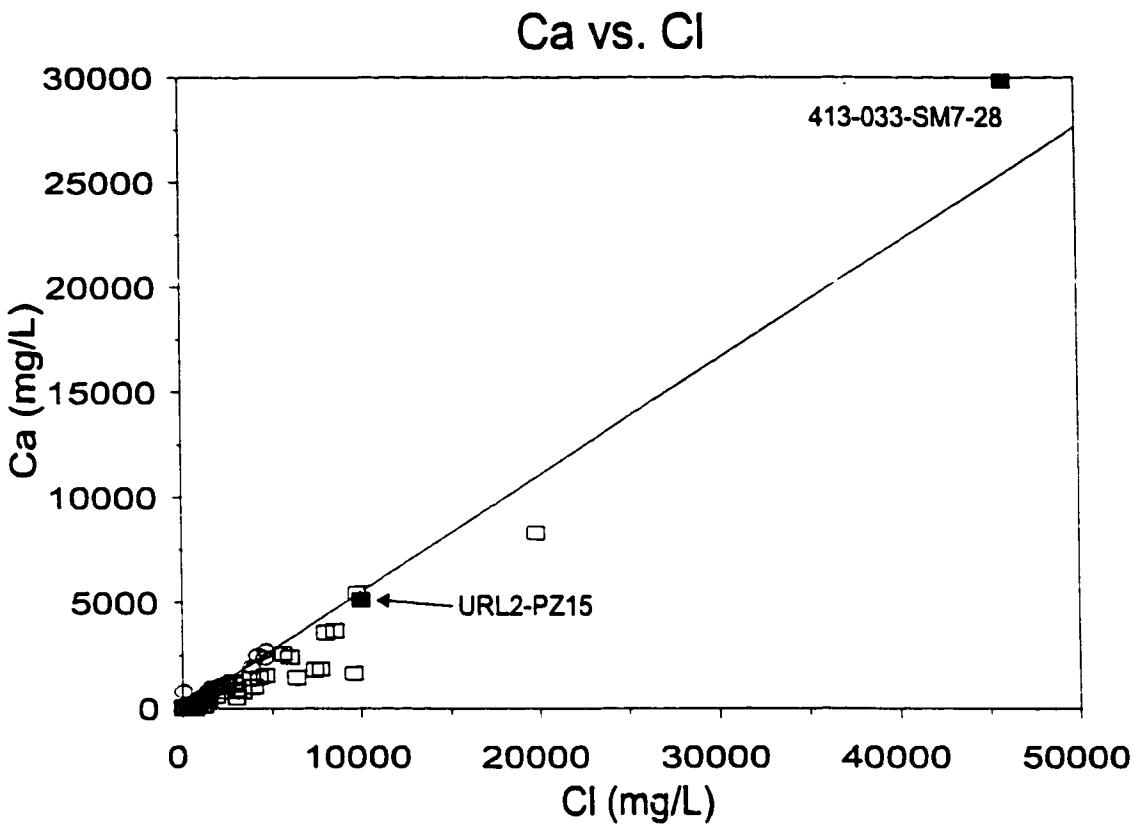
Ca vs. Cl
30000
25000
20000
15000
10000
5000
0
Ca (mg/L)
413-033-SM7-28
URL2-PZ15
0
10000
20000
30000
40000
50000
Cl (mg/L)

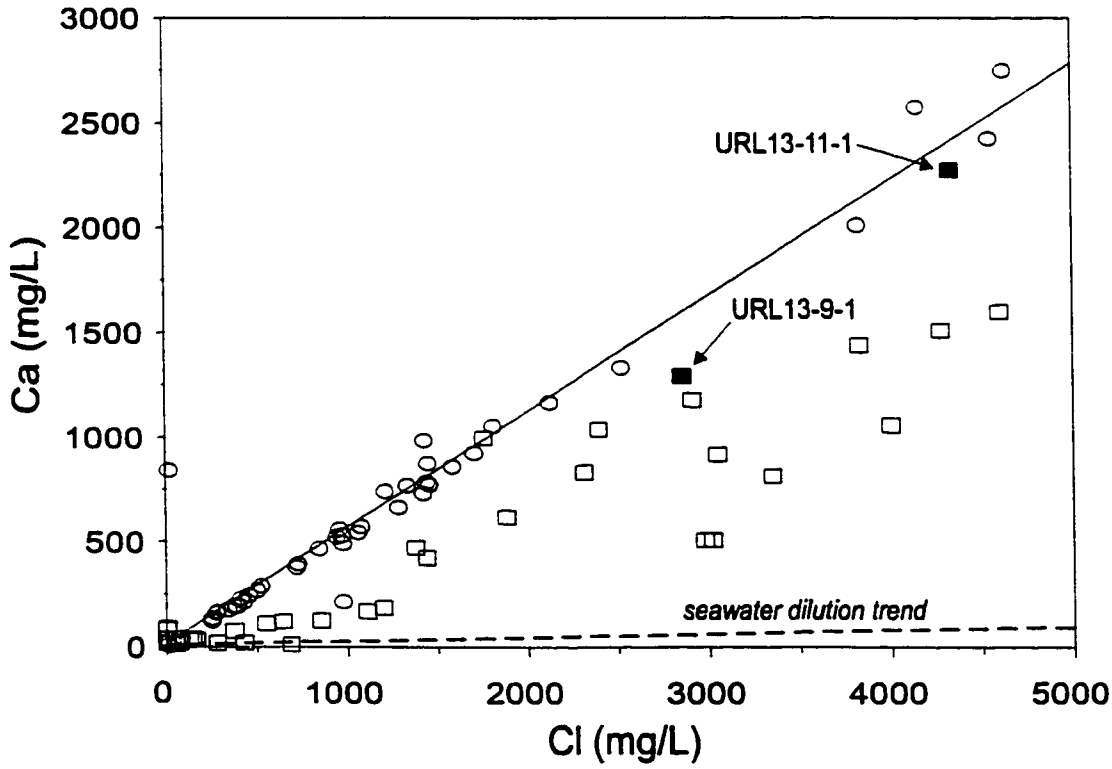
3000
2500
2000
1500
1000
500
0
Ca (mg/L)
URL13-11-1
URL13-9-1
seawater dilution trend
0
1000
2000
3000
4000
5000
Cl (mg/L)

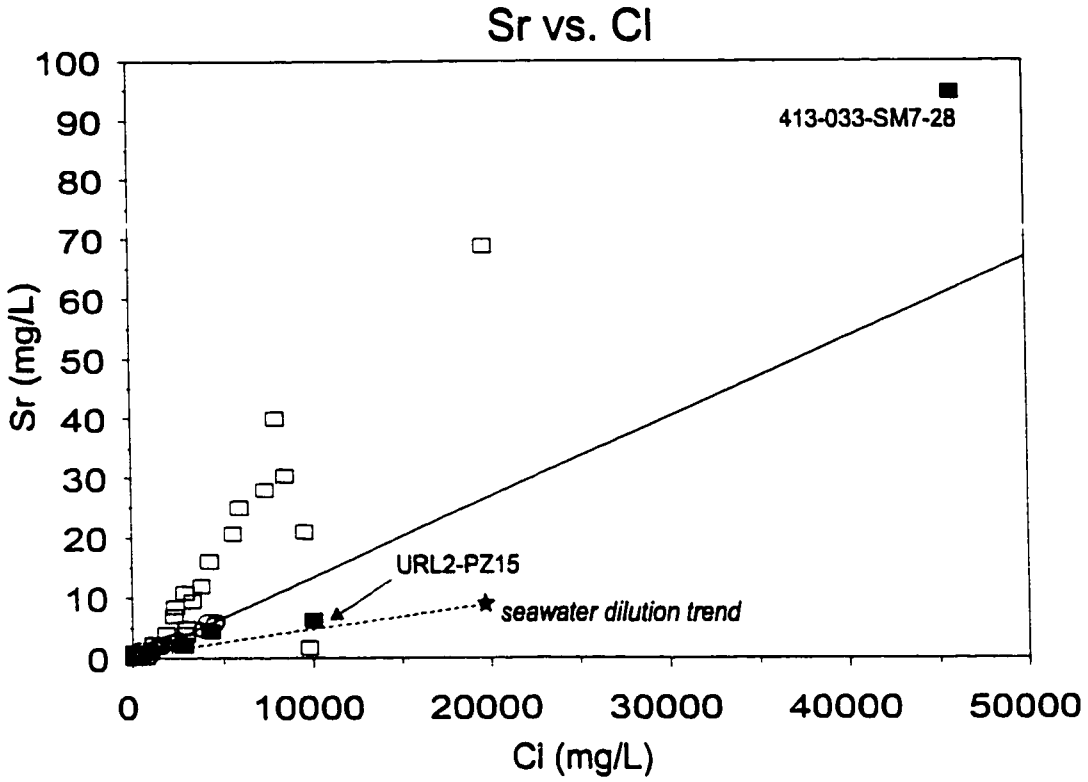
Sr vs. Cl
Sr (mg/L)
Cl (mg/L)
413-033-SM7-28
URL2-PZ15
seawater dilution trend
0
10
20
30
40
50
60
70
80
90
100
0
10000
20000
30000
40000
50000

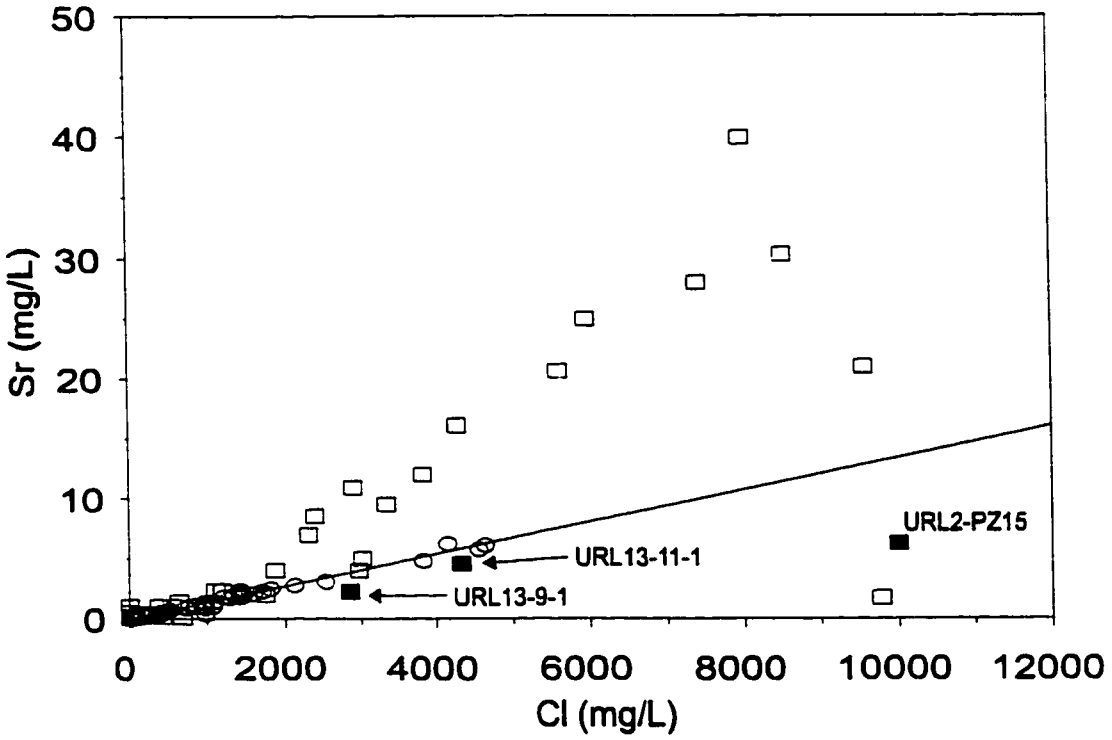
Sr (mg/L)
Cl (mg/L)
URL2-PZ15
URL13-11-1
URL13-9-1
0
10
20
30
40
50
0
2000
4000
6000
8000
10000
12000

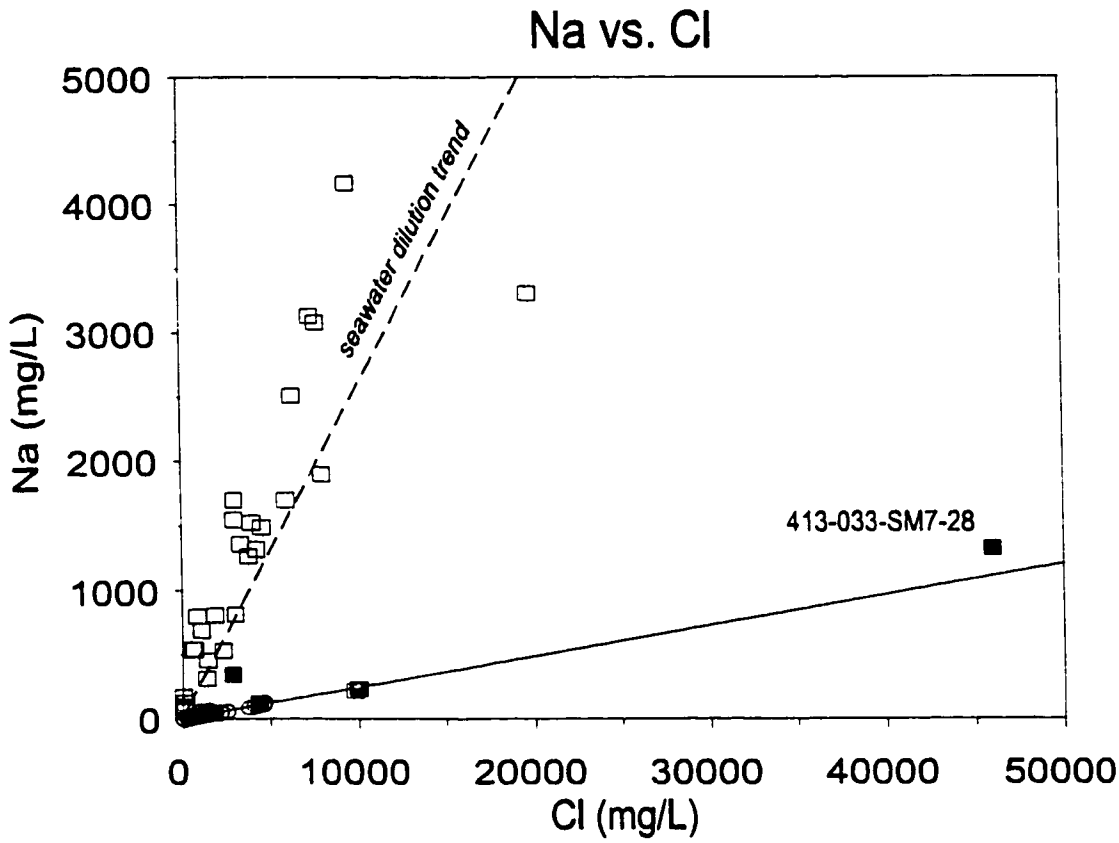
Na vs. Cl
5000
4000
3000
2000
1000
0
Na (mg/L)
seawater dilution trend
413-033-SM7-28
0
10000
20000
30000
40000
50000
Cl (mg/L)

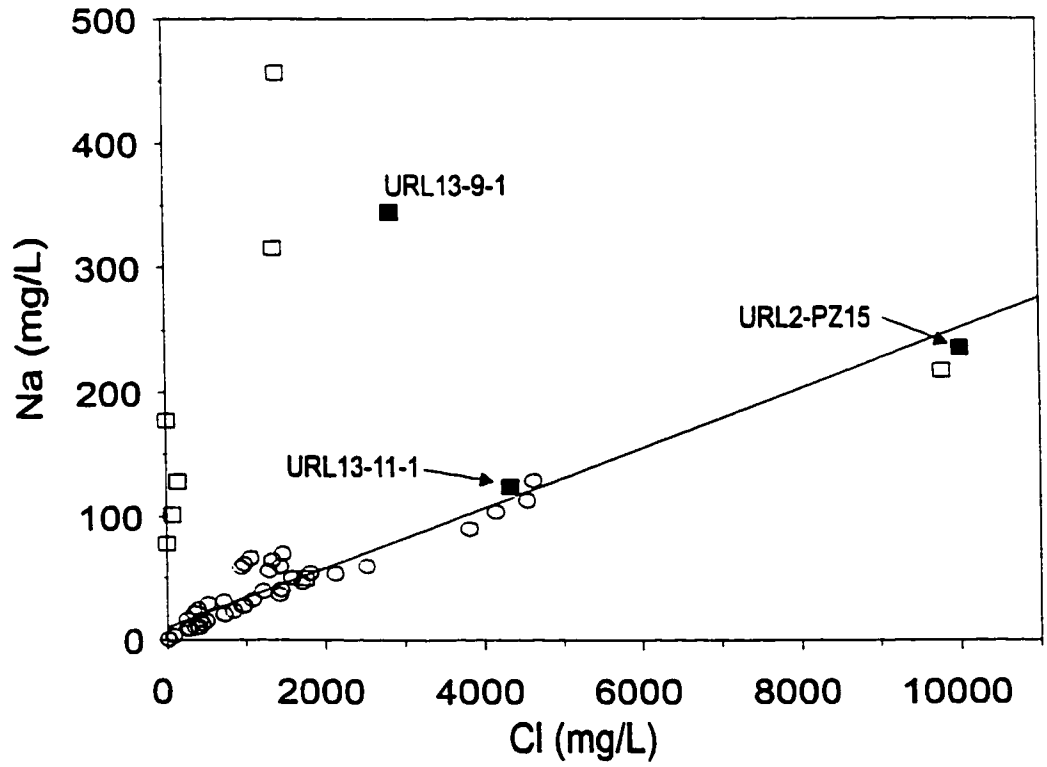
500
400
300
200
100
0
Na (mg/L)
URL13-9-1
URL2-PZ15
URL13-11-1
0
2000
4000
6000
8000
10000
Cl (mg/L)

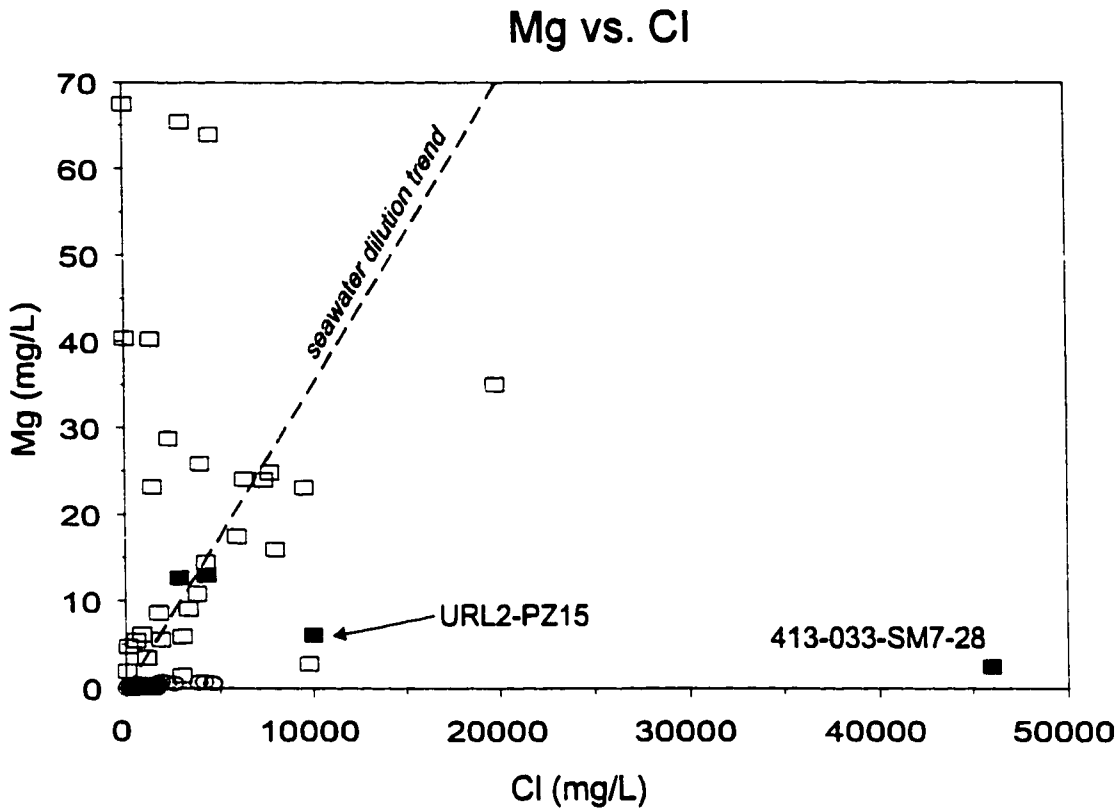
Mg vs. Cl
70
60
50
40
30
20
10
0
Mg (mg/L)
seawater dilution trend
URL2-PZ15
413-033-SM7-28
0
10000
20000
30000
40000
50000
Cl (mg/L)

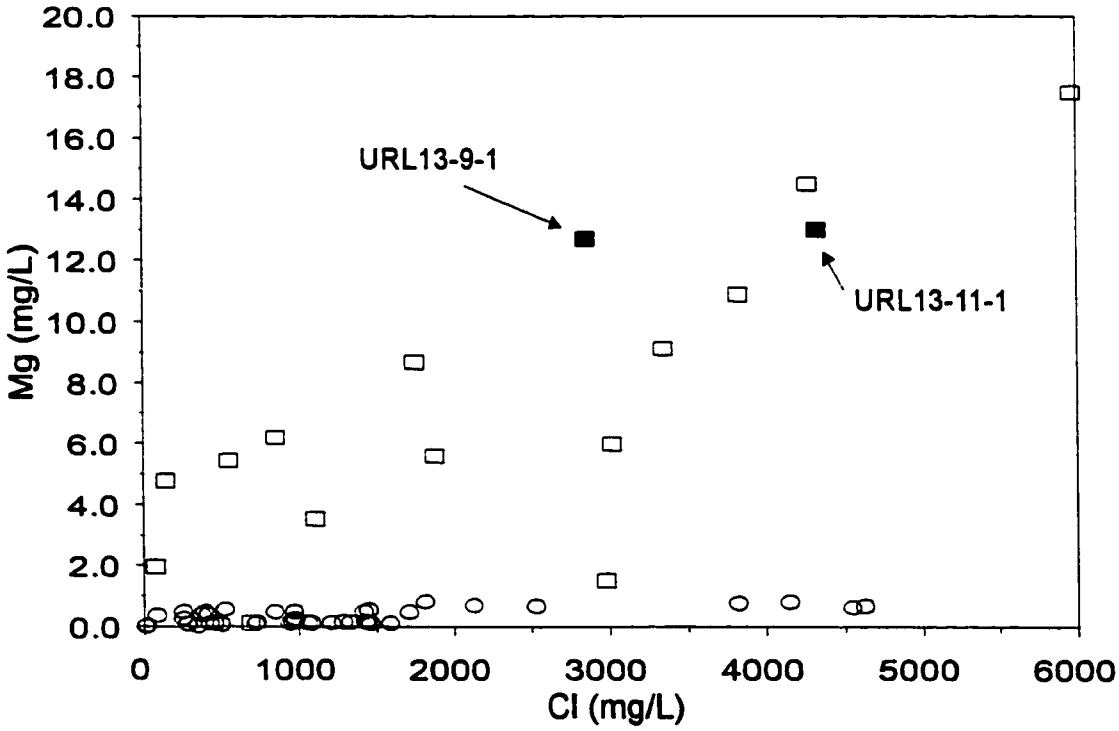
20.0
18.0
16.0
14.0
12.0
10.0
8.0
6.0
4.0
2.0
0.0
Mg (mg/L)
URL13-9-1
URL13-11-1
0
1000
2000
3000
4000
5000
6000
Cl (mg/L)

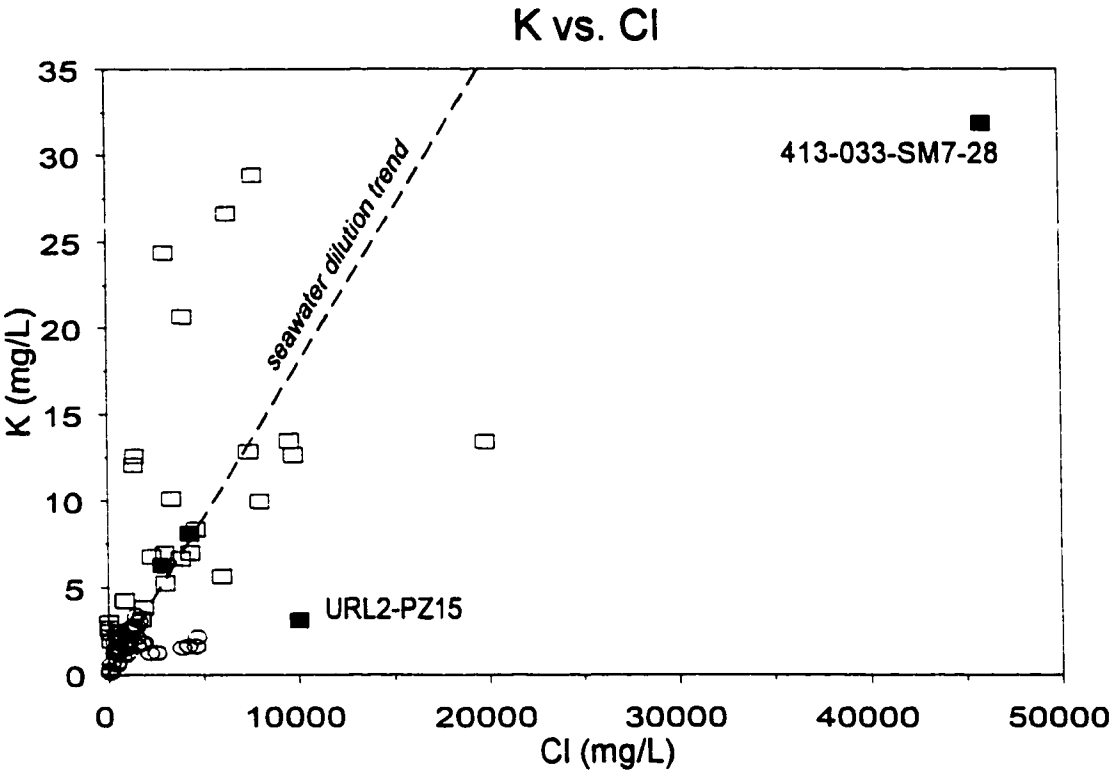
K vs. Cl
K (mg/L)
Cl (mg/L)
seawater dilution trend
413-033-SM7-28
URL2-PZ15
0
5
10
15
20
25
30
35
0
10000
20000
30000
40000
50000

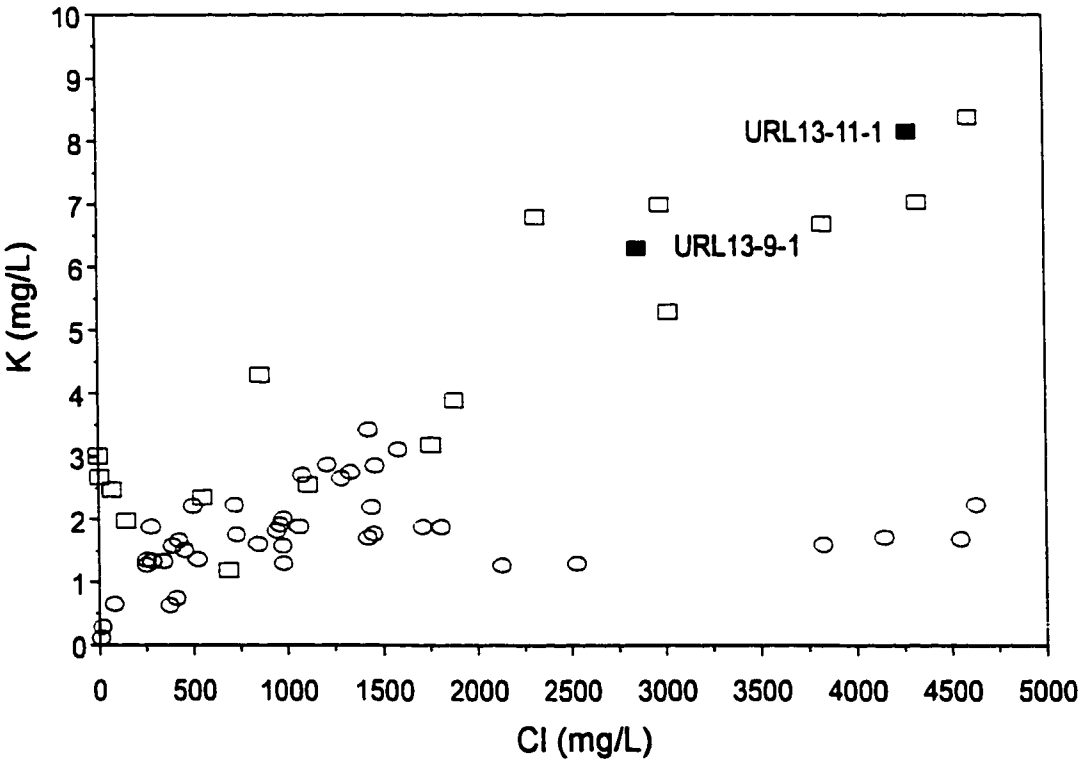
K (mg/L)
Cl (mg/L)
URL13-11-1
URL13-9-1
0
1
2
3
4
5
6
7
8
9
10
0
500
1000
1500
2000
2500
3000
3500
4000
4500
5000

Ratio	Fracture	URL2-PZ15	URL13-9-1	URL13-11-1	SM7-28	PSE	BLT
Na/Cl	0.55	0.04	0.18	0.04	0.04	-	0.04
Ca/Cl	0.49	0.45	0.40	0.46	0.58	-	0.52
Sr/Cl	0.0014	0.00025	0.00032	0.00042	0.00085	-	0.00056
K/Cl	0.0014	0.00029	0.0020	0.0015	0.00062	-	0.00077
Ca/Sr	236	1801	1263	1097	6589	-	918
Na/Ca	5.60	0.077	0.45	0.091	0.074	-	0.086
$^{87}Sr/^{86}Sr$	0.713-0.734	0.801	0.794	0.785	0.767	0.762-0.780	0.762

Table 2.2. Comparison of chemical composition of groundwater from fractured rock (Fracture), water samples from unfractured and sparsely fractured rock (URL2-PZ15, URL13-9-1, URL13-11-1 and 413-033-SM7-28), the Borehole Leaching Test sampled water (BLT) and the Pore Salt Extraction waters (PSE). Ratios are expressed as molar ratios.

zones early on in the experiment (< 1500 mg/L Cl) are probably more representive of the true ratio in the pore fluids than the ratios measured in the later stages of the experiment (>1500 mg/L).

The leaching test waters, are distinctly different from the fracture waters in their cation/Cl ratios. They are depleted in Na, Mg, and Sr, and are enriched in Ca.The most unusual feature is the depletion of Sr with respect to Ca in the BLT waters compared with the fracture waters (Fig. 2.8). Considering the similarity in geochemical behaviour of the two cations, the difference in Ca/Sr in the fracture waters and pore fluids may be important in determining the different Ca and Sr sources, or the different chemical processes controlling the Ca-Sr budgets in the two water types.

Although most fracture waters sampled at LDB are chemically distinct from the leaching test waters, four URL groundwater samples (URL13-9-1, URL13-11-1, URL2-PZ15 and 413-033-SM7-28) extracted from unfractured and sparsely fractured rock exhibit similar chemical characteristics. In most of the cation -chloride plots, the four samples plot near the line defined by the mixing trend of the BLT waters.

2.2.2 Sr Isotopes in Water Samples

In addition to major element analysis of the BLT waters, the $^{87}Sr/^{86}Sr$ ratio was also monitored in all six zones. The waters are distinctly different in their enrichment in radiogenic ^{87}Sr compared to the fracture waters in the Lac du Bonnet Batholith. The Sr isotopic composition of previously analysed fracture waters varies from a low value of 0.713 for shallow and typically dilute waters, to 0.738 in deeper and more saline groundwaters (Li, 1989). In contrast, the leach test waters are more radiogenic having values between 0.763 - 0.773 (Table 2.3). At the beginning of the experiment, there was a decrease in the $^{87}Sr/^{86}Sr$ with time, but as the experiment progressed, the Sr isotopic composition of the zones approached constant values, and in GC1-1 and MB2-1, the $^{87}Sr/^{86}Sr$ increased at the end of

Figures 2.8 Ca - Sr plot of the fracture and BLT sample waters. Solid line represents the dilution trend of the BLT samples. Similar to the cation/Cl plots, the four water samples from sparsely fractured and unfractured rock plot close to the dilution trend. Data for fracture waters compiled from Gascoyne et al. (1987) and Li (1989) and this study.

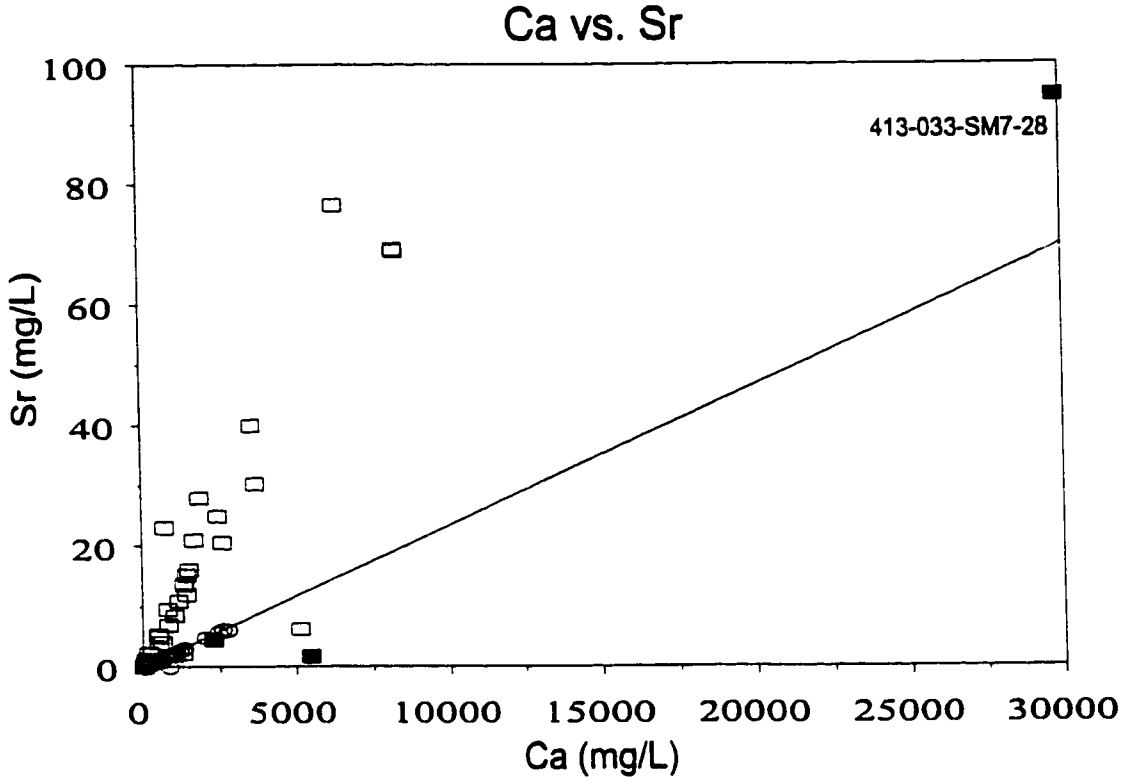
Ca vs. Sr
Sr (mg/L)
Ca (mg/L)
413-033-SM7-28
0
20
40
60
80
100
0
5000
10000
15000
20000
25000
30000

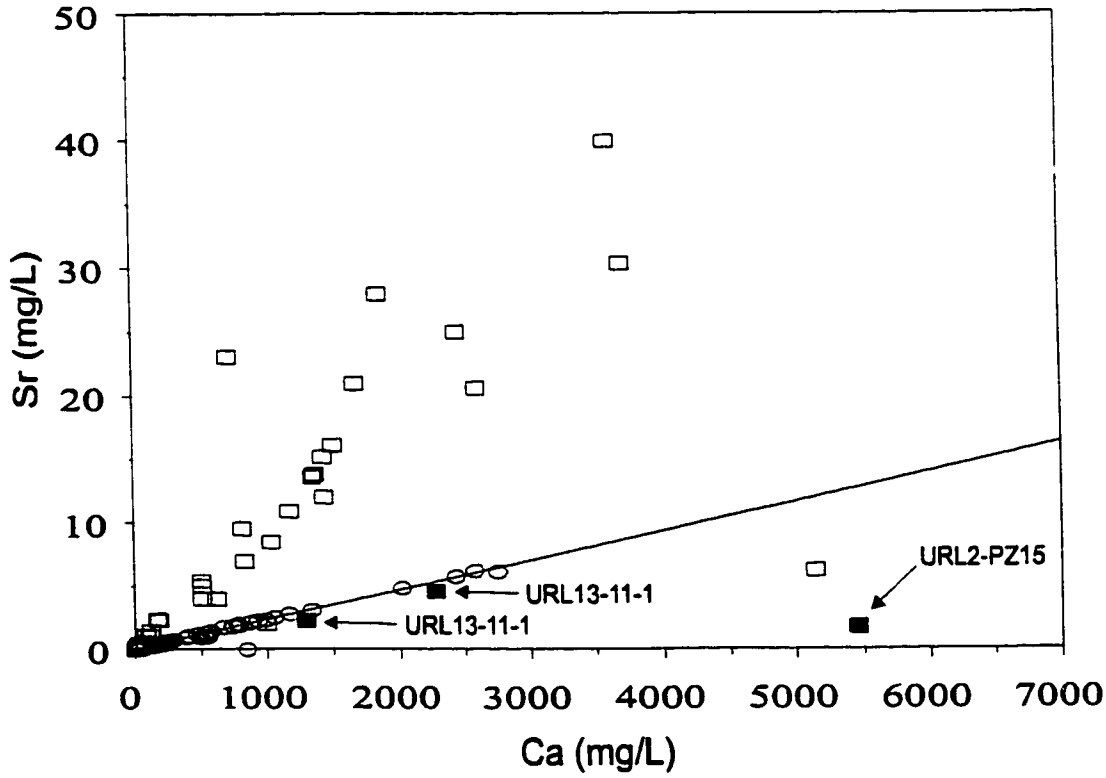
Sr (mg/L)
Ca (mg/L)
URL13-11-1
URL13-11-1
URL2-PZ15
0
10
20
30
40
50
0
1000
2000
3000
4000
5000
6000
7000

the experiment (Fig. 2.9).

2.2.3 Whole Rock Sr Isotopes

Whole rock samples were collected from the drill cores of 406-033-GC2, 404-017-GC1, and 403-014-MB2-Z1, and from several other localities in the Lac Du Bonnet (Table 2.4). Mineral separates were obtained from granite and granodiorite samples taken from drill core 403-014-MB2 and analysed for their Sr isotopic composition. The isotopic composition of whole rock and minerals of the grey granite and granodiorite are similar to minerals and whole rock of pink granite (Li, 1989). One exception is biotite, where a noticeably higher $^{87}Sr/^{86}Sr$ was obtained for this study. It is believed that this is related to the higher purity of the biotite separate used for analysis in this study and not a reflection of any geochemical difference between biotites sampled from the two lithological units.

Table 2.3. Sr isotopic data of water samples from the Borehole Leaching Test Experiment. Time refers to number of days after the initial introduction of distilled deionized water into the zone.

MB2-Zone 1				GC2-Zone 1			
Date	Time	$^{87}Sr/^{86}Sr$	Sr Conc.	Date	Time	$^{87}Sr/^{86}Sr$	Sr Conc.
92/05/12	132	0.76693	1.2	92/09/09	186	0.77295	1.0
92/09/09	251	0.76678	1.8	92/10/23	230	0.77271	1.4
93/01/04	368	0.76669	2.3	93/01/04	302	0.77254	1.9
93/03/18	441	0.76661	2.5	93/03/19	376	0.77232	-
93/8/31	576	0.76681	3.4	94/2/24	687	0.77208	4.8
94/2/23	752	0.76643	4.0	94/6/14	797	0.77204	5.0
94/6/13	862	0.76653	4.1	94/11/25	960	0.77189	6.5
94/11/23	1024	0.76692	4.9				
MB2-Zone 2				**GC2-Zone 2**			
92/02/19	4	0.76775	0.6	92/06/11	72	0.77259	0.7
92/05/12	132	0.76744	2.8	92/09/09	161	0.77184	1.4
92/09/09	251	0.76743	4.8	92/10/23	206	0.77147	1.8
93/01/04	368	0.76738	5.8	93/01/04	278	0.77119	2.1
93/03/18	441	0.76709	6.1	93/03/19	349	0.77126	2.3
93/8/31	576	0.76733	7.9	93/11/25	599	0.77082	2.6
94/2/23	752	0.76726	7.4	94/2/24	663	0.77078	2.7
94/6/13	862	0.76729	8.8	94/6/14	773	0.77073	2.6
94/11/24	1024	0.76723	9.0	94/11/24	935	0.77069	2.8
GC1- Zone 1				**GC2-Zone 3**			
92/10/23	198	0.76333	1.0	92/06/11	71	0.76869	0.9
92/12/02	238	0.76344	0.9	92/09/09	160	0.76825	1.8
93/01/04	270	0.76311	1.0	92/10/23	205	0.76798	2.0
93/03/18	343	0.76308	0.4	93/01/04	277	0.76781	2.0
93/8/31	478	0.76286	1.5	93/03/19	348	0.76786	2.2
93/11/24	563	0.76261	1.8	93/8/31	482	0.76765	2.7
94/2/23	654	0.76264	2.0	93/11/25	598	0.76754	2.8
94/6/13	764	0.76266	1.8	94/2/24	662	0.76753	3.1
94/11/24	926	0.76275	3.2	94/6/14	772	0.76749	3.1
				94/11/24	934	0.76742	3.4

Sample	$^{87}Sr/^{86}Sr$	Sr Conc. (μg/g)	Lithology/Mineral
401-1	0.76209	--	Grey Granite
GC2-36	0.77474	--	Grey Granite
URL2-791	0.80189	--	Grey Granite
GC1-1	0.78356	--	Grey Granite
MB2-1	0.78051	--	Grey Granite
403-A1	0.77868	--	Grey Granite
GC2-10	0.79570	--	Granodiorite
GC2-15	0.79000	--	Granodiorite
MB2-11	0.78870	--	Granodiorite
403-A1F	0.84333	224.4	K-Feldspar
403-A2F	0.84938	195.4	K-Feldspar
403-A5F	0.86448	293.3	K-Feldspar
403-A4F	0.88472	140.5	K-Feldspar
403-A6F	0.84930	217.6	K-Feldspar
403-A1B	5.9666	14.6	Biotite
403-A2B	5.2635	18.2	Biotitie
403-A4B	7.5910	15.0	Biotite
403-A5B	4.3312	--	Biotite
403-A6B	6.0968	23.0	Biotite
403-A1P	0.71131	--	Plagioclase
403-A2P	0.71079	197.3	Plagioclase
403-A5P	0.71257	--	Plagioclase
403-A6P	0.71104	--	Plagioclase

Table 2.4. Sr isotopic composition and concentrations of whole rock and mineral samples . MB2 and 403-series samples are from BLT borehole 403-014-MB2; GC2 series samples are from borehole 406-033-GC2; sample GC1-1 is from borehole 404-017-GC1; sample 401-1 is from borehole 401-S1-PH1;and URL2-791 is from borehole URL2.

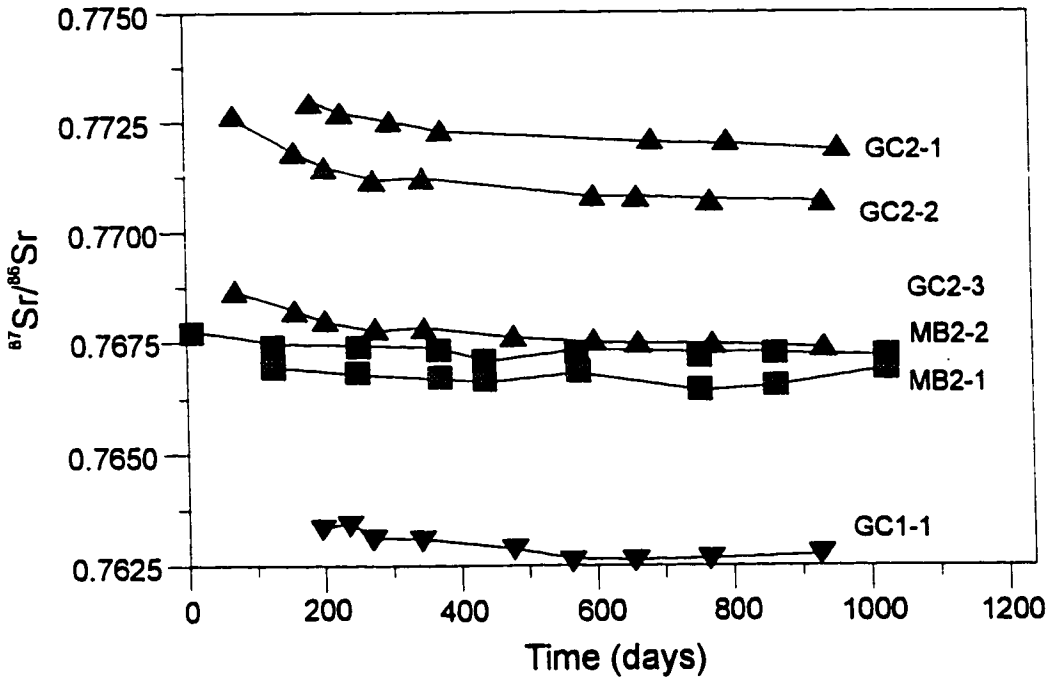

Figure 2.9. Change in $^{87}Sr/^{86}Sr$ in periodically sampled waters of the BLT experiment. All six zones show a slow decrease in their $^{87}Sr/^{86}Sr$ ratios with time. Line labels refer to borehole and zone (see Table 2.1 and Figure 2.1).

CHAPTER THREE
PORE SALT EXTRACTION EXPERIMENT

To investigate pore salts directly, a procedure and equipment previous used for radionuclide migration experiments (Drew and Vandergraaf, 1988), was modified to extract intergranular salts from unfractured rock samples. Grain boundary salts in the effective porosity were extracted by forcing distilled deionized water under high pressure through unfractured drill cores.

3.1 Experimental Procedure

Whole rock samples for the Pore Salt Extraction (PSE) experiment were obtained from large (61.2 mm diameter) unfractured drill cores of pristine grey granite, altered pink granite and granodiorite from the URL. Smaller cores with diameters of 2.5 cm, were drilled from the centre of the large cores and these smaller cores were used in the Extraction experiment while the remaining portions the large cores were crushed and analysed for $^{87}Sr/^{86}Sr$. The salts are removed or flushed from the grain boundary cavities, by using distilled deionized water as a carrier fluid to dissolve and remove any grain boundary salts present in the effective porosity of the small core. Entry and exit for the carrier fluid was provided by stainless steel plates and tubing affixed onto the sample cores' ends (Fig 3.1). To prevent slippage of the plates from the core's ends, RTV 108® Silicone Rubber was applied around the perimeter of the core where the plates and core were in contact. After the silicone rubber was dry, the core was placed in a Teflon mould and epoxy resin was poured into the mould. The sample and mould were allowed to set over night until the resin was hard. The mould was removed, thus leaving the sample and plates inclosed in a hard epoxy jacket.

Very high water pressures are required to force the carrier fluid through the unfractured cores. If there is no confining pressure applied to the sample as the carrier fluid is forced through the unfractured rock, the seal between core and epoxy jacket will be broken.

Figure 3.1. Schematic diagram of apparatus used in the Pore Salt Flush Experiment. An unfractured granite or granodiorite core is enclosed in a hard epoxy jacket and placed inside a pressure vessel. Intergranular salts are removed by forcing a carrier or transport solution through the core. To prevent rupture, the pressure in the confining pressure cavity is kept higher than the pressure in the transport fluid.

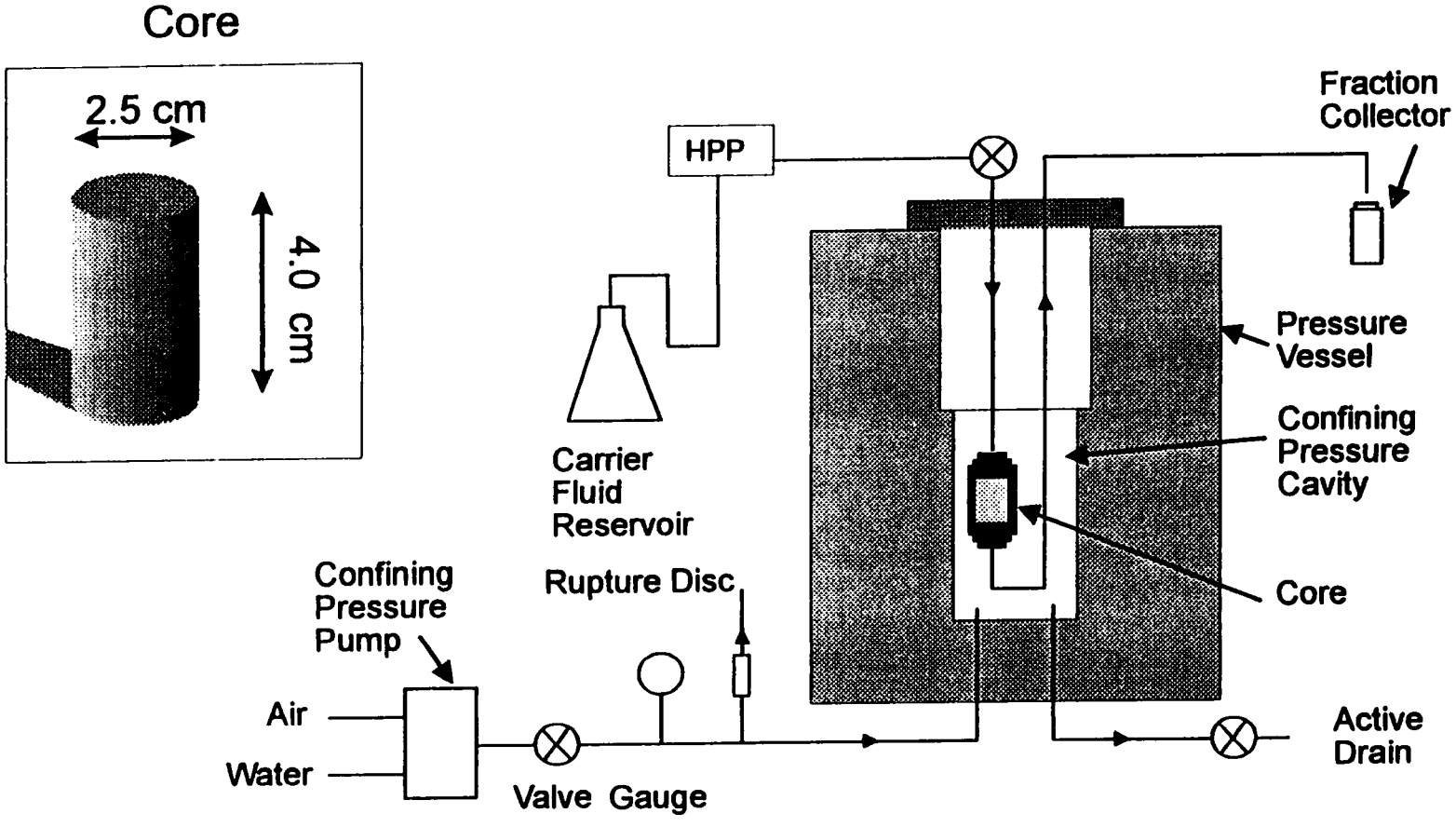
Core
2.5 cm
4.0 cm
HPP
Fraction Collector
Pressure Vessel
Confining Pressure Cavity
Core
Carrier Fluid Reservoir
Confining Pressure Pump
Rupture Disc
Air
Water
Valve
Gauge
Active Drain

To prevent the rupture of the epoxy jacket due to the pressure of the carrier fluid, the prepared core is placed in an autoclave (Fig. 3.1). Due to the small size of the pressure cavity in the autoclave, the length of the sample core is limited to no greater than 4 cm. The pressure cavity is filled with distilled water and pressurized using an ISCO LC-5000 high-pressure syringe pump. For the epoxy jacket not to rupture the confining pressure in the autoclave must be maintained at a higher pressure than that of the carrier fluid. The target pressure for the carrier fluid was 1.5 Mpa, but this was often difficult to maintain and the pressure often increased several Mpa for the less permeable whole rock cores.

3.2 Pore Salt Extraction Experiment - Results.

Between ½ ml and 11 ml of eluant was collected from each sample and was analysed for $^{87}Sr/^{86}Sr$. Although the grey granite samples allowed for the flow of the transport fluid through the 4 cm cores, the granodiorite and in particular the altered pink granite samples, were less permeable than the granite samples. The lengths of the cores were reduced, but even with the size reduction, some samples remained impermeable. Pink granite's low permeability is probably due to its high clay content.

Sr isotopic values were determined for eluant from granodiorite, grey granite and altered pink granite (Table 3.1). Eluant from the granodiorite sample and four of the grey granite samples have high $^{87}Sr/^{86}Sr$ between 0.75964 - 0.78110. The exception is sample MB2-22, which is less radiogenic having $^{87}Sr/^{86}Sr$ = 0.72110. There is no mineralogical difference between sample MB2-22, a grey granite, and the other grey granite samples used in the PSE experiment, however, it should be noted that MB2-22 was sampled immediately adjacent to a narrow fracture in zone 2 of borehole 403-014-MB2, while the other granite and granodiorite cores were sampled from unfractured rock. The low Sr ratio of MB2-22 eluant is in contrast to the pore fluids sampled from zone 2 in the Borehole Leaching Test. This discrepancy between isotopic values may indicate contamination of the MB2-22 eluant during the extraction process. Altered pink granite cores HC11-31 and HC29-17A were

sampled adjacent to Fracture Zone 2. The eluant from these cores also exhibit low $^{87}Sr/^{86}Sr$ values.

Sample	$^{87}Sr/^{86}Sr$	Std Err. (2σ)	Core Lithology
GC2-10APF	0.78110	0.000023	granodiorite
MB21APF	0.78088	0.000016	grey granite
GC2-36BPF	0.77694	0.000031	grey granite
403-A1PF	0.77503	0.000024	grey granite
401-1PF	0.75964	0.000250	grey granite
MB2-22PF	0.72110	0.000160	grey granite
HC11-31PF	0.72314	0.000300	altered pink granite
HC29-17APF	0.72225	0.000290	altered pink granite

Table 3.1. Sr isotopic composition of eluant extracted from whole rock cores in the Pore Salt Extraction Experiment.

CHAPTER FOUR
STRONTIUM GEOCHEMISTRY IN THE LAC DU BONNET BATHOLITH - DISCUSSION

Among geochemical tracers, strontium isotopes are good indicators of both water-rock interaction, and sources of Sr. Because of the similar geochemical behaviour of Sr and Ca, Sr isotopes may also be used to trace the source of Ca. An additional advantage is the absence of measurable isotopic fractionation during dissolution or precipitation. Strontium isotopes are therefore particularly well suited for investigating the deep Ca-dominated brines in the Canadian shield and have been used in identifying sources of Sr and Ca in groundwaters associated with crystalline rocks. (McNutt, 1987; Frape et al. 1984; Franklyn et al., 1991; Li, 1989; Li et al. 1989). In studies involving the interaction between groundwater and a plagioclase-bearing host rock, the dissolution of plagioclase was shown to be the main control on Sr isotopic composition of the groundwater. This empirical evidence for plagioclase's control, is also supported by geochemical modelling of water-rock interaction using thermodynamic and chemical principles (Madé, 1991).

When a groundwater-rock system is far from equilibrium, that is to say, the groundwater is highly undersaturated with regard to the primary minerals composing the rock, the groundwater isotopic composition is governed by the amount of Sr that each mineral phase can contribute to solution and the mineral's isotopic composition. The amount depends on the mineral's dissolution rate, Sr concentration, and modal abundance. In most granites, the feldspars are the main sources of Sr. Experimentally derived dissolution rates indicate that plagioclase's (Ab_{100}) rate is double that of K-feldspar (Lasaga et al.,1994) and two orders of magnitude faster than biotite (Ackar and Bricker, 1992). Calcium-rich plagioclase rate of dissolution is even greater than that of its Na-rich end member. Therefore, plagioclase's relatively high dissolution rate, modal abundance, and typically high Sr concentration insures that a large portion of Sr in solution is contributed by plagioclase.

Furthermore, it is probable that the solution will maintain its plagioclase affinity as the system progresses towards chemical equilibrium. As the chemical constituents build up in the water, the reaction path and the attainment of equilibrium between primary minerals and alteration products will become a factor in the solution's isotopic composition. For groundwater infiltrating granite, K-feldspar will likely be the first primary mineral phase to reach equilibrium with the alteration product kaolinite (Madé, 1991). This would prevent K-feldspar from contributing significant amounts of Sr to solution, thus allowing plagioclase, and to a lesser extent biotite, continued control over the solution's isotopic composition. In addition, the precipitation of $CaCO_3$ from a solution with high P_{CO2} will ensure the continuing dissolution of plagioclase.

Contrary to what has just been stated, plagioclase may not always control the isotopic composition of the solution. McNutt (1987) has suggested that Sudbury mine waters have reached chemical and isotopic equilibrium with their host rock based on the apparent similarity in $^{87}Sr/^{86}Sr$ of the mine waters and the associated norite. Unfortunately, the small difference in isotopic composition between plagioclase $^{87}Sr/^{86}Sr$ and whole rock makes this interpretation inconclusive. However, it will be shown that certain groundwater samples, BLT and PSE waters collected from the Lac du Bonnet Batholith also exhibit whole rock $^{87}Sr/^{86}Sr$, and due to the large difference in the isotopic compositions of the mineral phases, a stronger case can be that made that certain fluids from the batholith have obtained the Sr isotopic signature of the host granite.

4.1 Major Cation Chemistry

Despite their wide range of salinities, fracture waters can be grouped separately from the pore fluids according to their elemental proportions and their strontium isotopic composition (Fig 2.3 to Fig 2.7). One of the most distinguishing characteristics of the pore fluids is their very high Ca/Sr relative to the fracture waters. This may indicate that the Ca-Sr

budgets are controlled by two distinct processes.

Plagioclase dissolution has been shown to govern the Ca/Sr ratio in geothermal waters (Michaud, 1990) and in groundwater of a sandy silicate aquifer (Bullen et al. , 1996). A simple calculation can be made to see whether dissolution of plagioclase also controls the Ca/Sr in the fracture waters in the Lac du Bonnet Batholith. Using plagioclase strontium data collected in this study and from Li (1989), the average Sr concentration in plagioclase is 277 ppm. The specific range of plagioclase compositions is not known, but it has been identified as oligoclase (McCrank, 1985). Oligoclase has a compositional range Ab_{90} -Ab_{70}, therefore, the Ca/Sr molar ratio of the plagioclase of the Lac du Bonnet batholith is within the range 120 to 360 , which is similar to the distribution of Ca/Sr molar ratios of the fracture waters (Figure 4.1).

With such an obvious control of Ca and Sr by plagioclase in the fracture waters, interpreting the Sr depletion in the pore fluids is difficult. The pore fluids probably represent chemical conditions where Sr and Ca are no longer controlled by the dissolution of plagioclase, but are instead, governed by other water-rock reactions.

The precipitation of Ca and Sr-bearing minerals such as calcite, gypsum, and Ca-bearing clays may influence the Ca/Sr in solution if the partitioning of the two elements between fluid and solid are far from unity. Calcite is probably the most important sink for Ca and Sr. It is an abundant fracture-filling mineral in the Lac du Bonnet Batholith and many shallow groundwaters are strongly supersaturated with respect to calcite (Gascoyne et al., 1987). It is difficult to estimate the partition coefficient of Sr into calcite due to its dependency on temperature, reaction rate, and solution and solid composition (Morse and Bender, 1990). The partition coefficient, D_{Sr}, is defined as

$$D_{Sr} = \frac{(M_{Sr}/M_{Ca})_C}{(M_{Sr}/M_{Ca})_L} \qquad equ.\ 4.1$$

Figure 4.1. Ca/Sr versus $^{87}Sr/^{86}Sr$ plot. Shaded rectangle is possible range of the Ca/Sr molar ratio and isotopic composition of plagioclase in the Lac du Bonnet Batholith. Most fracture waters (□) plot near to the plagioclase compositional range, while pore fluids (■) exhibit a positive correlation between isotopic composition and molar ratios. The BLT waters are sampled water from all six zones in the Borehole Leaching Test Experiment. (Compilation of this study and Li, 1989)

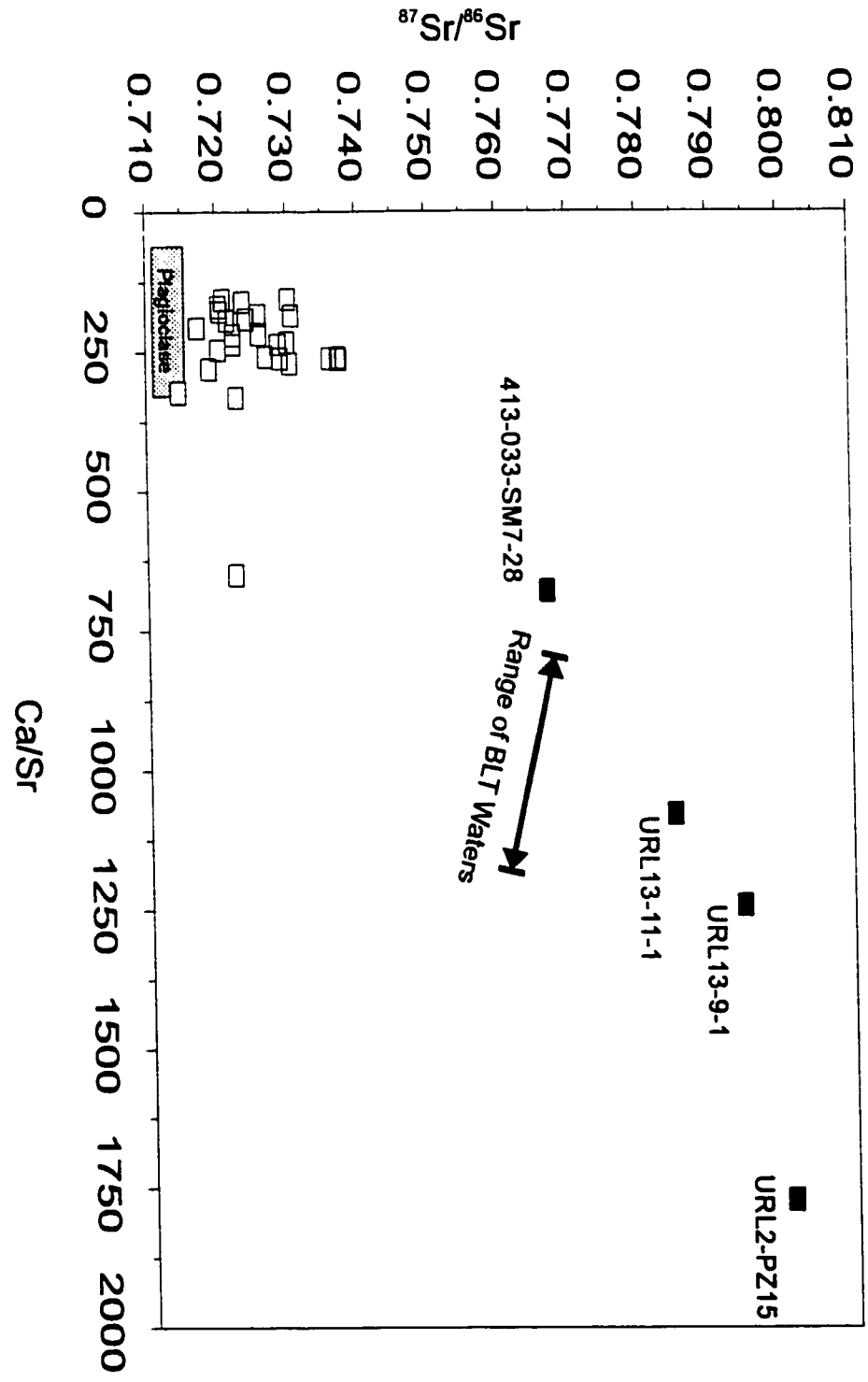
$^{87}Sr/^{86}Sr$
0.810
0.800
0.790
0.780
0.770
0.760
0.750
0.740
0.730
0.720
0.710
0
250
500
750
1000
1250
1500
1750
2000
Ca/Sr
URL2-PZ15
URL13-9-1
URL13-11-1
413-033-SM7-28
Range of BLT Waters
Plagioclase

where $(M_{Sr}/M_{Ca})_C$ is the molar ratio in calcite and $(M_{Sr}/M_{Ca})_L$ is the molar ratio in solution. Experimental studies on Sr-partitioning under various conditions indicate that partition coefficient does not exceed 0.25 (Mucci and Morse, 1983; Lorens, 1981; Pingitore and Eastman, 1986; Katz et al., 1972). With a partition coefficient less than 1, precipitation of large amounts of calcite would result in the enrichment of Sr relative to Ca in the water phase. Enrichment of Sr is opposite to what is seen in the pore fluids, therefore, calcite precipitation is not the cause of the higher Ca/Sr ratios in the pore fluids relative to the fracture waters. Alternately, gypsum is supersaturated in the deeper waters of the LDB batholith and is a possible sink for Ca and Sr. However, the occurrences of gypsum as a secondary mineral is rare, and similar to calcite, the Sr partition coefficient of gypsum is estimated to be << 1 (Ichikimi and Musha, 1978). Clays are not considered important in controlling the Ca content in the LDB Batholith (Gascoyne et al. 1987). Consequently, an alternative Sr sink to the more obvious secondary minerals must be considered.

Garrels (1967) noted that when water reacts with crystalline rocks during weathering, it develops a Na/Ca molar ratio with about the same value as that of the plagioclase feldspars in the rock. In the Lac du Bonnet Batholith, the fracture waters' average Na/Ca molar ratio (5.6) is not identical to the ratio expected by the dissolution of a plagioclase with an oligoclase composition (Na/Ca molar ratio of 4), however, the Na abundance is still greater than Ca in solution and is what would be expected for the dissolution of a Na - rich plagioclase such as oligoclase. In contrast, the pore fluids are characterized by low Na/Ca molar ratios (0.5). Sodium depletion is a feature of the Canadian shield mine waters and has been attributed to the albitization as a result of low temperature water-rock interaction (Pearson, 1987; Davisson and Criss, 1996). Secondary albite may also incorporate Sr and Ca into its structure and the formation of significant amounts of secondary albite may alter the proportions of Na, Ca and Sr in solution. Extensive albitization will obviously lower the concentration of Na in solution, but no information on how Ca and Sr are partitioned into albite at low temperatures is available. However, Lagache and Dujon

(1987) did investigate the partitioning of strontium between plagioclase of various compositions in a one molar aqueous chloride solution at 600 °C and at 1.5 Kbar pressure. They found that the degree of partitioning of Sr into the plagioclase was dependent on the composition of the plagioclase, where Sr is incorporated into the albite end member to a greater extent than in anorthite. Furthermore, Sr enters more easily into plagioclase with albite components greater than 0.6, than does Ca despite strontium's larger ionic radius. The greatest preferential partition of strontium into the solid phase relative to calcium is in the albitic plagioclase, where the Sr partition coefficient is 1.5 times higher than for Ca. At these high pressures and temperatures, mineralogic control on the partitioning of Sr and Ca is more important than temperature or pressure on partitioning (Blundy and Wood, 1991). It is uncertain, however, whether plagioclase composition remains the primary control on partitioning at the low temperatures presently found in the Lac du Bonnet batholith. If Sr is preferentially incorporated into albite relative to Ca then, albitization or recrystallization of preexisting plagioclase may increase the Ca/Sr and Ca/Na in solution.

4.2 Sr Isotopes

Most fracture waters in the Lac du Bonnet Batholith have $^{87}Sr/^{86}Sr$ ranging from a low value of 0.713 for shallow and typically dilute waters, to 0.738 in the deeper more saline groundwaters (Li, 1989). In contrast, the pore fluids are more radiogenic with values between 0.761 and 0.809 and are the highest $^{87}Sr/^{86}Sr$ values determined so far, in the Lac du Bonnet Batholith groundwaters. The control on the $^{87}Sr/^{86}Sr$ of fracture waters by plagioclase as suggested by Li (1989), is evident in the similarity of their $^{87}Sr/^{86}Sr$ and Ca/Sr ratios (Fig. 4.1). However, four samples from sparsely fractured and unfractured rock fall within the range of whole rock values, and can be grouped separately from other fracture waters (Fig. 4.2). As well, most of the pore fluid samples (ie. the BLT waters and the PSE waters) fall within the range of whole rock values. This would suggest that the pore fluids

have reached isotopic equilibrium with the whole rock; or alternately, biotite has contributed a larger proportion of Sr to solution. A larger biotite contribution is a distinct possibility. Although biotite is a minor constituent in granite and granodiorite and Sr occurs in low concentrations in biotite, the $^{87}Sr/^{86}Sr$ in biotite is very high and only a small amount of biotite derived ^{87}Sr is required to greatly affect the isotopic composition of the solution. If plagioclase is indeed stable in the pore fluids as evidenced by the low Na/Ca molar ratios in the pore fluids, then biotite may be the only mineral continuing to dissolve. For example, an estimate of the amount of dissolved biotite that is needed to be dissolved for pore fluid sample URL2-PZ15 to obtain its present day $^{87}Sr/^{86}Sr$ of 0.809 can be calculated. If the solution, prior to plagioclase becoming stable, had an $^{87}Sr/^{86}Sr$ value of 0.718, then 2.6% of Sr presently in solution was contributed by biotite (assuming an average biotite isotopic composition of 4.2). Sample URL2-PZ15 has a Sr concentration of 6 mg/L, therefore, 0.156 mg of Sr has been contributed by biotite per litre of pore fluid. This requires the dissolution of 421 g of biotite. Although, this may appear to be an unreasonably large amount of dissolved biotite, it is small compared to the amount of biotite in contact with 1 L of fluid in the pore network. One litre of fluid will be contained in approximately 0.3 m^3 of granite having a porosity of 0.3%. Assuming that 5% of the rock is biotite, 50,000 g of biotite can potentially contribute Sr to one litre of pore fluid. Only, 0.8% is required to dissolve (421g/50000g) for pore fluid URL2-PZ15 to acquire an isotopic composition of 0.809.

The extremely close correlation between PSE waters and whole rock is, however, strong evidence that fluids found in intergranular cavities are in isotopic equilibrium with their host rocks. In Fig. 4.2, solid lines connect grey granite and granodiorite samples with their associated pore fluids extracted in the PSE experiment. There is a good correlation between whole rock $^{87}Sr/^{86}Sr$ and the rocks associated intergranular pore fluids. One PSE water derived from grey granite (MB2-22) has an isotopic signature closer to the PSE waters derived from altered pink granite than from the grey granite from which it is derived. This low value may indicate contamination of the sample, alternatively, the value may represent the true

Figure 4.2. Compilation of $^{87}Sr/^{86}Sr$ analyses of groundwater, pore fluids/salts, minerals and whole rock. Open squares (□) are fracture waters, filled squares (■) are pore fluids taken from sparsely fractured and unfractured rock, Open circles (O) are PSE waters sampled from altered pink granite, filled circles (●) are PSE waters sampled from grey granite, open triangles (▽) are whole rock grey granite, and filled triangles(▼) are whole rock granodiorite. Plagioclase and fracture water values are compilations of data from this study and Li (1989).

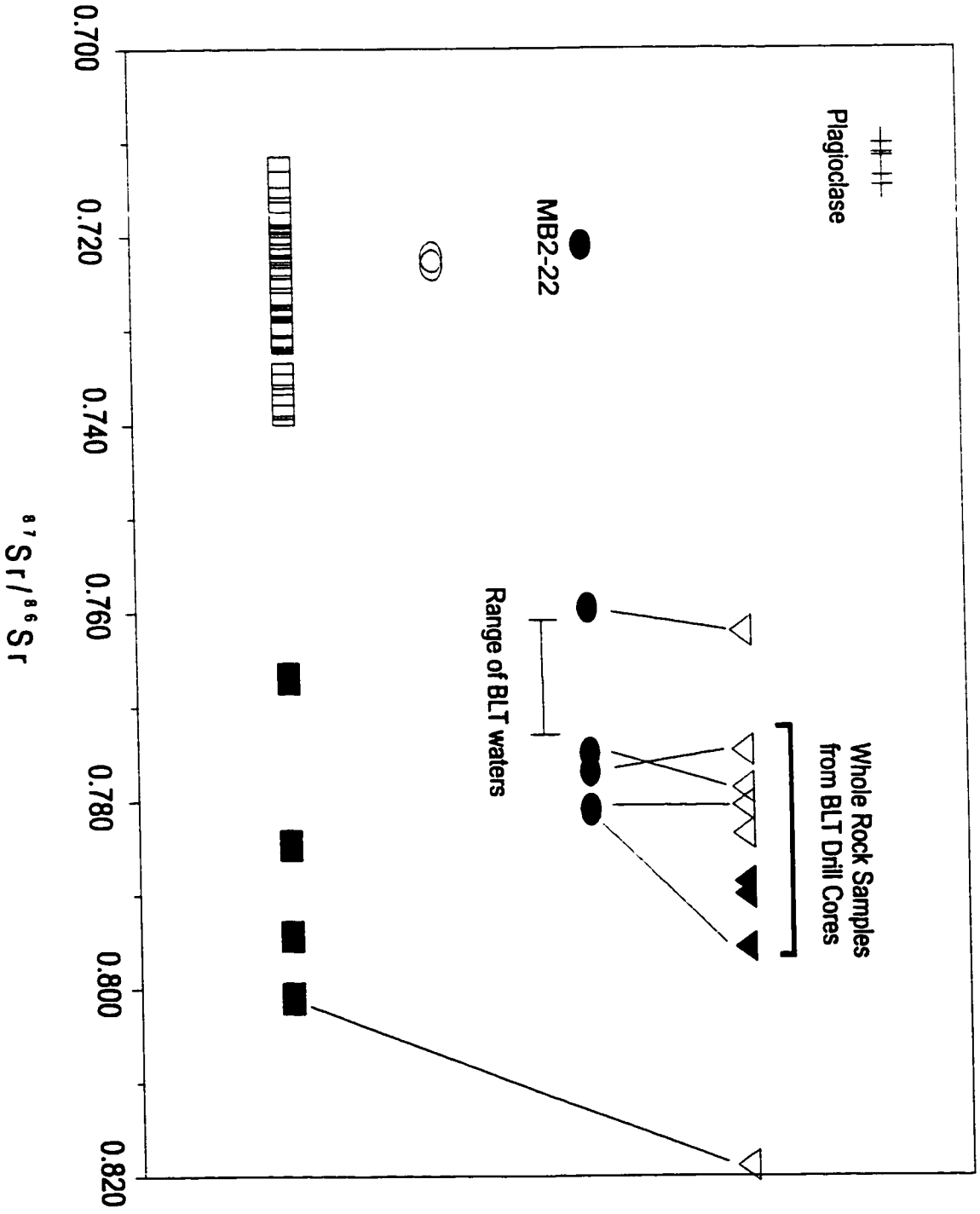
Plagioclase
MB2-22
Range of BLT waters
Whole Rock Samples
from BLT Drill Cores
0.700
0.720
0.740
0.760
0.780
0.800
0.820
$^{87}Sr/^{86}Sr$

isotopic composition of the intergranular salts from MB2-22. The grey granite sample was extracted adjacent to a narrow fracture and, in this respect, it is unique compared to the other fresh grey granite and granodiorite samples. The Borehole Leaching Test water sampled from MB2-Zone 2, however, exhibits an high $^{87}Sr/^{86}Sr$ ratio compared to the MB2-22 eluant. This may indicate that contamination of the MB2-22 eluant during the extraction process is the reason for the low $^{87}Sr/^{86}Sr$ in the eluant.

A good correlation would also be expected between the BLT sampled water and their associated granite and granodiorite whole rock values as well, but isotopic values in solution are approximately 1% lower than the surrounding granite. This difference may be an artifact of the sampling technique. Removal of salts by forcing distilled water through unfractured cores has the advantage that salts can be quickly extracted from a small known volume of rock, thus allowing for comparisons between the extracted salts and the granite in which they are in direct contact. In contrast, the BLT waters' salinity is derived from a much larger volume of rock and in this respect, the $^{87}Sr/^{86}Sr$ measured can be considered an average of all pore fluids immediately surrounding the borehole. This does not however, effectively explain the consistently lower isotopic ratios found in the leach hole experiment.

In all zones there is a measurable decrease in the solution's $^{87}Sr/^{86}Sr$ with time. Sampling techniques for the Borehole Leaching experiment requires that distilled water is initially introduced into each borehole and that water removed for sampling must be replaced by an equivalent amount of distilled water. Due to the BLT waters being far from equilibrium with respect to the minerals within the granite, dissolution will occur around the perimeter of the borehole and so contribute to the chemical composition of the solution. Furthermore, this dissolution may be enhanced by the process of drilling the boreholes by producing fine grains of crushed rock . These grains would increase the mineral surface area within the boreholes resulting in an increase in the dissolution rate. The $^{87}Sr/^{86}Sr$ of the BLT waters are therefore a mixture of several Sr sources entering into solution. The slow $^{87}Sr/^{86}Sr$ decrease may indicate that ^{87}Sr enriched K-feldspar may have quickly reached equilibrium in

the solution early in the experiment and stopped dissolving. It is probable that $^{87}Sr/^{86}Sr$ in all six zones may level off and eventually rise as plagioclase approaches equilibrium. This may already be occurring in MB2-1 and GC1-1, where $^{87}Sr/^{86}Sr$ has been increasing slightly over the last 200 days of the experiment.

The proportion of Sr contributed by leaching pore fluids and from the dissolution of minerals from the perimeter of the borehole, can be determined if the $^{87}Sr/^{86}Sr$ values are known for the pore fluid and the rock derived Sr. The proportion of Sr contributed by leaching pore fluids (P_p) is given by:

$$P_p = (R_m - R_r) / (R_p - R_r) \qquad equ.\ 4.2$$

where R_m is the ratio measured in the Borehole Leaching test waters, R_r is the Sr ratio contributed from the alteration of plagioclase, and R_p is the ratio found in the pore fluids. The R_r and R_p are not known but can be estimated. The flush waters suggest that pore fluids will have a whole rock ratio, therefore whole rock data obtained from analyses of cores should give a close approximation of the isotopic signature of pore fluids surrounding each zone. MB2-1 is composed of 80% grey granite and 20% granodiorite having $^{87}Sr/^{86}Sr$ values of 0.780 and 0.788, respectively. Weighting these values accordingly gives an average of 0.782. The isotopic ratio of Sr contributed by plagioclase is 0.712. Taking an average of 0.7665 for the solution in MB2-1 a P_p of 0.758 is calculated. This means that approximately 75% of the Sr in MB2-1 is attributable to the seepage of rock matrix fluids, the remainder being introduced by mineral dissolution over the duration of the experiment. This mixing between two Sr sources may also explain the lower Ca/Sr value found in the Leach test waters compared with the ^{87}Sr-enriched groundwaters URL2-PZ15, URL13-9-1, URL13-11-1 (Fig. 2.8). The dissolution of minerals in the granite and granodiorite (mainly plagioclase with it's lower Ca/Sr) would lower the value in the solution.

Evidence from the BLT experiment and from the flush experiment strongly supports

the model that fluids found in intergranular cavities have reached isotopic equilibrium with the host rocks. It has been suggested that once groundwater reaches chemical equilibrium with the country rock then it should have the same $^{87}Sr/^{86}Sr$ value as the host rock (McNutt, 1987). This assumption may not necessarily be correct. In contrast to the ion composition of a solution at chemical equilibrium which is independent of the reaction path of the system, the $^{87}Sr/^{86}Sr$ ratio of a solution that has reached chemical equilibrium is dependent on the reaction path. For a solution to have a whole rock signature at chemical equilibrium, the amount of each mineral dissolved must be in proportion to it's modal abundance within the rock. Considering that the modal abundance of the minerals is only one of several factors determining the amount of Sr each mineral contributes to solution, it is improbable that the isotopic composition of the solution would reflect modal dissolution. This reasoning argues against a contemporaneous attainment of a whole rock isotopic composition of a solution and its chemical equilibrium. Therefore, it would appear that at low temperatures, when a groundwater reaches chemical equilibrium with the host rock, it does not *necessarily* have a whole rock isotopic signature.

If it is improbable that a solution will attain a whole rock isotopic composition as it approaches chemical equilibrium, then exchange of Sr between rock and solution must be occur after chemical equilibrium has been reached. This implies that Sr in these fluids "freely" exchanges with the bulk. For this to occur, rapid volumetric diffusion of Sr to and from the grains interior is necessary and requires high temperature to facilitate such volumetric diffusion. At low temperatures, solid state diffusion is an extremely slow process, making it impossible for complete exchange between Sr in minerals and solution. There arises then a contradiction in the fracture water's apparent low temperature isotopic equilibrium and extremely low diffusion rates. This contradiction can be eliminated if it is assumed that thermodynamic isotopic equilibrium between mineral surfaces and solution is sufficient to impart a whole rock isotope signature to the solution. A mass balance calculation can be used to determine the feasibility of this model.

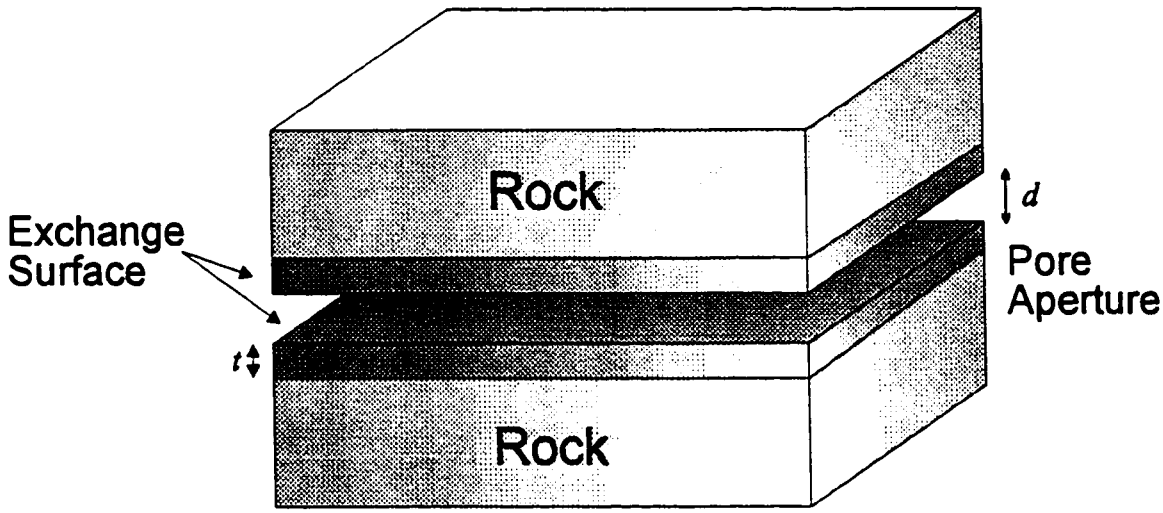

Figure 4.3. The wetted surface area can be calculated using a simple planar geometry for a fracture. The area is inversely portional to the pore diameter (*d*). The exchange surface has thickness *t* and is defined as the mineral layer at the mineral - solution interface where rapid exchange of ions occurs.

If Sr exchange between mineral and solution is relegated to surface reactions, then to a first approximation, the amount of Sr that each mineral can contribute is fixed by its surface area in contact with the solution and the Sr concentration in the mineral surface. If a fluid is introduced into an intergranular cavity and reaches chemical equilibrium, given a sufficient amount of time, the $^{87}Sr/^{86}Sr$ in solution (R_s) will be a result of complete exchange of Sr on the wetted surface of the minerals and the Sr in the initial solution. This can be expressed as,

$$R_s = \sum P_i R_i \qquad equ.\ 4.3$$

where R_i is the ratio of a mineral or the ratio of Sr in the solution first introduced into the pore cavity, and P_i is the proportion of total Sr in the system that is contributed by phase I. P_i is a function of the mineral surface area in contact with solution and the amount of Sr in the surface layer. In turn, the wetted surface area is a function of water volume and pore diameter. For simplicity a planar geometry is used to relate water volume to the wetted surface area (Fig. 4.3). The relationship between wetted surface area and pore diameter is given by the following equation,

$$A = \frac{2V}{d} \qquad equ.\ 4.4$$

where A is the surface area of a mineral in contact with the solution, V is the volume of solution, and d is the pore diameter. When groundwater is present in pores that are only a fraction of a micron in diameter, this area can be extremely large. For example, if 0.001 m^3 (1 Kg) of water is situated in a contiguous pore network having an average pore diameter of 1 μ, it would be in contact with a surface area equalling 1000 m^2.

Finally, the exchange surface and the amount of Sr in the exchange surface must be defined. The exchange surface is defined as the interface where direct and rapid exchange of

ions occurs between solution and mineral at equilibrium. Although no research has been done on determining the thickness of the exchange surface or layer at chemical equilibrium, an estimate may be obtained by using data collected on the dissolution of feldspars far from equilibrium. It has been postulated that the initial step in the hydration of feldspars involves the formation of a surface layer of hydrated feldspar by exchange of proton-bearing species for alkali cation (Helgeson et al., 1984) According to the surface reaction hypothesis, ions within the feldspar that are next to neighbours of the solution-mineral interface are exchanged for hydrogen ions. The thickness of the alkali-free layer would not be expected to exceed the distance between successive planes containing alkali ions, about 7 Å (Petrović et al., 1976). There have been several attempts to detect and measure the thickness of this layer. Eggelston et al. (1988) detected layers ranging in thickness from 30 to 90 Å on albite surfaces after hydrothermal dissolution under different pH conditions. Similar studies failed to show leached layers within the detection limits of the methods used. If present, these layers were less than 30Å in thickness (Petrović et al., 1978; Yang and Kilpatrick, 1989). Therefore, rapid ion exchange probably occurs at the first and possibly the second molecular layer (i.e 7Å - 23Å)under most natural conditions.

Knowing the exchange surface thickness (t), the amount of Sr in a particular mineral phase (Sr_i) can be determined by the equation,

$$Sr_i = C_i\ A\ t\ \rho_i\ m_i \qquad equ.\ 4.5$$

where C_i is the concentration of Sr in mineral i, t_i is the thickness of the surface layer and ρ_i is the density of the mineral, and m_i is the modal % of the mineral. The relationship between Sr_i and pore diameter is found by substituting for A from equation 4.4 into equation 4.55.

$$_i = \frac{2\ C_i\ m_i\ V\ t\ \rho_i}{d} \qquad equ.\ 4.$$

P_i is then found by substituting equation 4.6 into the following.

$$P_i = \frac{Sr_i}{(Sr_1 + Sr_2 + \ldots)} \qquad equ.\ 4.7$$

Once the proportions (P_i) that each mineral contributes is calculated, and knowing the isotopic composition (R_i) of the phases, the isotopic composition of a solution that has reached chemical and isotopic composition can be determined. What must also be considered is the amount and isotopic composition of Sr in solution as the system reaches chemical equilibrium. One possible scenario for the isotopic evolution of Sr in the pore fluid involves the infiltration of dilute meteoric water with little Sr, into the intergranular cavities of a granite. Initially the solution will be far from equilibrium and the Sr in solution will be derived from the dissolution of minerals, again mainly plagioclase. In this respect, these hypothetical pore fluids are analogous to the fracture water and will have a low $^{87}Sr/^{86}Sr$. The initial amount of Sr in solution and its isotopic composition at the establishment of chemical equilibrium may be important factor determining whether the pore fluid achieves a whole rock isotope signature. If the initial amount of Sr in solution far exceeds the amount of Sr available for exchange in the mineral surface layer, the solution will *not* reflect the whole rocks isotopic composition.

This dependency on the amount of Sr available for exchange on the minerals surface and the Sr concentration in the fluid may limit isotopic equilibrium to environments with very high A/V ratios and pore fluids with low Sr concentrations. Figure 4.4 illustrates the relationship between pore diameter and the maximum $^{87}Sr/^{86}Sr$ attainable in solution (ie. R_s in equation 3). The parameters of the model are chosen in accordance to the evolution of the

hypothetical pore fluid model described above. The modal abundances, Sr concentrations and isotopic composition of the minerals are averages calculated from compiled mineral data. The initial Sr concentration and $^{87}Sr/^{86}Sr$ in solution is based on data from shallow fracture waters and are 6 mg/L and 0.720, respectively. It is apparent from figure 4.4, that a pore aperture of 0.01μ or less is necessary for the solution to obtain a whole rock value, if the exchange layer thickness of between 7 - 25 Å is assumed. In the Lac du Bonnet Batholith the diameter for natural microcracks are less than 4 μ with a geometric mean of 0.01 μ (Chernis and Robertson, 1987). In unfractured rock, 0.01 μ could be considered an upper estimate on the average pore diameter. The actual surface area has been assumed to be perfectly smooth, which is an over simplification of a natural system. Mineral surface microtopography is variable with kinks, and steps of variable height (Hochella, 1990) and will increase the surface area. In addition, dislocations can act as narrow conduits for the exchange of Sr, further increasing the surface area in contact with the solution. Exchange between solution and mineral surfaces is therefore, a plausible mechanism for attainment of isotopic equilibrium between pore fluids and host rock.

4.3 Mixing of Fracture Waters and Rock Matrix Salts.

With the discovery of very saline pore fluids in the LDB, it is probable that a portion of the dissolved load in the fracture waters is attributable to diffusion of salts from the rock matrix. The total volume of intergranular fluid could be substantial; with an average effective porosity of 0.36% (Katsube and Hume, 1987), 1 m^3 of granite may contain as much as 3.6 L of saline water. It has been suggested that rock matrix salts do contribute significantly to the salinity of the fracture waters in the Lac du Bonnet batholith (Gascoyne et al 1989b).

If there is mixing between pore fluids and groundwater, it should be evident in ^{87}Sr - enrichment in the fracture zone waters. The $^{87}Sr/^{86}Sr$ ratios measured in the fracture waters do increase in conjunction with Sr and Cl concentration. Li (1989) proposed that the isotopic

Figure 4.4 Graph showing the relationship of R_s (the Sr isotopic ratio in solution after complete exchange of Sr has occurred between solution and exchange surface) and intergranular pore diameter. Parameters for model are given in upper left box. Curves represent the value R_s in a contiguous network system having an average pore diameter (d) for different thicknesses (t) of the mineral exchange surface. If the exchange surface thickness is 7 Å, then a fluid must be situated in a pore network having an average diameter > 0.01 μ . If the exchange surface thickness is greater, then fluids may obtain a whole rock value at pore diameters > 0.01 μ.

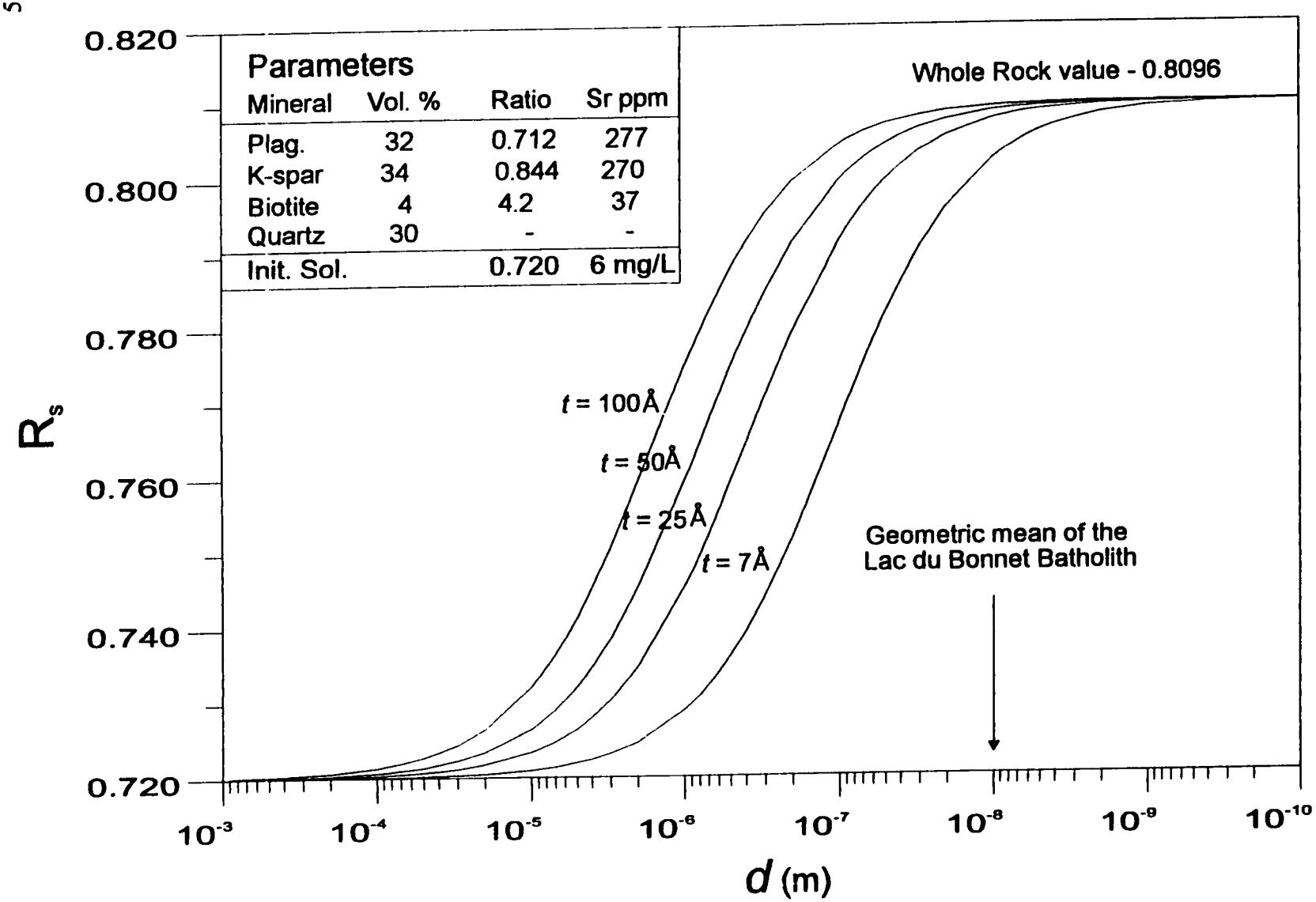
Parameters
Mineral Vol. % Ratio Sr ppm
Plag. 32 0.712 277
K-spar 34 0.844 270
Biotite 4 4.2 37
Quartz 30 - -
Init. Sol. 0.720 6 mg/L
Whole Rock value - 0.8096
t = 100Å
t = 50Å
t = 25Å
t = 7Å
Geometric mean of the Lac du Bonnet Batholith
R_s
0.820
0.800
0.780
0.760
0.740
0.720
10^-3 10^-4 10^-5 10^-6 10^-7 10^-8 10^-9 10^-10
d (m)

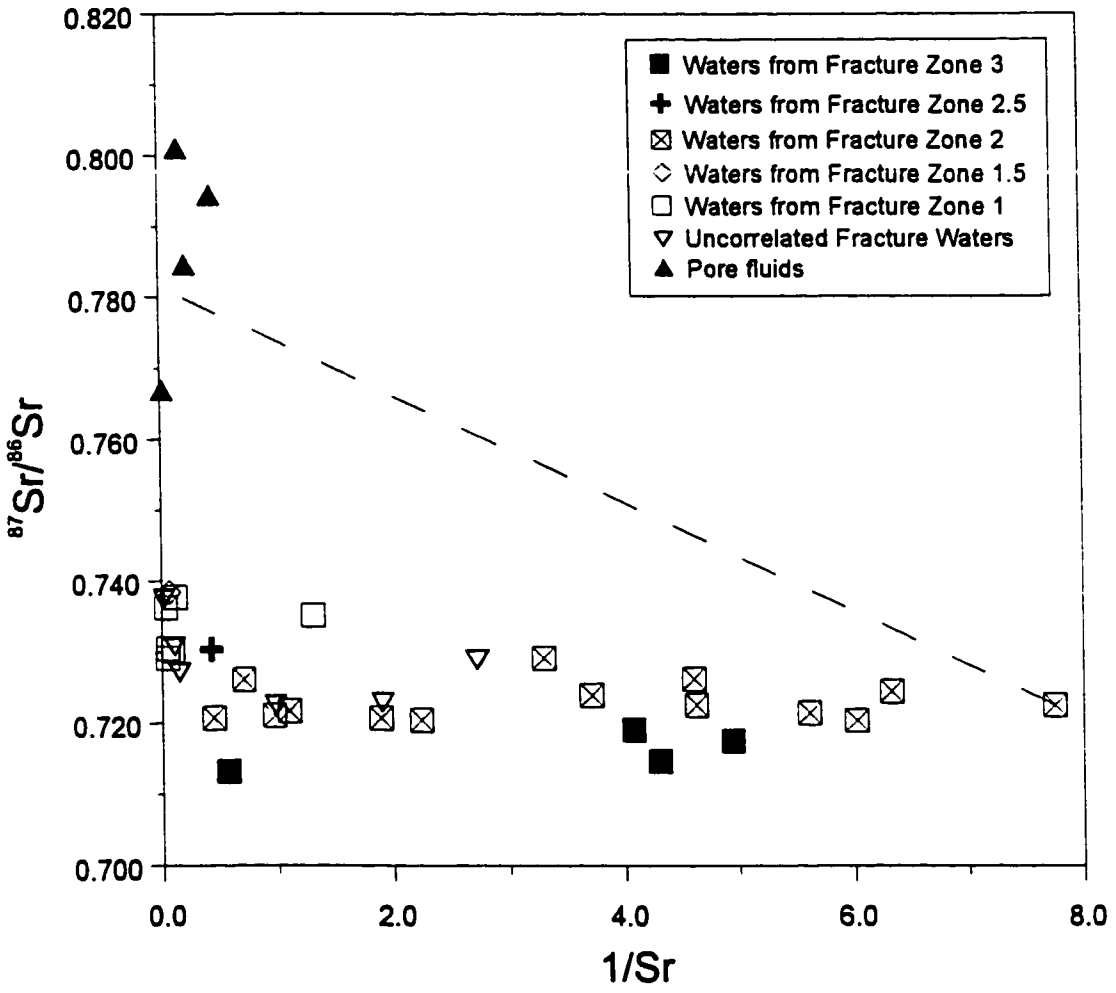

Figure 4.5. Mixing plot of groundwaters from the Lac du Bonnet Batholith.Dashed line represents possible mixing trend between a dilute shallow water end-member and a pore fluid end-member. Uncorrelated fracture waters are groundwaters taken from fractures that are not correlated with any of the 3 main or intermediate fracture zones. Compilation of data from this study and Li (1989).

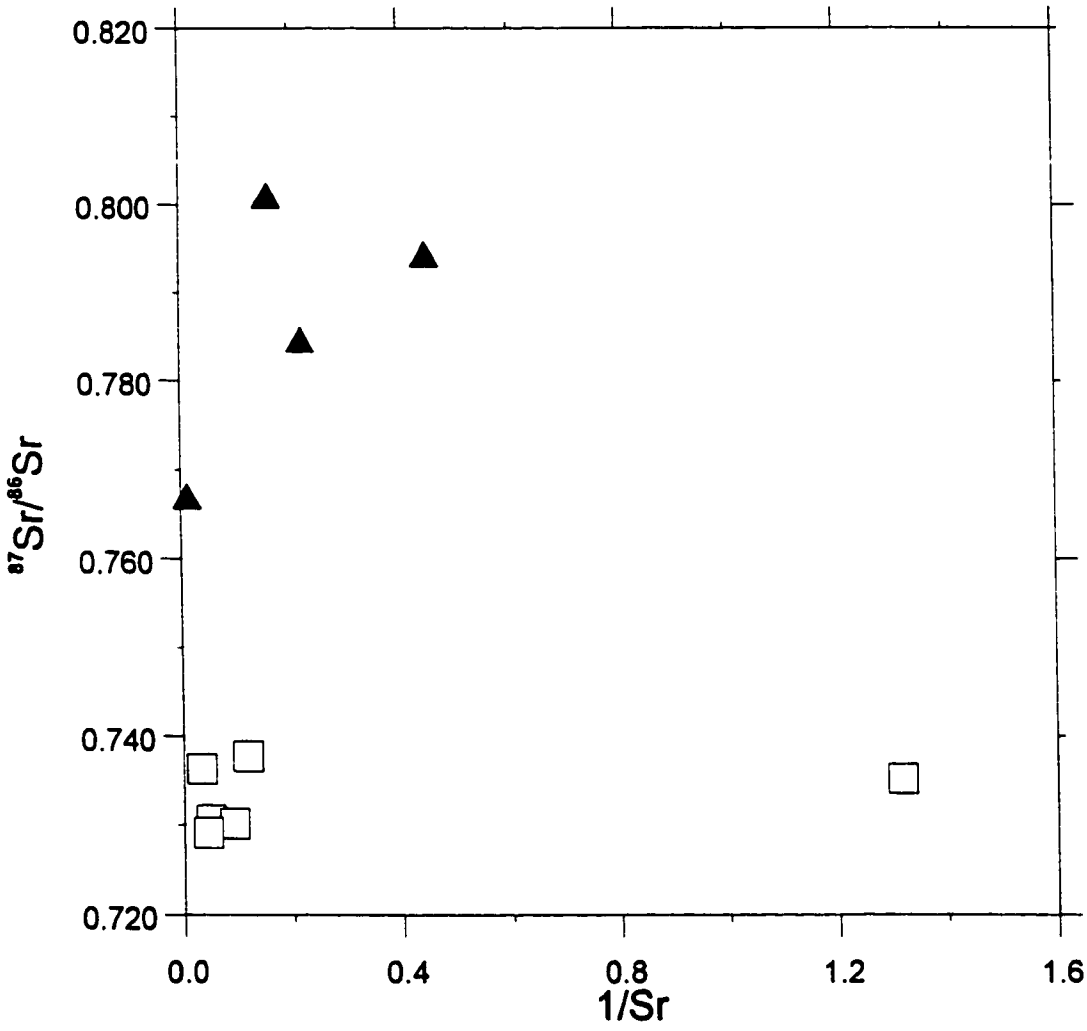

Figure 4.6. Mixing plot of Fracture Zone 1 water and pore fluids. Fracture Zone 1 water exhibits the highest $^{87}Sr/^{86}Sr$ values compared to groundwaters from the other two fracture zones. This may indicate that Fracture Zone 1 water has a greater component of pore fluid derived Sr. The distribution of data points, however, does not indicate an obvious mixing trend. Symbols are the same as those in Fig. 4.5.

signature of the shallow waters in the LDB was due to rapid dissolution of plagioclase, while the higher $^{87}Sr/^{86}Sr$ of the deeper waters, indicated a greater Sr contribution by the slower dissolving K-feldspar. However, the attainment of partial equilibrium between rock and solution was not considered. K-feldspar can only contribute a larger portion of Sr if the dissolution rate of plagioclase decreases relative to the rate of K-feldspar (ie. plagioclase becomes stable before K-feldspar). This is a possibility as the higher dissolution rate of plagioclase, along with removal of potassium from solution by the formation of K-bearing clay minerals such as illite, may prevent K-feldspar from reaching equilibrium with the solution. Modelling of the evolution of groundwaters in granite systems, however, suggests that K-feldspar (microcline) becomes stable before plagioclase (oligoclase) (Madé 1991; Grimaud et al, 1990).

If there are only two sources mixing, then there should be a linear trend, in $^{87}Sr/^{86}Sr$ - 1/Sr space, between the pore fluids and samples that are most representative of dissolution controlled chemistry (ie. dilute and chloride poor waters having low $^{87}Sr/^{86}Sr$ ratio). As shown in Fig. 4.5, this simple two-component model does not explain the data. The fracture zone waters, although showing a linear trend, do not fall on the predicted mixing line (dashed line in Fig. 4.5) but exhibit only slight ^{87}Sr-enrichment with increasing strontium concentration. In fact, the $^{87}Sr/^{86}Sr$ ratios in most fracture waters are relatively constant over most Sr concentrations, indicating continued control of plagioclase alteration on the fracture waters. If pore fluids are contributing to the salinity of the fracture waters, then continuing water-rock interactions have modified the Sr isotopic composition of the introduced pore fluid. Waters from the Fracture Zone 1 show the greatest ^{87}Sr-enrichment and may reflect a greater degree of mixing between the deeper fracture zone and pore fluids. There is however, no distinct mixing trend between the two water types indicating that mixing is occurring (Fig. 4.5).

CHAPTER FIVE
BORON ANALYSIS

Compared to other stable isotopes, boron has not been widely applied to geological studies. This under utilization is a result of analytical difficulties associated with chemical extraction of boron, and fractionation effects during ionization. Due to the large relative mass difference between ^{11}B and ^{10}B, a high yield must be achieved after sample preparation to minimize the effects of fractionation. This has been most difficult for the analysis of boron in solid samples, in particular silicates. In contrast to water samples, which typically require no preparation, other than purification using an ion-exchange resin, rock samples must be decomposed using acids - HF, HCl, HNO, $HClO_4$ or H_2SO_4. In these acid solutions, boron is easily volatilized as a gaseous species such as BF_3 or BCl_3 with a consequence that a large boron isotopic fractionation results (Nakamura et al., 1992).

Several techniques have been developed to analyse the isotopic composition of boron. The first attempts used gas-source mass spectrometry, but the results proved to be unreliable due to the memory effects of reactive BF_3 (Thode et al., 1948). However, subsequent solid-source mass spectrometry techniques have produced reliable results. Two solid source techniques have been developed; 1) Positive thermal ionization mass spectrometry (P-TIMS) where the molecular species analysed are $Na_2BO_2^+$, $Cs_2BO_2^+$, or $K_2BO_2^+$ and, 2) negative thermal ionization mass spectrometry (N-TIMS) where the molecular ion BO_2^- is analysed. The precision of P-TIMS varies depending on which alkali metal-borate is used. The earliest attempts in P-TIMS measured sodium borate ions achieving an analytical uncertainty of 2 - 3‰ (2σ), while more recent boron isotope analyses have used the Cs-borate method with an uncertainty 0.012‰. N-TIMS typically had an analytical uncertainty of 2‰, although improvements to sample preparation and mass-spectrometric techniques have lowered the uncertainty to 0.07‰ (Hemming and Hanson, 1994). The greater precision of the Cs-borate method compared to N-TIMS and the other alkali metal-borates is, in large part, attributable to the higher molecular mass of the

measured $Cs_2BO_2^+$ ion. A high molecular mass reduces the relative mass difference between isotopic species thus limiting thermally induced mass-dependent isotopic fractionation.

Although precision of N-TIMS to date is lower than P-TIMS, it does have advantages in its considerably higher analytical sensitivity. Also, surface waters may be directly sampled with little or no sample preparation (Vengosh et al, 1989; Vengosh et al. 1991c; Klötzli , 1992). As practically no complicated chemical treatment is necessary, the boron blank is considerably reduced. Therefore, the N-TIMS method can potentially analyse as little as 0.1 ng B. In contrast, the P-TIMS method normally requires microgram amounts, however an improved technique allows isotopic measurement as low as 0.5 μg boron (Xiao et al., 1988; Nakamura et al.; 1992).

Inductively coupled plasma mass spectrometry (ICP-MS) has also been used for boron analysis (Gregoire, 1987; Bottomley et al. 1994). It has the potential for easy and rapid analyses of boron in water samples, however, the method has a high analytical uncertainty of 4 ‰. It has been used in the analysis of mine waters from the Canadian Shield (Bottomley et al. 1994).

In this study, N-TIMS is used to determine the isotopic composition of the water samples and P-TIMS is used to analyse whole rock and mineral separates. Boron concentration in both silicate and water samples was determined using isotope dilution by spiking samples with the National Bureau of Standards standard reference material NBS SRM 952.

Boron isotopic compositions are expressed as both permil differences relative to the NBS SRM 951 standard and as absolute abundance ratios. The permil difference is defined as:

$$\delta^{11}B = \{[(^{11}B/^{10}B)_{sample}/(^{11}B/^{10}B)_{standard}]-1\} \times 10^3$$

NBS SRM 951 is a boric acid and a National Bureau of Standards standard reference

$\delta^{11}B$	B (μg/g)	Location	Method	Reference
--	4.3	Pacific/Atlantic	$Na_2BO_2^+$	Schwarcz et al. (1969)
39.5	--	Pacific/Atlantic	$Cs_2BO_2^+$	Spivack and Edmond (1987a)
39.6	4.45	Atlantic	$Cs_2BO_2^+$	Aggarwal et al. (1992)
37.9	4.66	Pacific	$Cs_2BO_2^+$	Nomura et al. (1982)
40.2	4.76	Florida Bay	BO_2^-	Hemming and Hanson (1992)
39.9	--	Tavernier Cay, Florida	BO_2^-	Hemming and Hanson(1994)
38.4	4.69	Jervis Bay, eastern Australia	BO_2^-	Vengosh et al. (1989)
40.5	**5.41**	Atlantic (NASS-1)	BO_2^-	**This Study**

Table 5.1. Compilation of boron concentration and isotopic composition of seawater.

material certified for total H_3BO_3 and absolute abundance ratio $^{11}B/^{10}B$ (4.0436) (Catanzaro et al., 1970). NBS SRM 951 was repeatedly analysed to determine the analytical precision of the N-TIMS method.

To determine $^{11}B/^{10}B$ for samples, measured ratios must be corrected as follows:

$$\text{Correction Factor} = \text{NBS 951}_{\text{certified}} / \text{NBS 951}_{\text{measured}}$$

Therefore, the normalized $^{11}B/^{10}B$ is given by:

$$(^{11}B/^{10}B) = (^{11}B/^{10}B)_{\text{measured}} * \text{Correction Factor}$$

In the absence of a natural certified standard, the North Atlantic Seawater Standard (NASS-1) was analysed repeatedly as an additional check on the reproducibility of the analytical method. Although the seawater standard is not certified for $^{11}B/^{10}B$ or B concentration, both the isotopic composition and B concentrations determined from previous studies indicate that these values vary little in sea water (Table 5.1).

Reagents used for boron analysis were prepared using the methods described by Zhai (1996) and Nakamura et al. (1992). The procedure was modified by using a quartz rather than a Teflon still in the distillation of the reagents. Low blank levels were obtained by distilling reagents in the presence of mannitol.

5.1. Analysis of Water Samples using N-TIMS

The N-TIMS method was chosen initially for water sample analysis for its high sensitivity and low procedural blank. Because of the expected large isotopic variation in the groundwaters of the Lac du Bonnet, it was believed that the lower precision of N-TIMS would not prevent the defining of trends and water types. The absence of complicated

purification procedures would allow for rapid sample analysis and the low procedural blank would be advantageous in the analysis of the Lac du Bonnet groundwater samples having low B concentrations.

In the early stages of this study, the procedure of Klötzli (1992) was strictly followed. One µl of groundwater along with 1 µl of an aqueous 1000 µg/g $La(NO_3)_3$ solution was loaded onto an outgassed Re-filament. The groundwater sample received no prior chemical treatment. Ion beams produced from these untreated samples were weak and short lived. Increasing the sample amounts to 5 µl produced no noticeable improvement in beam strength and actually decreased beam stability . The poor beam strength may be due to other chemical species affecting the ionization of the groundwater samples. The presence of Fe, Si and organic carbon may interfere with the ionization of boron (Hemming and Hanson, 1994). Although the organic content in deep groundwaters is low, concentrations of Fe and Si are typically higher than that found in surface waters. For example, seawater Fe, Si, and B concentrations are 6×10^{-5}, 2.8, and 4.6 µg/g, respectively (Faure, 1994). Groundwaters in the Lac du Bonnet Batholith have Fe and Si concentrations in excess of 4 µg/g and 7 µg/g, while having B concentrations < 1.6 µg/g. The combination of low B concentration and high Fe and Si probably prohibits the formation of a strong ion beam.

To overcome the matrix effects and allow for greater concentration of B, boron-specific ion exchange resin was used to purify the sample before loading. The methodology is described in detail in section 5.1.1.

The ion ratio measured is molecular ions 43 to 42. The ion species at mass 42 is $^{10}B^{16}O^{16}O^-$ and at mass 43, $^{11}B^{16}O^{16}O^-$ and $^{10}B^{16}O^{17}O^-$. Therefore a correction must be made to eliminate the additional contribution of the $^{17}O^-$ bearing molecular ion at mass 43. Adopting Klötzli's (1992) method, the corrected $^{11}B/^{10}B$ ratios are calculated using equation,

$$^{11}B/^{10}B = [(I_{43} - (0.0007482 \cdot I_{42})]/I_{42}$$

where I_{42}, I_{43} are the measured ion beam intensities of masses 42 and 43, respectively.

5.1.1 Separation and Concentration of Boron in Water Samples

The method used to purify boron is a modification of the procedure presented by Hemming and Hanson (1994).

Prior to loading onto the ion-exchange column, water samples are evaporated in Teflon® beakers under infrared lamps in a laminar flow hood. To avoid volatile loss of boron during evaporation in acidic media (Ishikawa and Nakamura, 1990), all samples were evaporated at temperatures < 60°C. The dried samples are taken up in 0.25-1.0 ml of water adjusted to a pH ~ 8.5 by the addition of NH_4OH, and loaded on the ion-exchange column. The eluate is collected in a Teflon beaker and the sample is placed under a heat lamp (< 60 °C) and evaporated until approximately 10 µl of the sample remains.

The ion-exchange apparatus consists of a Teflon® tubing (0.05 mm I.D. and 0.12 mm O.D.), peristaltic tubing (0.12 mm- I.D.), 50 mesh Amberlite IRA-743 ion-exchange resin, and a peristaltic pump having an adjustable flow rate. The Teflon® tubing is connected to the peristaltic pump tubing (Fig. 5.1). The resin is introduced into the column by placing one end of the Teflon® tubing in a beaker containing the resin beads in water. The peristaltic pump will pull the beads into the tubing. The inside diameter of the Teflon® tubing is such that 50 mesh resin enters the tubing as a column of single grains. The progression of the beads into the peristaltic tubing is stopped by crimping the Teflon tubing with a clip near the connection between the tubing and peristaltic tubing. In this study, 18 cm of beads was used. The column is cleaned and conditioned using distilled deionized water, 0.5 *M* HCl, and 0.5 *M* NH_3. The flow rate and amount of reagent used for each procedural step is outlined in Table 5.2. After each sample, the beads are cleaned by repeating steps 1 through 5.

Figure 5.1. Schematic drawing of ion-exchange column and peristaltic pump for the separation of boron from aqueous samples (modified from Hemming and Hanson, 1994).

Table 5.2. Cleaning and elution steps for boron separation (modified from Hemming and Hanson, 1994).

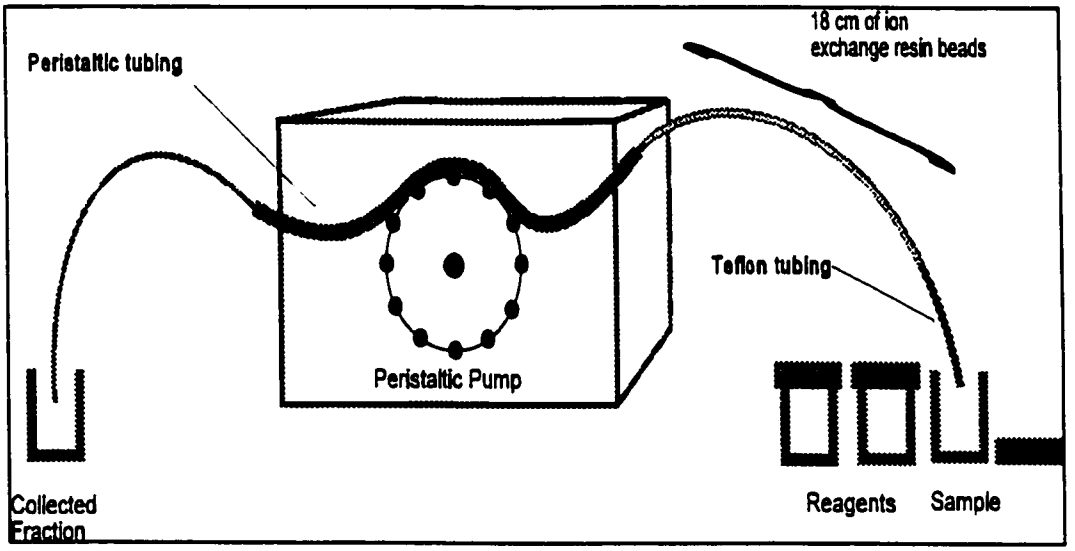

Step	Reagent	Amount (µl)	Flow Rate (µl min^{-1})	Purpose
1	water	100	30	wet beads
2	0.5 M HCl	500	30	clean column
3	water	100	30	condition column
4	0.5 M NH_3	50	30	condition column
5	water	100	30	condition column
6	sample	250-1000	15	separate boron
7	water	100	30	remove cations
8	0.5 M NH_3	50	30	remove cations
9	water	100	30	remove cations
10	0.5 M HCl	1000	30	elute boron

5.1.2 Mass Spectrometry.

The mass spectrometry procedure was modified from Klötzli (1992) and Hemming and Hanson (1994). The borium analyses were carried out on a VG 354 solid source mass spectrometer. The machine was modified to allow for the analyses of negative ions by reversing the polarities of the magnetic field and the acceleration potential.

At the beginning of this study, focussing problems became evident. The peak shape of the ion beams collected using the axial Faraday Cup collector were noticeably asymmetrical with sloping peaks while the side collectors exhibited flat peaks. The reason for this is unclear, but may be related to the acceleration of electrons and the electrons' interaction with the ion beam (Hemming and Hanson, 1994). In their study, Hemming and Hanson (1994) reduced the interaction of the electrons with the ion beam by deflecting the electrons with a small magnet placed close to the ionization filament. A similar procedure was attempted in this study to improve focussing, however, this failed to improve peak shape. Considering these difficulties, a side collector (H1 Faraday Cup) next to the axial collector was used instead of the axial.

Loading Sample:

To enhance the formation of BO_2^- ions and lower the optimum filament temperature an activator is added to the sample. Nitrates of Ca, Na, and La have been used in previous studies (Heumann and Zeininger, 1985; Klotzli, 1992), but the addition of sea water has been shown to be superior to other compounds in increasing ion yield (Hemming and Hanson, 1994). For seawater to be used as an activator, boron must be removed; this was accomplished by processing 0.5 ml of NASS-1 with the ion-exchange column using the procedure described in section 5.1.1. 0.5 µl of B-free seawater (see Table 5.7 for blank levels) is deposited on an outgassed single Re filament and evaporated close to dryness. 1-

10 µl of sample solution is deposited on top of the activator (typically 100 - 500 ng of B) . The solution is then evaporated under a heat lamp at temperatures under 60°C. Although 16 filaments could be loaded simultaneously into the mass spectrometer, only 8 samples are analysed at one time to reduce the potential for cross-contamination effects. Additional precautions included cleaning sample holders between analyses, and analysing spiked samples separate from unspiked samples.

Operation of Mass Spectrometer:

A Fluke® high voltage power supply was used as the external power source and the accelerating voltage was set at 3200 V. Once the accelerating voltage has stabilized (after several hours) and the ion source has been evacuated to $< 2.0 \times 10^{-7}$ Torr, the filament heating procedure begins. The procedure is controlled manually and the timing and operation conditions must be strictly repeated to insure the reproducibility of the analyses. The heating steps are as follows:

(1) *0 -10 min:*

The filament current is initially set to 0.5 A and is increased manually every 30 sec. by 0.1 A. At a filament current of 1.8 A, a $^{11}BO_2^-$ ion beam is usually detectable.

(2) *10-20 min:*

The signal is optimized by manually focussing the ion beam and/or slowly increasing the filament current until a stable, slowly increasing or decreasing ion beam is obtained. The preferred ion intensity for analysis is 0.5-2 V (beam current of 5×10^{-12} to 2×10^{-11} A) .

(3) *20 - 40 min:*

A standard computer-controlled peak jumping routine is used to collect data for boron at masses 43 ($^{11}BO_2^-$) and 42 ($^{10}BO_2^-$) (2 second integration times for both the

Method	$^{11}B/^{10}B$	Precision (%) 2σ	Reference
$Na_2BO_2^+$	4.0436	0.034	Catanzaro et al. (1970)
$Cs_2BO_2^+$	4.0512	0.010	Nakamura et al. (1992)
$K_2BO_2^+$	4.0500	0.074	Zhai (1996)
$K_2BO_2^+$	**4.0389**	0.149	**This Study**
BO_2^-	4.0160		Zeininger and Heumann (1983)
BO_2^-	4.0100	0.249	Vengosh et al. (1989)
BO_2^-	3.9960	0.200	Vengosh et al. (1991a)
BO_2^-	3.9949	0.426	Klötzli (1992)
BO_2^-	4.0014	0.067	Hemming and Hanson (1994)
BO_2^-	**4.0053**	0.325	**This Study**

Table 5.3. Compilation of NBS 951 analyses and methods.

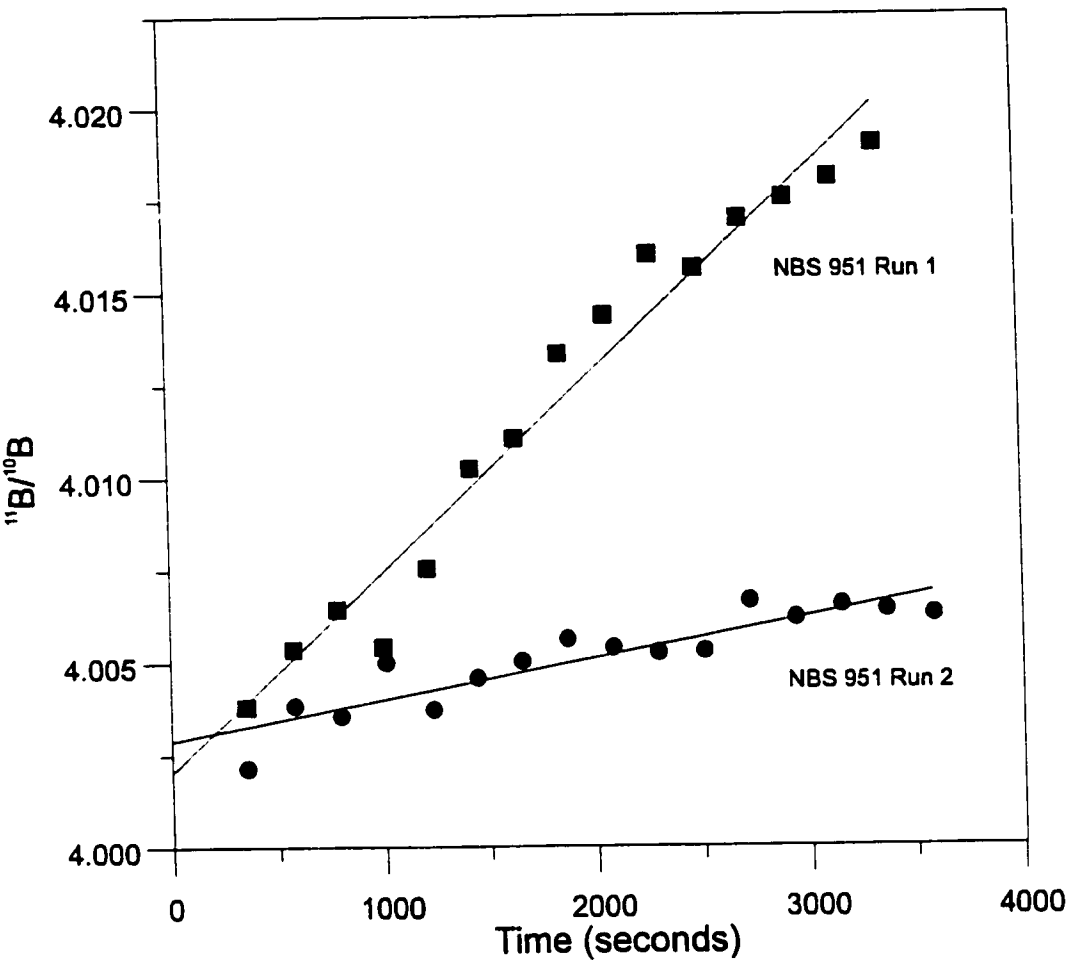

Figure 5.2. Time-dependent fractionation trend of 2 analyses of NBS 951 boric acid. Data points can be regressed back to t=0 (beginning of data aquisition procedure). Each point is the average isotopic ratio of one data block (10 isotopic analyses).

masses). The mass range is scanned 10 times and a mean value of $^{11}B/^{10}B$ calculated for the block of data. It was found that regression of more than 5 data blocks did not significantly improve the precision of the procedure. For example, in Figure 5.2, NBS 951 Run1 and Run 2 have Y- intercepts of 4.00204 and 4.00288, respectively calculated from 15 data blocks. Regression using the first 5 data blocks gives intercept values of 4.00207 and 4.00295 for Run 1 and Run 2. Therefore, 5 data blocks are acquired for each sample run. Baseline values are taken before each set at mass 41.5.

5.1.3 Data Reduction

The average isotopic composition for SRM-951 reported here ($^{11}B/^{10}B = 4.0053$) is ~ 1 % lower than the recommended value reported by the U.S. National Bureau of Standards (Cantanzaro et al., 1970). However, the value calculated in this study is similar to values reported by other investigators using N-TIMS (Table 5.3). This discrepancy reflects the difference between the N-TIMS method and the Na-borate method used by the U.S. National Bureau of Standards. It's generally agreed that the large molecular mass difference of BO_2^- ions leads to greater fractionation than would be expected for $Na_2BO_2^+$. An additional factor contributing to the fractionation in the N-TIMS method may be the "salt pan" effect on the filament, where early precipitates on the outside of the sample load take up the isotopically lighter boron (Hemming and Hanson, 1994).

Theoretically, the fractionation during evaporation from the filament can be described as a Rayleigh distillation process. If it is assumed that the evaporation rate is constant with time, the fractionation of N-TIMS is approximately linear with time within the first 40% of the evaporation process (Klötzli, 1992). Relatively good external reproducibility can be achieved if the slope of the fractionation trend is used to correct the ratio to time zero (Fig. 5.2). Klötzli (1992) used standard linear regression to correct for variations in the time-dependent fractionation of the ion beam and used the calculated ratio at t=0 as the measured

I_{43}/I_{42} ratio of the sample.

In this study, 5 block ratios were regressed and the Y-intercept (the calculated ratio at t=0) was determined. The calculated ratio was then corrected to eliminate the $^{17}O^-$ bearing molecular ion at mass 43 as described in section 5.1. In addition to the regressed value, the mean of the 5 block ratios was calculated for all samples and standards. The analytical reproducibilities of the regressed value and the calculated mean for NBS 951 and NASS-1 were compared to determine whether regression did, in fact, improve uncertainty.

5.1.4 Analytical Reproducibility and Accuracy

Twenty three replicate analyses of NBS SRM 951 are presented in Table 5.4. As would be expected (see Fig 5.2), the mean of each analysis is higher than the value determined for t = 0. The averages of the 23 regressed and non-regressed analyses are 4.0015 ± 0.36% and 4.0053 ± 0.32% (2σ), respectively. What is interesting to note is the similarity in precision for the two methods . The external errors are also similar in the analysis of NASS - 1 (Table 5.5). This would suggest that the error resulting from fractionation during ionization is insignificant compared to error caused by sample loading and machine setup. Therefore, regression analysis of data as outlined by Klötzli (1992) does not improve the statistical error of the data. Due to the slightly larger error produced by the y-intercept method and for simplicity, the measured mean of the 5 data blocks is used instead of the regressed value. Repeat analyses were carried out on a number of groundwaters sample and the external errors varied between 0.22% to 1.12% (Table 5.1).

Although seawater's $\delta^{11}B$ is not used as a standard, its uniform boron isotopic composition can still be used as an indication of accuracy. NASS-1 was analysed 7 times using negative thermal ionization giving an average $\delta^{11}B = 40.7‰$. This value is ~2% higher than the average $\delta^{11}B$ of seawater of 39.5‰ (Barth, 1993) indicating a possible bias in the analytical procedure adopted for this study.

Run	Y-intercept		Mean	Std. Err. %
1	4.0026		4.0068	0.006
2	3.9986		4.0029	0.007
3	4.0044		4.0142	0.013
4	4.0081		4.0098	
5	4.0059		4.0079	0.003
6	4.0110		4.0129	0.001
7	4.0049		4.0077	0.003
8	3.9816			
9	3.9973		4.0005	0.016
10	4.0052		4.0068	0.010
11	4.0002		4.0032	0.011
12	4.0020		4.0107	
13	3.9968		3.9977	0.014
14	4.0041		4.0065	0.007
15	4.0080		4.0092	0.010
16	4.0023		4.0027	0.003
17	3.9910		3.9926	0.004
18	4.0052		4.0085	0.005
19	4.0013		4.0029	0.005
20	4.0109		4.0128	0.006
21	4.0075		4.0093	0.007
22	4.0016		4.0063	0.006
23	3.9841		3.9855	0.007
Average	4.0015	±0.36 %	4.0053	±0.32 %

Table 5.4. Analyses of NBS 951 boric acid. *Y-intercept* represents the apparent $^{11}B/^{10}B$ at t=0 determined from the regression of 5 data points. *Mean* is the average of the data points.

Table 5.5. Analyses of sea water standard NASS-1. Y-intercept represents the apparent $^{11}B/^{10}B$ at t=0 determined from the regression of 5 data points. Also shown is the mean of the 5 data points.

Table 5.6. Boron yields using Amberlite IRA-743 boron-specific resin. Seawater standard NASS-1 was used to determine yields.

	Y-intercept			Mean		
Run	Measured	Corrected	$\delta^{11}B$	Measured	Corrected	$\delta^{11}B$
1	4.174	4.217	43.1	4.176	4.214	42.4
2	4.169	4.212	41.9	4.174	4.212	41.9
3	4.156	4.199	38.5	4.162	4.200	39.0
4	4.163	4.206	40.4	4.171	4.209	41.1
5	4.163	4.207	40.5	4.172	4.211	41.4
6	4.159	4.202	39.4	4.169	4.207	40.5
7	4.160	4.203	39.5	4.160	4.198	38.3
Average	4.163	4.207	40.5	4.169	4.207	40.7 ± 2.8‰

Run	Amt. (*μg*)	Yield (*μg*)	% recovery
1	0.69	0.66	95.5
2	0.73	0.70	94.7
3	1.21	1.18	97.3
4	0.83	0.82	98.8
Average			96.6

High yields in the purification process are important to overcome the fractionation effects on the sample. Boron may be lost due to the volatility of boron complexes during evaporation in acidic media (Ishikawa and Nakamura, 1990), or by inefficient ion-exchange chemistry. To insure that complete recovery of boron was accomplished during sample purification, a procedural yield was determined using NASS-1. As can be seen in Table 5.6, there is no significant loss of boron during sample preparation.

Reagent and procedural blanks are 1.2 ng and 1.7 ng, respectively (Table 5.7). The typical amount of boron analysed varied between 100-500 ng, therefore for any given sample, the proportion of the boron contributed by reagent and handling did not exceed 1.7%.

5.2 Boron Isotopic Analysis of Silicate Samples

5.2.1 Analysis using N-TIMS

Mineral and whole rock B isotopic analysis using N-TIMS has previously been successful when coupled with the K-fusion procedure for purifying boron (Vengosh. et al, 1991a). In this study, an attempt was made to analyse silicate samples using N-TIMS and a purification procedure previously used by Zhai (1996) and Nakamura et al. (1992) with P-TIMS. Due to the nature of N-TIMS, this procedure was modified to include an additional stage of boron separation by boron-specific resin.

In the original procedure mannitol is added to the powdered sample prior to the addition of HF to prevent the volatilization of BF_3. Once the sample is decomposed, the boron is removed using both cation and anion exchange resins to obtain a pure boron eluate. Mannitol is again added to the sample to prevent boron loss during the final evaporation in a 6 M HCL solution. The sample loaded into the mass spectrometer contains 40-50 μg of mannitol; for P-TIMS, the presence of mannitol does not affect the analysis, however problems may occur if the method of analysis is N-TIMS as mannitol may prevent formation

Reagent	ng/g
Average Boron Content in "B-Free Seawater"	35.61
Average Boron Content in HCL (6M)	1.07
Average Boron Content in H_2O	0.50
Boron Content NH_4	1.29
0.5 M HCL	0.65

Reagent Blank

Amount of Reagents used	ng
Dissolve in 0.5 ml H_2O	0.24
0.1 ml H_2O	0.05
0.05 ml NH_4	0.06
0.1 ml H_20	0.05
Sample	
0.1 ml H_2O	0.05
0.05 ml NH_4	0.06
0.1 ml H_20	0.05
1.0 ml HCL (0.5 M)	0.61
Seawater (0.5 µl)	0.02
Total	1.18

Procedural Blank

Run	ng
1	1.66
2	1.71
Average	1.68

Table 5.7. Blank levels in reagents and and procedures.

of the ion beam and interfere with $^{10}BO_2^-$.

Mannitol is an organic compound and has the formula $CH_2OH\text{-}(CHOH)_4\text{-}CH_2OH$ (Barbier and Rosset, 1968) and therefore contains reduced carbon. The presence of reduced carbon may inhibit B ionization and cause interference of peak 42 by combining with N to form cyanogen (CNO^-) (Hemming and Hanson, 1992). Therefore, it is important that mannitol not be present in the sample when loaded onto the filament. To achieve this, the initial purification procedure as outlined by Nakamura et al. (1992) was modified by not adding mannitol to the eluate retrieved from the anion-exchange column. A further modification was made, in replacing the final anion-exchange procedure of Nakamura et al.(1992) with the boron purification procedure for water samples used in this study.

Results from whole rock and NASS-1 standard analysis using N-TIMS proved to be unreliable. Ion beams were typically weak, or short lived and reproducibility was poor. Spiking of samples before and after processing indicated that most boron was lost during processing. A yield of <20% was achieved.

5.2.2 Analysis using P-TIMS

In an attempt to obtain better results, the P-TIMS method was adopted. Similar to N-TIMS, the majority of samples produced weak or short lived ion beams, but when replicate data was obtained, the reproducibility was noticeably better than N-TIMS. Unfortunately, because yields were also < 20%, the possibility of fractionation effects cannot be ignored.

The $K_2BO_2^+$ molecular ion was analysed according to the procedure outlined by Zhai (1996). The ion ratio analysed is molecular ion 121 to molecular ion 120. The ions at mass 121 are $^{39}K^{39}K^{11}B^{16}O^{16}O^+$, $^{40}K^{39}K^{10}B^{16}O^{16}O^+$, and $^{39}K^{39}K^{16}O^{12}O^+$; the ion at mass 120 is $^{39}K^{39}K^{10}B^{16}O^{16}O^+$. It is evident that a correction must be made to remove interference of peak 121 by ^{40}K and ^{17}O . Taking this into consideration $^{11}B/^{10}B$ can be calculated using equation,

$$(^{11}B/^{10}B) = I_{121}/I_{120} - 0.00105$$

(Spivack and Edmond, 1986)

5.2.3 Boron Separation Procedure for Silicate Samples.

The procedure for silicate dissolution and boron separation was adopted and modified from Zhai (1996) and Nakamura et al.(1992).

Sample Decomposition:

0.1 to 0.3 g of powder is placed in a Teflon bomb. If B concentration is to be determined, the spike is added to the sample at this stage. The sample is then soaked in 0.5 ml of 1% mannitol solution. Two ml of 30 M HF acid are added and the bomb is sealed and agitated to suspend powder in the acid. The bomb is placed on a hotplate for 1 -2 days at a temperature of 80 °C. After the bomb has cooled down to room temperature, the solution and precipitate was transferred to a centrifuge tube. The bomb was rinsed once with 0.5 ml of concentrated HF to remove any remaining residue and this was added to the centrifuge tube. The solution was centrifuged for 10 minutes and the supernatant transferred to a Teflon beaker, and evaporated to dryness on a hot plate in a laminar flow hood at < 60 °C. The dried sample is dissolved in 0.5 ml of 6 M HCl and is again evaporated to dryness under a heat lamp at a temperature < 60 °C.

Cation Exchange:

Three ml of AG 50WX12 cation-exchange resin was placed in a polypropylene column. The resin bed was cleaned twice by 5ml of 6 M HCl and conditioned with 3 ml of 0.02 M HF. The dried sample was re-dissolved in 1 ml of 0.1 M HCl and the solution loaded onto the cation-exchange column. The beaker was rinsed with 0.5 ml of 0.02 M HF and this solution was loaded on the column. The boron fraction was collected in a Teflon

beaker using 5 ml of 0.02 M HF as the eluent. The eluate was evaporated at < 70 °C under a heat lamp to incipient dryness.

Anion Exchange:

Anion-exchange resin is used to separate boron from Si, Ti, and Fe. 0.3 ml of AG 1-X4 (200 - 400 mesh) anion-exchange resin was placed in a polyethylene column. The Column was cleaned using 2 ml of 6 M HCl twice and conditioned with 3 ml of 3 M HF. The dried sample was dissolved in 0.6 ml of 3 M HF, the beaker sealed and heated under a heat lamp for 15 min. at a temperature < 60 °C. After the beaker had cooled to room temperature, the sample was loaded onto the anion-exchange column. The beaker was rinsed with 0.25 ml of a mixed acid solution of 2M HCl and 0.5 M HF, and this solution was also loaded onto the column. 1.2 ml of the mixed acid was added to the column. The boron fraction was eluted using 2 ml of 6 M HCl and the eluate was collected in a Teflon beaker containing 0.02 ml of mannitol solution, and evaporated to incipient dryness as described above. The sample was reprocessed by repeating the anion-exchange procedure.

Loading and Mass Spectrometry:

If using P-TIMS, the final boron fraction was collected in a Teflon beaker containing 0.01 ml of 0.01 M potassium solution and 50 μg of mannitol. This final solution was evaporated to dryness at <60 °C and the dried sample was loaded on a tantalum filament for mass spectrometry.

Prior to loading the sample, a v-shaped groove is made cross-wise in the filament. The top of the filament is coated by 1μl of graphite -ethanol-water slurry containing 50 μg of graphite. Just before complete dryness of the graphite slurry, the boron sample, dissolved in 2 μl of 0.02 M HF, is loaded on the graphite layer. The sample is slowly dried under a heat lamp, then loaded into the mass spectrometer and the ion source evacuated to < 3.0×10^{-7} Torr. Because of the gaseous nature of the samples, they are preheated for 3 minutes at a

filament current of 1.3 A, before analysis.

Data acquisition was made by peak jumping using the Daly Collector. The integration time for each Peak was 4 secs and 150 ratios were collected in 15 blocks.

If using N-TIMS, the final boron fraction was collected in an empty Teflon beaker. The solution was evaporated at a temperature <60 °C. When the sample was close to complete dryness, the sample was dissolved in 0.25 ml of water adjusted to a pH ~ 8.5, then loaded onto a column containing boron-specific resin following the procedure outlined in section 5.1.1.

5.2.4 Analytical Reproducibility and Accuracy.

Fifteen replicate analysis of NBS 951 are presented in Table 5.8. The isotopic composition of NBS 951 reported here (4.0389 ± 0.2%) is about 0.1 % lower than the certified value (4.0436) and about 0.3% lower than the value determined by Zhai (1996) using the $K_2BO_2^+$ ion (4.0510 ±.02%). This difference and the larger uncertainty when compared to Zhai (1996), is probably due to the lower ionization temperature and smaller ion beam used in this study because detection was by the Daly detector. To estimate the precision and accuracy of the P-TIMS and separation procedure, NASS-1 was processed in a similar fashion as the silicate samples. The isotopic composition determined for NASS-1 is $\delta\ ^{11}B$ =40.6‰ (Table 5.9) is 0.1‰ lower than the value determined using the N-TIMS method (Table 5.5).

5.3 Spike Solutions and Calibration.

Because there is no natural standard for B concentration, Fisher boric acid (Reagent grade) was used to calibrate the spike NBS SRM 952 ($^{11}B/^{10}B$= 0.0532). The isotopic composition of the Fisher boric acid is 4.0501 ± 0.12% as determined from 10 analyses using

Run	Amount (μg)	$^{11}B/^{10}B$	Std. Err. (2σ)
1	1	4.0345	0.014
2	1	4.0432	0.017
3	1	4.0377	0.017
4	1	4.0358	0.014
5	1	4.0384	0.017
6	0.5	4.0377	0.017
7	0.3	4.0397	0.019
8	0.5	4.0367	0.015
9	0.5	4.0451	0.021
10	1	4.0352	0.014
11	1	4.0400	0.016
12	1	4.0357	0.017
13	1	4.0444	0.015
14	1	4.0375	0.016
15	1	4.0424	0.014
Average		4.0389	± 0.16 %

Table 5.8. Boron isotopic composition of standard NBS 951 determined using P-TIMS.

Table 5.9. Boron isotopic composition of NASS-1 determined using P-TIMS.

Table 5.10. Determination of $^{11}B/^{10}B$ of Fisher boric acid

Table 5.11 Determination of boron spike (NBS 952) concentration.

Run	Measured	Corrected		$\delta^{11}B$	
1	4.200	4.204		41	
2	4.196	4.200		40	
3	4.207	4.210		43	
4	4.196	4.199		40	
5	4.198	4.202		40	
Average	4.199	4.203	± 0.008	40.6	± 2.0‰

Run	$^{11}B/^{10}B$	Std Err% (2σ)
1	4.0114	0.004
2	4.0136	0.008
3	4.0082	0.005
4	4.0128	0.007
5	4.0132	0.008
6	4.0114	0.003
7	4.0093	0.004
8	4.0136	0.004
9	4.0146	0.005
10	4.0170	0.004
Average	4.0125	±0.12 %
Corrected	4.0501	

Run	Conc. (µg/g)	
1	0.45	
2	0.45	
3	0.49	
4	0.50	
5	0.48	
6	0.46	
7	0.44	
8	0.47	
Avg	0.47	
Std (1σ)	0.02	± 4.3 %

N-TIMS (Table 5.10). The boric acid was weighed and dissolved in mannitol-distilled water. The solution was agitated and allowed to sit for 15 minutes and was inspected to confirm complete dissolution. A second solution was made by diluting a portion of the initial solution and this final solution was used to calibrate the spike.

Eight solutions were spiked and the B concentration of the spike was calculated. The average concentration of the spike was 0.465 μg/g ± 4.3% (Table 5.11). The B concentration of NASS-1 was determined 5 times by isotope dilution giving an average concentration is 5.41 μg/g ± 1.0% This is approximately 20% higher than the B concentration reported from various seawater samples taken from the Atlantic and Pacific oceans (Table 5.1). It is not known whether this is the "true" value of NASS-1, considering that the standard is not certified for boron concentration. The high concentration may indicate that a bias has been introduced by errors in spike calibration. One possibility is that the boric acid was not fully dissolved in the calibrating solutions. Inspection of the calibrating solutions prior to dilution, however, seem to indicate complete dissolution. Alternately, the boric acid used could have adsorbed a significant amount of water, but boric acid is not considered hygroscopic.

The spike solution was analysed twice to determine its' isotopic composition. The two values obtained were 0.05614 and 0.05610. This ratio is 5.5% higher than the certified value of 0.0532 for NBS 952. The higher ratio of the spike solution probably indicates a small degree of contamination during handling of the spike solution. The ratio 0.05612 is used in calculations to determine the concentrations of samples.

CHAPTER SIX
BORON GEOCHEMISTRY IN THE LAC DU BONNET BATHOLITH

6.1 Introduction

The isotope geochemistry of boron is a potential tracer of salinity in natural waters (Spivak and Edmond, 1987b; Basset, 1990; Vengosh et al. 1991a; Vengosh, 1992) and has been used to determine the origin of Canadian shield brines (Bottomley et al. 1994). The usefulness of boron isotopes is their ability to distinguish between boron of marine and terrestrial origin. Natural boron is composed of 2 stable isotopes ^{10}B and ^{11}B, whose approximate abundances are 20 and 80%, respectively. The large relative mass differences between the two isotopes and the high chemical reactivity of boron, results in significant isotope fractionation in natural samples from different geological environments. Seawater reactions involving sea floor basalt, detrital clays, and biogenic calcium carbonate, has enriched present-day seawater in ^{11}B to a $\delta^{11}B$ of about 40‰, relative to the NBS-951 boric acid standard of the National Bureau of Standards (Agyei and McMullen, 1968; Spivak and Edmond, 1987a; Spivak et al, 1987; Vengosh et al., 1991b). This is approximately 40‰ higher than the calculated average for $\delta^{11}B$ of continental igneous rocks (Agyei and McMullen, 1968; Schwarcz et al., 1969; Barth, 1993).

This large difference in the isotopic composition of the marine and terrestrial reservoirs, has been used to distinguish ^{11}B-enriched marine evaporitic borates from their ^{11}B-depleted non-marine counterparts (Swihart et al. , 1986; Oi et al. 1989; Vengosh et al. 1992). Boron isotopes have also been used to distinguish between marine and terrestrial boron in surface waters such as in Australian salt lakes (Vengosh et al. 1991a), in groundwaters from various geological environments (Vengosh et al. 1991a, Bottomley et al., 1994) and in geothermal waters (Palmer and Sturchio, 1989; Vengosh et al., 1991c; Aggarwal et al., 1992; Leeman et al., 1990). The distinctive isotopic composition of boron in seawater makes it an

Figure 6.1. Boron co-ordination in solution at 25°C as a function of *p*H). Equilibrium constant used is *p*K = 8.83 as determined by Hershey et al. (1977)(modified after Palmer et al., 1987).

Figure 6.2. Isotopic composition of boric acid ($B(OH)_3$) and borate anion ($B(OH)_4^-$) in solution at 25°C as a function of pH. The theoretical fractionation factor used is 1.0194 as calculated by Kakihana et al., (1977). Star (★) represents the isotopic and pH conditions of present day sea water (modified after Palmer et al., 1987).

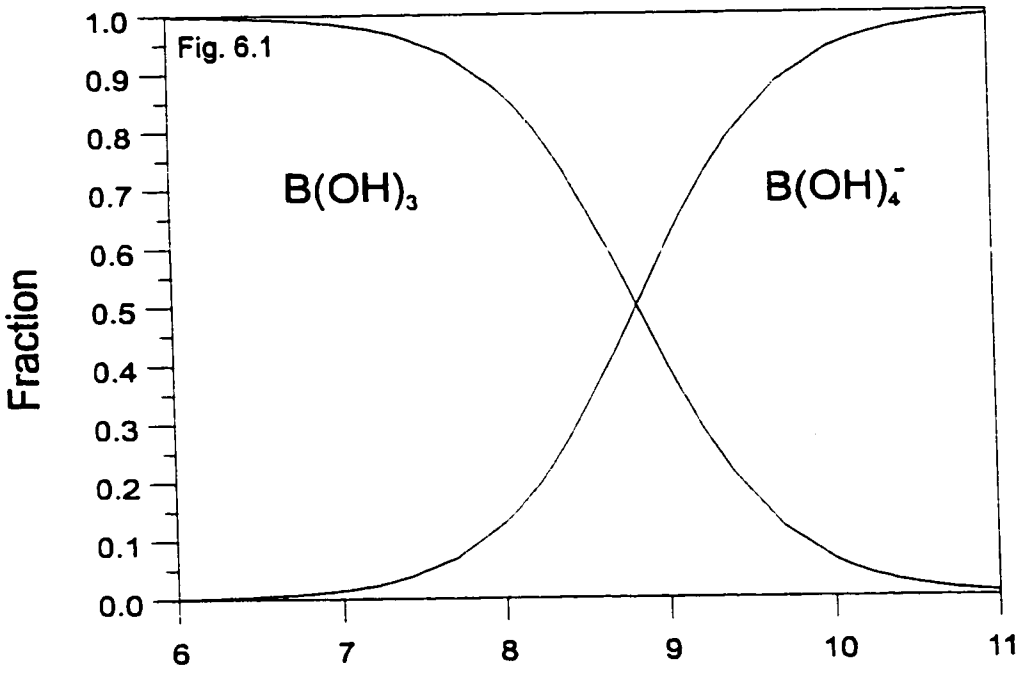
Fig. 6.1
Fraction
1.0
0.9
0.8
0.7
0.6
0.5
0.4
0.3
0.2
0.1
0.0
B(OH)3
B(OH)4-
6
7
8
9
10
11

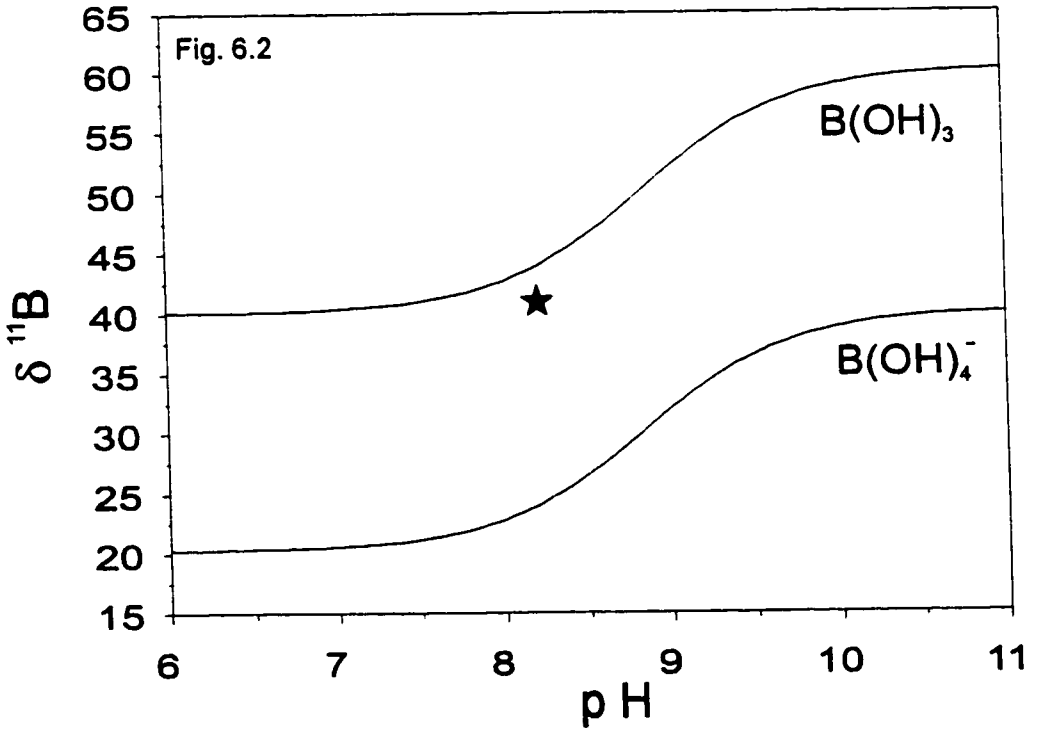
Fig. 6.2
δ 11B
65
60
55
50
45
40
35
30
25
20
15
B(OH)3
B(OH)4-
6
7
8
9
10
11
p H

attractive geochemical tracer, however, due to boron's susceptibility to fractionation, a thorough understanding of the mechanisms governing boron fractionation and the magnitude of possible fractionation effects is essential. Moreover, boron isotopes should not be used alone in interpreting the origin of salinity in groundwaters, but should be used in conjunction with other chemical criteria (Vengosh, 1992).

Dissolved boron occurs as various aqueous species, as boric acid ($B(OH)_3$), the borate anion $B(OH)_4^-$, and as different borates and polyborates depending on the chemical composition of the solution (Christ and Harder, 1978). In most natural aqueous systems, the dominant species are $B(OH)_3$ and $B(OH)_4^-$ (Hershey et al., 1986). The relative proportions of these species are mainly a function of *pH* and are given by the relation:

$$B(OH)_3 + H_2O \leftrightharpoons B(OH)_4^- + H^+ \qquad equ.5.1$$

At low *p*H, virtually all of the boron in solution is in the $B(OH)_3$ species; conversely, at high *p*H (>8.5), virtually all of the boron is in the $B(OH)_4^-$ species (Fig. 6.1). When both species are present the ^{10}B is preferentially partitioned into $B(OH)_4^-$. The isotope-exchange reaction between these species is given by Kakihana et al. (1977) :

$$^{10}B(OH)_3 + {}^{11}B(OH)_4^- \leftrightharpoons {}^{11}B(OH)_3 + {}^{10}B(OH)_4^- \qquad equ.5.2$$

Differential uptake of the two boron species during the interaction of dissolved boron with solid phases leads to significant isotope fractionation. Experiments on the adsorption of boron onto clays indicate that $B(OH)_4^-$ is adsorbed preferentially onto the reactive surfaces of clays. Considering the relationship between the proportion of $B(OH)_3$ and $B(OH)_4^-$ present in solution and pH, the amount of boron adsorbed is not constant but changes according to the pH of the solution (Keren and Mezuman, 1981; Palmer et al., 1987). Therefore, in

alkaline solutions, there will be a greater proportion of boron removed from solution as the $B(OH)_4^-$ is adsorbed. The individual fractionation factors for the two species ($\alpha = R_{ad}/R_{sol}$, where R_{ad} and R_{sol} are the $^{11}B/^{10}B$ ratios of the adsorbed and dissolved B, respectively) have also been determined for boron adsorption onto clays. The fractionation factor for the $B(OH)_3$ and $B(OH)_4^-$ is 0.969 ± 0.002 and is 0.992 ± 0.002, respectively (Palmer et al., 1987). Thus there is a greater degree of isotopic fractionation (preferential adsorption of ^{10}B onto clay) associated with the adsorption of $B(OH)_3$ than $B(OH)_4^-$. In this respect the degree of boron adsorption and fractionation is strongly dependent on the *p*H of the groundwater.

In seawater, these boron complexes are adsorbed onto reactive surfaces in the marine environment such as detrital clays, and on neogenic minerals formed by alteration on sea floor basalts. The isotopically lighter $B(OH)_4^-$ is adsorbed preferentially onto the active surfaces, resulting in the dissolved marine boron becoming enriched in the isotopically heavier $B(OH)_3$ species.

The boron concentration in seawater and its isotopic composition has probably achieved steady state (Harriss , 1969; Schwarcz et al, 1969) where the input of boron into the oceans from the weathering of continental material and the high temperature alteration of sea floor basalt is equal to the removal of boron by adsorption onto detrital clays, low temperature alteration of sea floor basalts, and formation of carbonates (Seyfried et al., 1984, Spivak and Edmond, 1987a, 1987b; Thompson and Melson, 1970). This steady state has resulted in a uniform B concentration in open oceans of 4.5 μg/g. The isotopic composition of the oceans has probably remained relatively constant for much of of earth's history as evidenced by the narrow range of isotopic composition of marine evaporites (Barth ,1993).

6.2 Results

6.2.1 Boron in Groundwaters

Boron concentrations and isotopic compositions of the Lac du Bonnet Batholith groundwaters are shown in Table 6.1. The boron concentrations are relatively low compared to seawater (4.5 mg/L) ranging from 0.038 to 1.57 mg/L, but are similar to concentrations determined in the Canadian Shield mine waters (Bottomley et al., 1994; Frape and Fritz, 1987)and in groundwater of the East Bull Lake pluton (Bottomley et al., 1986). Isotopically, the LDB fracture waters are also similar to the Canadian Shield mine waters, but waters from the LDB do show a greater degree of ^{11}B-enrichment (Fig. 6.4). Fracture waters having low concentrations plot close to the mean $\delta\ ^{11}B$ of the grey granites and minerals (-5‰ ± 3.2‰), while samples with the highest concentrations show ^{11}B enrichment to 52.7 ‰. This positive correlation of $\delta\ ^{11}B$ and concentration is also seen in the mine waters, but it is not as well constrained, reflecting the wide range of rock types and different locations from which the mine waters were sampled.

There is a very poor correlation between the chlorinity and boron concentration (Fig. 6.3) and chlorinity and isotopic composition (Fig 6.5). The lack of correlation between boron and chloride geochemistry indicates that processes controlling boron are different from the processes controlling chloride.

Boron concentration and isotopic composition, like other chemical criteria, can be used to distinguish between fracture waters and pore fluids. Based on concentration and $\delta\ ^{11}B$ alone, the pore fluids are indistinguishable from the fracture waters (Fig. 6.4), but they are distinct, in B/Cl and $\delta\ ^{11}B/Cl$. The pore fluids are some of the most saline fluids in the Lac du Bonnet Batholith and have significantly lower B concentrations and $\delta\ ^{11}B$-values compared to fracture waters with comparable chlorinities.

Sample	$^{11}B/^{10}B$	Err %(2σ)	(Repeats)	$\delta^{11}B$	Conc. (μg/g)
208-HC8-Z2	4.202		(1)	39.1	0.91
208-HC16-Z2	4.140		(1)	23.8	0.40
209-056-OC1-28	4.054	0.24	(3)	2.5	0.11
B34-1-4	4.168		(1)	30.6	0.31
B37-1-2	4.136		(2)	22.8	0.20
B37-2-1	4.141	0.63	(3)	24.1	0.52
JE1-2	4.197		(1)	38.0	0.76
M13-2-3	4.071		(1)	6.9	0.15
M14-1-4	4.174		(1)	32.2	0.33
M4B-2-5	4.105		(2)	15.1	0.25
URL2-PZ15	4.073	1.00	(3)	7.4	0.27
URL12-10-3	4.237	0.49	(6)	47.9	1.57
URL12-11-4	4.211	1.11	(3)	41.3	1.05
URL12-12-2	4.233		(1)	46.9	0.94
URL13-5-1	4.136		(1)	22.9	0.67
URL13-7-1	4.225		(2)	44.8	0.55
URL13-9-1	4.098		(1)	13.5	0.16
URL13-11-1	4.096		(1)	13.0	0.20
URI14-8	4.231		(1)	46.4	0.99
413-033-SM7-28	4.082	0.38	(3)	9.5	0.04
WB2-13-4	4.234		(1)	47.0	0.77
WB2-19-5	4.218	0.36	(3)	43.2	1.41
WB3-Pz3	4.203		(1)	39.3	0.56
WD3-895-10	4.257		(1)	52.7	0.76
WN4-6-8	4.200		(1)	38.8	1.21
WN4-6-42	4.168		(1)	30.7	1.37
WN4-6-7	4.235		(1)	47.3	1.18
WRA1-4-SW10	4.206		(1)	40.1	0.45
WG2-2-8	4.070		(1)	6.7	0.26

Table 6.1. Boron isotopic compositions and concentrations of the Lac Du Bonnet groundwaters.

Figure 6.3. Boron concentration vs chloride plot of water from fracture zones and unfractured rock. Open squares (□) are fracture waters and closed squares (■) are pore fluids. Boron concentrations in Fracture waters show a very poor correlation with chloride content. For a given chloride concentration, pore fluids are depleted in boron relative to the fracture waters.

Figure 6.4. A compilation of boron isotopic and boron concentrations data from the Lac du Bonnet fracture waters (□), pore fluids (■), formation brines from south west Manitoba (Δ), and mine waters from the Canadian Shield (●) (Bottomley, 1994). The composition of present day seawater is represented by a star (★). The $\delta^{11}B$ of the LDB groundwaters and Shield mine waters increase with boron concentration and both exhibit low boron concentrations (< 2.0 μg/g). The groundwaters are distinct from the mine waters in the higher degree of boron-11 enrichment. The mine waters exhibit a poorer correlation between $\delta^{11}B$ and concentration compared to the groundwaters and is probably a reflection of the wider geographical area of sampling for the mine waters and the diverse lithologies of the host rocks from which they were sampled. Although, the mine waters trend towards a seawater composition, the LDB groundwaters show no apparent relationship with seawater or brines from south west Manitoba.

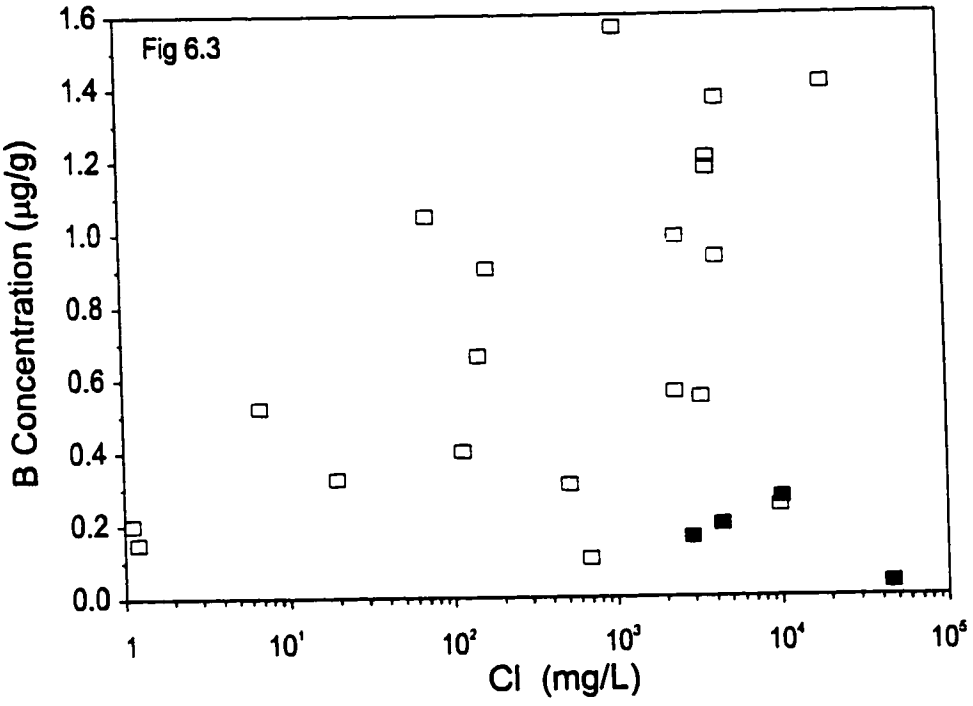
Fig 6.3
B Concentration (µg/g)
1.6
1.4
1.2
1.0
0.8
0.6
0.4
0.2
0.0
1
10¹
10²
10³
10⁴
10⁵
Cl (mg/L)

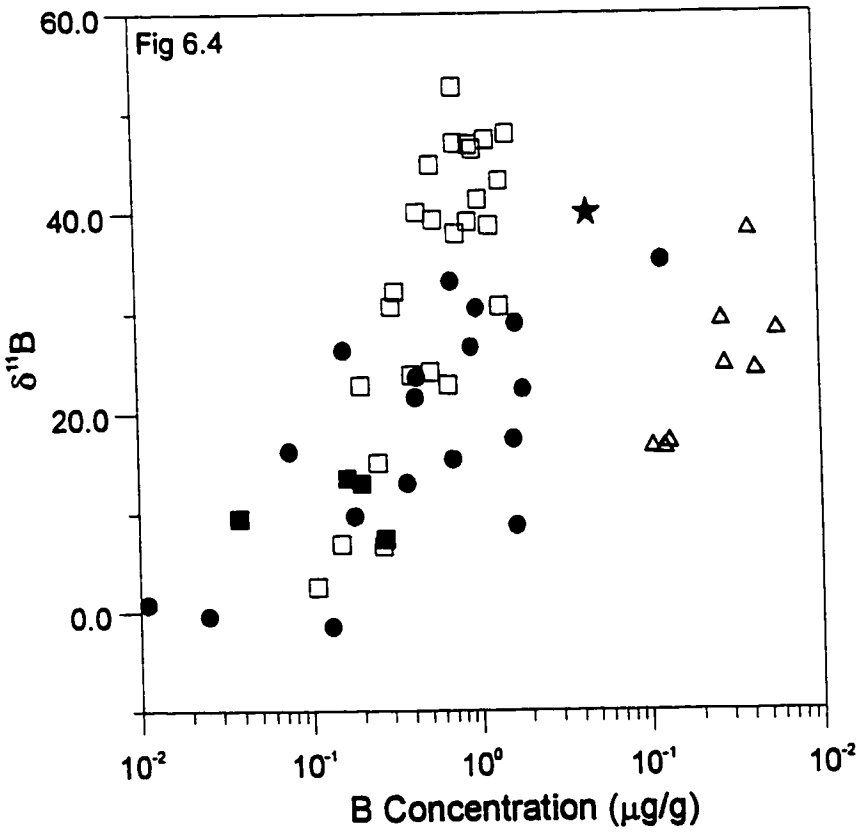
Fig 6.4
δ¹¹B
60.0
40.0
20.0
0.0
10⁻²
10⁻¹
10⁰
10¹
10²
B Concentration (µg/g)

Figure 6.5. Relationship of isotopic composition and chloride concentration in the groundwaters of the Lac Du Bonnet Batholith, mine waters of the Canadian Shield (Bottemley et al., 1994), and sea water. Symbols are the same as in Figure 6.4. The mine waters and LDB groundwaters, if considered separately, exhibit a very poor positive correlations. The LDB fracture waters are typically enriched in boron-11 relative to mine waters having a similar chloride concentration and pore fluids are depleted relative to fracture water samples having similar chloride concentrations.

Figure 6.6. Relationship of bromide and chloride in the groundwaters of the Lac Du Bonnet Batholith, mine waters of the Canadian Shield (Bottemley et al., 1994), and sea water. Symbols are the same as in Figure 6.4. The similarity of the Br/Cl ratios in fracture waters and pore fluids is evidence for a common origin of the two fluids and the horizontal trend between the pore fluids and more dilute fracture waters, can be interpreted as a simple dilution of a pore fluid end member. The Br/Cl ratio of the SW Manitoba are distinct from both the mine waters and the LDB groundwaters having ratios lower than present-day seawater.

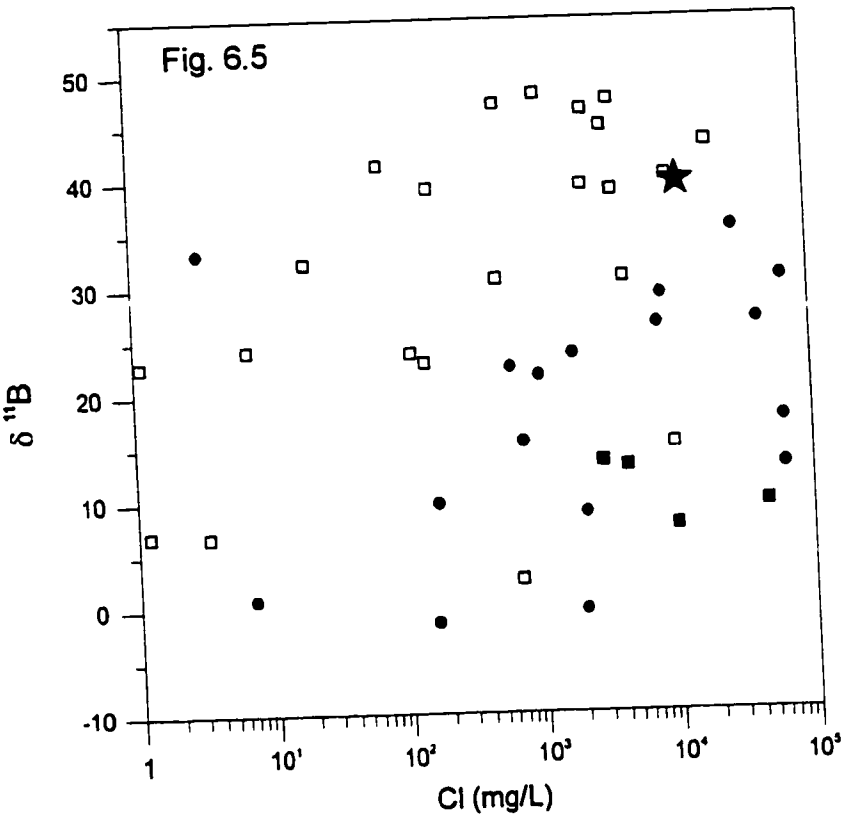
Fig. 6.5
δ 11B
50
40
30
20
10
0
-10
1
10¹
10²
10³
10⁴
10⁵
Cl (mg/L)

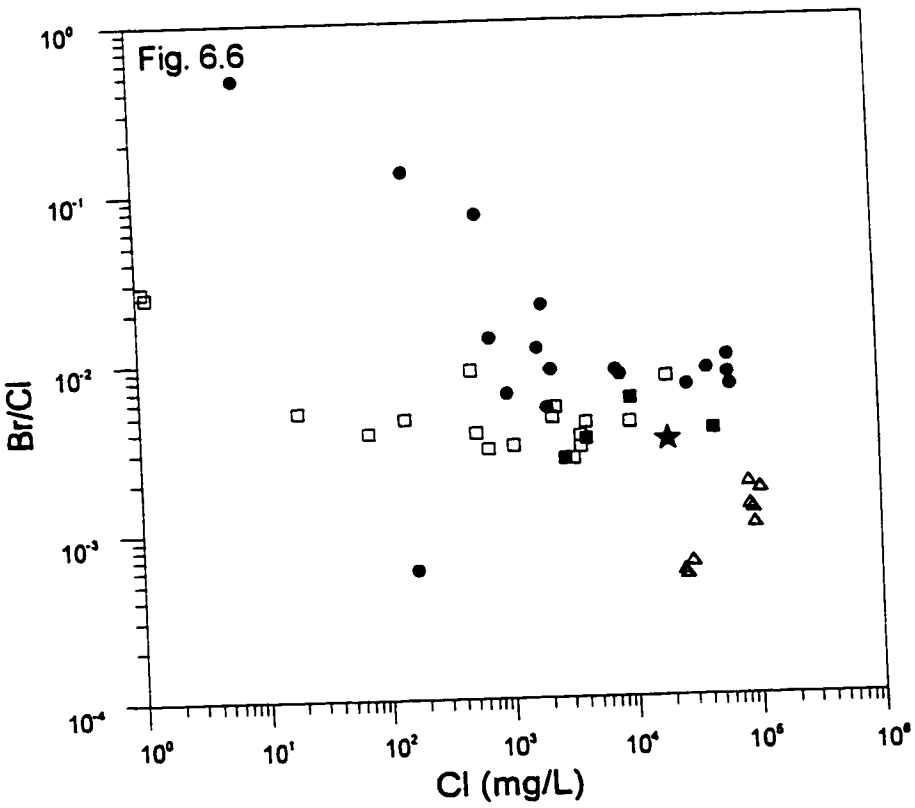
Fig. 6.6
Br/Cl
10⁰
10⁻¹
10⁻²
10⁻³
10⁻⁴
10⁰
10¹
10²
10³
10⁴
10⁵
10⁶
Cl (mg/L)

6.2.2 Boron in whole rock and minerals

Boron concentrations and isotopic compositions were determined for whole rock samples of grey granite, pink granite and mineral separates of K-feldspar and plagioclase. Isotopic analysis of boron from biotite was attempted but no results were obtained. The concentrations determined from whole rock samples are given in Table 6.2. As stated in section 5.2.1, significant loss of boron occurred during whole rock and mineral sample preparation. The resulting low yields may well have affected the accuracy of the isotopic analyses, however, despite the possible error introduced in the $\delta^{11}B$ of the silicate sample analyses, resulting errors in the determination of boron concentrations using isotope dilution should be minor. Therefore, it is believed that concentrations in this study are representative of the concentrations in the granite. Based on the small number of whole rock and mineral separates analysed, there is no significant difference in the concentrations between the grey granite, pink granite and feldspars. No distinction can be made isotopically between mineral separates and whole rock, with the exception of the altered pink granite which exhibits higher $\delta^{11}B$ than the other silicate samples.

Table 6.2. Boron isotopic composition and boron concentrations in Whole rock samples and mineral separates from the Lac Du Bonnet Batholith

Table 6.3. Boron isotopic composition and concentration of southwest Manitoba oil field brines.

Rock Type	Sample Name	$^{11}B/^{10}B$	$\delta^{11}B$	Concentration	Duplicate
Grey	401-1	4.033	-2.7	6.4	
	GC2-18	4.039	-1.2		
	403-A1	4.035	-2.0		
	MB2-1	4.015	-7.2	1.7	1.7
	GC2-19	4.027	-4.1	1.3	
	GC1-1	4.016	-6.9	2.0	
	URL2-791	4.031	-3.1		
Pink Granite	HC11-31	4.082	9.5	3.7	3.4
	HC29-17	4.080	9.0		
K-feldspar	403-A2 FSP	4.033	-2.5		
	403-A6 FSP	4.025	-4.5		
	GC1-1 FSP	4.024	-4.9	0.7	
Plagioclase	GC1-1PLAG	3.988	-13.8	1.9	
	200-APLAG	4.015	-7.0	4.5	
	403-A2PLAG	4.024	-4.9	4.5	

Sample	$^{11}B/^{10}B$		$\delta^{11}B$	Conc. (μg/g)
1062.1	4.1222	(1)	29.2	27.3
1076.1	4.1023	(1)	24.2	43.1
1058.1	4.1171	(1)	27.9	57.4
1080.1	4.0712	(1)	16.5	12.5
1078.1	4.0716	(1)	16.6	10.6
1064.1	4.1042	(1)	24.7	28.4
1070.1	4.1583	(1)	38.2	40.4
1054.1	4.0734	(1)	17.0	13.3

6.3 Discussion

6.3.1 Fracture waters

There is a positive correlation between boron concentration and $\delta^{11}B$ in the fracture waters. This can be interpreted as mixing of two groundwater end members, whose boron content is derived from two distinct sources (Fig. 6.4). One end member is characterized by a low boron concentration and a low $\delta^{11}B$ ($\approx$5 ‰). The low $\delta^{11}B$ suggests that its boron is mainly derived from a terristrial source (ie. the dissolution of minerals). The relationship between B concentration and Cl (Fig. 6.3) indicates that this end member represents a dilute and shallow groundwater, most likely of meteoric origin. Surface waters infiltrating to shallow depths would dissolve small amounts of minerals resulting in the low boron concentrations and low $\delta^{11}B$-values seen in these shallow fracture waters.

The second end member is characterized by a relatively high boron concentration and ^{11}B-enrichment ($\delta^{11}B \approx 45$ ‰) and is typical of deeper more saline fracture waters. If the boron isotopic composition is used alone to interpret the origin of the boron in this end member, then its marine-like signature would suggest an allochthonous origin, the source of boron being either Paleozoic seawater or connate brines from sedimentary basins adjacent to the Canadian Shield.

However, as stated above, boron is highly reactive and isotopic values cannot be used alone in interpreting the origin of boron. Evidence for a possible allochthonous or autochthonous origin is discussed below.

It has been proposed that groundwater salinity in the Canadian shield is derived from dense, Devonian-aged residual evaporitic brines that infiltrated into the shield rocks through major faults and fracture zones (Bottomley et al. 1994). Alternately, it has been suggested that shield brines represent connate waters derived from Paleozoic aged rocks adjacent to the Canadian shield (Kelly et al., 1986)or from sediments that once overlaid the Shield but

Figure 6.7. Plot of Cl versus Br concentrations for Lac du Bonnet fracture waters (□) and pore fluids (■). Line "A" and "B" are evaporation trajectories for seawater (S). Progressive evaporation leads to gypsum (G) and halite (H) saturation. Line "C" is created by regressing all data points and represents an hypothetical mixing line between a fresh meteoric water and evaporated seawater end member (modified from Bottemley et al., 1994).

Figure 6.8. Plot of B/Cl wt. ratios versus the Cl concentrations of the Lac du Bonnet groundwaters. Symbols are the same as in Fig. 6.7.

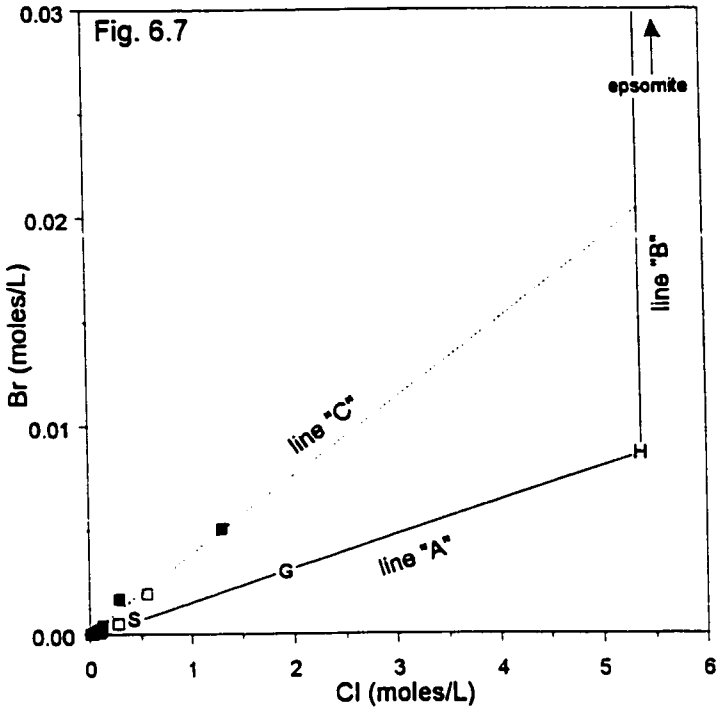
Fig. 6.7
epsomite
line "B"
line "C"
line "A"
H
G
S
Br (moles/L)
Cl (moles/L)
0.03
0.02
0.01
0.00
0
1
2
3
4
5
6

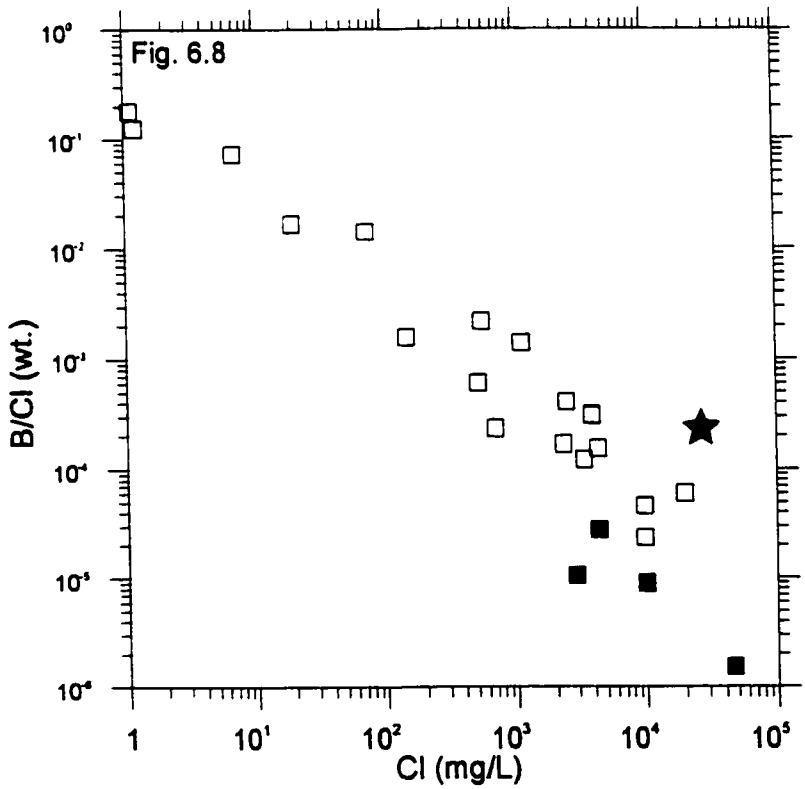
Fig. 6.8
B/Cl (wt.)
Cl (mg/L)
1
10¹
10²
10³
10⁴
10⁵

have subsequently being removed by erosion. It has been necessary to invoke an evaporitic modification of the seawater precursor because 1) the salinity of these Canadian Shield groundwaters are often higher than seawater salinity, and therefore any hypothetical marine precursor must be concentrated to obtain the salinities observed in the groundwaters; and 2) Br/Cl ratios in shield groundwaters are typically higher than ratios found in present day seawater; the enrichment of bromide relative to chloride being a characteristic of seawater that has undergone significant evaporation. During evaporation the Br/Cl ratio of the water remains constant until halite saturation is reached, at this point, continued evaporation will increase the ratio because the chloride concentration is buffered by the precipitation of halite. Due to the conservative behaviour of the halogens, this high ratio may be retained in the evolved brines. Similar to other groundwaters in the Canadian Shield , many of the fracture waters in the Lac du Bonnet batholith show Br/Cl ratios higher than present day seawater (Fig 6.6). This may indicate that Br and Cl in certain fracture waters of the LDB are derived from a marine source that has undergone evaporation. If true, the degree of evaporation can be estimated from the Br-enrichment in groundwater.

The evolution of chloride and bromide concentrations in evaporating seawater is illustrated in figure 6.7. Progressive evaporation of seawater (S) leads to gypsum (G) and halite (H) saturation (line "A") . Once halite saturation is reached, progressive evaporation will increase the bromide concentration in the residual brine while the chloride concentration remains constant (line "B"). With continued evaporation, to a degree of 60x, epsomite ($MgSO_4.7H_2O$) precipitation occurs. If it is assumed that bromide and chloride in the Lac du Bonnet groundwaters are derived from evaporated seawater then the data points in figure 6.7 represent a mixing line joining a fresh meteroic water end member with an evaporated seawater end member. The degree of evaporation of the hypothetical evaporated seawater, as represented by the Br concentration, is given by the intersection of the regressed line ("C") with line "B". Due to the similarity in bromide and chloride in the pore fluids and fracture waters and the pore fluids high salinity, pore fluid and bromide and chloride data are also

included in the regression. The estimated degree of evaporation is estimated at 25x.

Similar to bromide, boron increases in the residual brine during seawater evaporation, and as a consequence, the B concentration and B/Cl ratio increases in the solution. Along with increasing B concentration, isotopic fractionation will occur as neogenic phases are formed in the evaporating seawater. Beyond a degree of evaporation of about 30x, the $\delta^{11}B$ sea water boron will increase because of the precipitation of $MgSO_4$ and K-$MgSO_4$ salts and their selective uptake of ^{10}B. From the bromide-chloride relationship, the hypothetical evaporated seawater end member would not have been evaporated to a sufficient degree to precipitate out $MgSO_4$ salts. Therefore the similarity of the boron isotopic composition of the most saline fracture waters of the LDB to seawater is not incompatible with the model in which boron is derived from an evaporated seawater brine. In contrast, the B/Cl ratios found in fracture waters cannot be explained by an evaporated seawater model. If the seawater end member was evaporated to halite saturation, the B/Cl ratio in the end member should exhibit a higher ratio than seawater. The B/Cl ratios in the most saline fracture waters, in fact, are lower than that of seawater (Fig 6.8).

It also has been suggested that the Lac Du Bonnet saline fluids originated as connate brines from Formations in Southwestern Manitoba (Gascoyne et al., 1987). To see whether such a contribution of salinity is evident in the boron geochemistry of the LDB groundwaters, oil field brines from the late Paleozoic and early Mesozoic were analysed for B concentrations and isotopic compositions. The oil field brines exhibit high concentrations of boron (Table 6.3), which are compatible with an evaporitic origin. The isotopic ratios, however, are low, with most $\delta^{11}B$ - values being less than +30‰. Considering the probable marine origin of these fluids, the low $\delta^{11}B$ - values are unexpected. Possible causes for the lower $\delta^{11}B$ are modifications of connate brine by the dissolution/alteration of silicate, carbonate or evaporitic minerals having lower $\delta^{11}B$ compositions. This is supported by the Br/Cl ratios in the Manitoba brines. They are significantly lower than that of seawater and more characteristic of a marine precipitate, than a evaporitic residual brine (Fig 6.6). Similar modifications to

other isotopic systems have also been found in sedimentary basin brines. For example, formation waters are commonly enriched in ^{18}O relative to sea water. It has been proposed that this enrichment is a result of isotopic exchange between water and ^{18}O-rich phases such as carbonate minerals and silicate minerals (Clayton et al., 1966; Knauth et al., 1980; Longstaffe, 1987).

The low $\delta^{11}B$-values of the oil field brines are distinctly different from what is found in the Lac du Bonnet. Consequently, boron content in the LDB groundwater, cannot be explain by a simple infiltration-dilution model. If the Manitoba brines were the source of boron in the LDB groundwaters and boron behaved conservatively, then B/Cl and $\delta^{11}B$ in the Manitoba brines and the LDB groundwater should be similar. As can be seen in Figure 6.5, this is not the case.

It is possible that the Manitoba brines have contributed to salinity in the LDB groundwaters and that the low [B] and low B/Cl relative to the brines reflect the sorption of boron onto fracture minerals. If the parent brine contained B concentrations similar to the oil brines, adsorption would have to be an extremely efficient process to reduce these concentrations to the low values now present in the Lac du Bonnet Batholith (ie. > 96% removal of B from solution) . Moreover, because of preferential sorption of ^{10}B, massive boron sorption would be accompanied by Rayleigh distillation effects leading to ^{11}B enrichment in the solution. For example, if a basin brine having a boron concentration of 30 μg/g, has most of its boron removed, so that the final brine has a concentration of 1 μg/g, the expected $\delta^{11}B$ in the final solution would be >150‰. This is assuming a fractionation factor of 0.963, and an initial $\delta^{11}B$ of 14‰. Such large enrichment in ^{11}B is not observed in the LDB groundwaters.

Based on the differences in Br/Cl ratios, boron isotopic composition and concentration between the LDB fracture waters and the Manitoba brines, the boron content in the fracture waters cannot be attributable to the infiltration of Manitoba brines into the batholith. As stated above, evaporated seawater is also an improbable source of boron in the

LDB groundwaters due to the low B/Cl ratios compared to seawater, therefore, it is improbable that boron in the LDB fracture waters has a marine origin.

6.3.2 Evidence for an autochthonous origin of boron.

It may be argued that the boron in the LDB waters is entirely of autochthonous origin and has been isotopically fractionated to heavier $\delta\ ^{11}B$ values by boron adsorption onto fracture minerals. This hypothesis is appealing because the low B concentrations are more compatible with the low concentrations determined for the whole rock and minerals of the Batholith. Furthermore, there are very poor correlations between chlorinity and boron concentration, and chlorinity and $\delta^{11}B$. This lack of correlations indicates that the processes governing the isotopic composition of boron and it's concentrations are not related to the controls on the chlorinity of the groundwaters of the Lac du Bonnet Batholith. Such 'decoupling' of boron from the more conservative element chloride, suggests that boron of LDB groundwaters has not behaved conservatively, having being modified by water-rock interactions. In this regard, the boron isotopic composition of the groundwater is unlikely to reflect the original isotopic composition of a precursor fluid.

A further problem arises in the allochthonous model, when the pore fluids and their relationship to the fracture waters are considered. In the LDB, some of the most saline groundwaters are the pore fluids. If boron is of marine origin, then it would be expected that the boron isotope compositions and concentrations of these fluids would more closely reflect a marine origin than the less saline fracture waters. It is apparent that the opposite is true, the fracture water exhibits a marine-like signature, while the pore fluid's boron composition is more characteristic of boron derived from a terrestrial origin. A simple interpretation would be that the fracture waters are marine in origin, while the pore fluid salinity is terrestrial (ie. deuteric or hydrothermal in origin) and that little or no mixing between the two water types has occurred. It is unlikely, however, that two separate saline waters, having distinct origins,

could remain isolated from each other for 500 million years (assuming that the deeper waters are Devonian-aged brines).

There is evidence indicating that pore fluids do contribute to the fracture water salinity. Gascoyne et al. (1989a) measured the chloride content in intergranular pores in the Lac du Bonnet Granite adjacent to a fracture. They showed that the chloride content in pores decreased towards the fracture. Additional evidence is the similarity between the Br/Cl ratios of the pore fluids and the fracture waters. The similarity in the halogens compositions of the pore fluids and fracture waters is in contrast to the differences in cation composition between the two water types. Due to the conservative chemical behaviour of Br and Cl and the relatively low concentrations of the elements found in granite, the halogens are not as susceptible to water-rock interaction as are cations. In this respect, the similar Br/Cl ratios may indicate a common origin for the halogens in the two water types. The pore fluids may have contributed a significant portion, if not most of the chloride and bromide to the fracture waters. If true, then pore fluid boron, must also be contributing to the fracture waters. Since, the pore fluids are depleted in boron relative to the fracture waters, they could not produce the higher concentrations seen in the fracture waters. Therefore, a secondary boron source is required to explain the elevated concentrations in the fracture waters relative to the pore fluids. The most obvious source is boron derived from the dissolution and alteration of minerals in the fracture zones.

Finally, the boron chemistry in the LDB groundwaters can be interpreted in the context of Canadian Shield groundwaters. The mine waters and the LDB groundwaters exhibit a relatively constant boron concentration over a wide range of salinities, rarely exceeding 2 μg/g (Fig. 6.5). This is more indicative of element being buffered by reactions in the groundwater system than dilution of a marine end member.

If the boron is terrestrial in origin, then the high $\delta\ ^{11}B$-values in the fracture waters must be explained. Dark red granite is present along fractures in both the pink and grey granite. It is characterized by numerous microfractures and an abundance of secondary

minerals. Biotite is altered to chlorite and vermiculite and plagioclase is altered to sericite, haematite and illite. The prevalence of low temperature minerals shows that this alteration is due to meteoric groundwater circulation (Brown and Davison, 1986). The abundant secondary clays and Fe-oxyhydroxides provides ample sorption sites for boron to be removed from solution. If significant amounts of boron is removed from solution, fractionation of boron in solution will result.

6.3.3 Controls on boron concentration in fracture waters.

When a parcel of water reacts with granite at a low temperature, boron is released into the water and contemporaneously adsorbed onto newly formed clays. This evolution can be considered in a simple model where a parcel of water progressively alters more granite such that instantaneous chemical and isotopic equilibrium are achieved but back-reaction between altered rock and fluid is not allowed. This is equivalent to a system where the continuous addition of a reactant (fresh granite), is followed by the instantaneous removal of the solid reaction products (clay). This model is similar to chemical models devised for mid-ocean ridge hot springs (Bowers et al. 1985; Bowers and Taylor, 1985) and for isotopic exchange between seawater and ocean crust (Spivak and Edmond 1987a).

If a fracture system is viewed as an "open" system, where boron is added to and removed from the fracture water by alteration of the adjacent rock, the concentration of boron in solution is dependent on the partitioning of boron between solution and clays. If equilibrium is reached between boron in solution and boron on clays, the partitioning of boron can be expressed by the equilibrium partition coefficient K_d (Palmer et al., 1987).

$$K_d = \frac{[B]_c}{[B]} \qquad \textit{eqn. } 6.1$$

where, [B] is the concentration of boron in the solution and $[B]_c$ is the adsorption density

parameter of boron adsorbed onto clay. It should be emphasised that $[B]_c$ is a measure of the mass of boron adsorbed relative to the mass of clay and *not* the concentration of structurally bound boron. This distinction is important, in the respect, that $[B]_c$ is dependent on the size of the clay particles.

If the total amount of boron in the system (the combined total of boron in solution and sorbed onto clay) remains constant, then once equilibrium has been reached the concentration in solution will remain constant. In the proposed model however, a packet of water progressively reacts with fresh granite releasing boron into solution and forming new clay surfaces. As a consequence, the total amount of boron in the system changes as the water alters additional granite. To determine the progressive changes in the boron concentration in solution, the incremental changes in the boron introduced and removed from solution must be considered.

The change in concentration of a chemical species in any aqueous environment is described mathematically by a conservation of mass equation (Wigley et al., 1978).

$$dB = \sum_{i=1}^{M} d\Gamma_i - \sum_{i=1}^{N} d\Theta_i \qquad \textit{eqn. } 6.2$$

Where dB is the change in the molality of boron in solution, $d\Gamma_i$ and $d\Theta_i$ are the molal contributions to B from M sources (inputs) and N sinks (outputs). The model is simplified further by assuming that there is only one source and one sink for boron in the system. This simplification should be a close approximation to the actual conditions found in the fracture zones, considering there are no significant differences in boron concentrations between the feldspars or whole rock. Moreover, strontium isotopic evidence suggests that much of the fracture water chemical composition is, in fact, dominated by one mineral phase (ie. plagioclase).

The mass of boron entering into solution is given by $\Gamma = M_r[B_r]$, where M_r is the mass

of rock or mineral, reacting with a mass of water W and $[B_r]$ is the concentration of boron in the rock. The amount of boron leaving the solution (Θ) by way of sorption onto clay surfaces is a function of the boron concentration in solution and the amount of clay present and the partition coefficient (equation 6.1). Therefore boron output is,

$$\Theta = \frac{M_r}{W} B K_d \qquad \textit{eqn. } 6.3$$

Since both the input and output of boron into solution is now related to the amount of rock altered (M_r), equation 6.2 can now be solved with respect to M_r/W, the amount of rock altered for a given mass of water. The solution of equation 6.2, where the amount of boron in solution is expressed as boron concentration is (see appendix 1.1 for full derivation of model),

$$[B] = \frac{[B_r]}{K_d}\left(1 - e^{-K_d\left(\frac{M_r}{W}\right)}\right) \qquad \textit{eqn. } 6.4$$

As a packet of initially boron-free water reacts with ever increasing amounts of rock, the boron concentration in solution increases (Fig. 6.9). A consequence of equation (6.4) is that, the boron concentration of the aqueous phase must tend to a limiting or asymptotic value. For large reaction progress the aqueous boron concentration tends to the limit $[B] = [B_r]/K_d$. Although the variable $[B_r]$ can be determined by isotope dilution, partition coefficients must be estimated empirically from experimental results.

Partition coefficients have been determined under varying experimental conditions of temperature, clay mineralogy, grain size, boron concentrations of the solutions, and ionic strength of solutions (Schwarcz et al., 1969; Palmer et al. 1987; Keren and Mezuman, 1981; Shivi and Mattigod, 1992). This variability in conditions is evident in the range of K_d - values

Figure 6.9. Model of the change in boron concentration in a solution that reacts with plagioclase having a boron concentration of 3.7 μg/g. R/W is the integrated rock/water ratio, where R is the total amount of rock that has reacted with a mass of water (W). Assuming an initial boron concentration of 0 μg/g, the boron concentration increases in solution with the progressive reaction of the plagioclase until the concentration approaches an asymptotic value. The asymptotic value is dependent on both the boron concentration in the plagioclase and the bulk partition coefficient (K_d) of boron between solution and clays. The model is plotted for values K_d = 2, 5, 10.

Figure 6.10. Model of the change in the isotopic composition of boron in a solution reacting with plagioclase having a boron isotopic composition of 4.035 and a boron concentration of 3.7 μg/g. The isotopic ratio in solution increases from an initial composition of 4.035 and with progressive reaction approaches an asymptotic value, which is dependent on the isotopic composition of the plagioclase and the equilibrium fractionation constant (α) of the system. The model is plotted three times using α = 0.96, 0.97, 0.99.

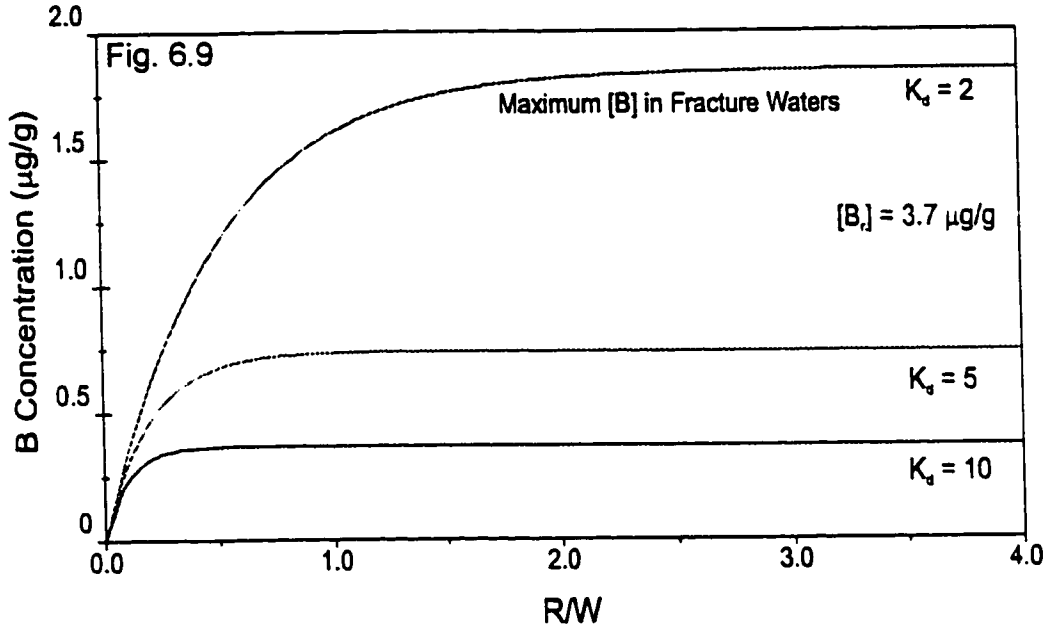
Fig. 6.9
Maximum [B] in Fracture Waters
K_d = 2
$[B_r]$ = 3.7 µg/g
K_d = 5
K_d = 10
B Concentration (µg/g)
2.0
1.5
1.0
0.5
0
0.0
1.0
2.0
3.0
4.0
R/W

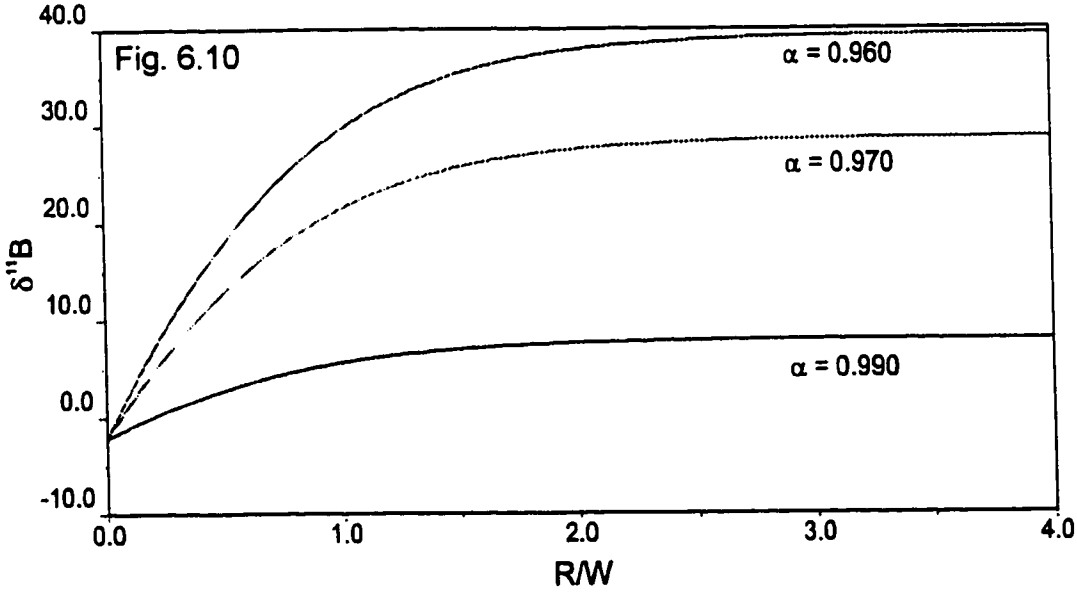
Fig. 6.10
α = 0.960
α = 0.970
α = 0.990
$\delta^{11}B$
40.0
30.0
20.0
10.0
0.0
-10.0
0.0
1.0
2.0
3.0
4.0
R/W

determined (0.75 to 10), therefore, the partition coefficient chosen for the model must be appropriate for the conditions found in the Lac du Bonnet fracture waters. The study that best approximates these conditions is Palmer et al., (1987). They determined the K_d values using Mississippi delta sediment consisting of mixed layer illite-smectite, and discrete illite and kaolinite in a sea water solution under pH conditions ranging from 6.75 to 7.8. Although the salinity in the fracture waters does not reach the concentration of seawater, the most saline fluids do exhibit very high TDS contents (up to 25 g/L). The *p*H values measured in the fracture waters are also similar to the experimental conditions of Palmer et al. (1987). The K_d-values determined, range from 1.4 to 2.6, with the increase of K_d related to the increase in the alkalinity of the experimental solution. An average K_d value of 2 is therefore used in equation 6.4.

If it is assumed that plagioclase is the main contributor of boron having a $[B_r]$ of 3.7 µg/g, the average boron concentration in the LDB plagiocase separates, then the predicted maximum concentration attainable in solution would be 1.85 µg/g. The highest boron concentration measured in the fracture waters is 1.6 µg/g, close to this theoretical maximum. Considering the possible variations in clay mineralogy, the presence of other adsorption substrates, such as Fe-oxyhydroxides where the degree of partitioning is unknown, and changes in *p*H, the predicted solution concentration, is very similar to the predicted value.

This process may also explain the consistently low boron concentrations in the Canadian Shield mine waters. Although the B contents in the host rocks from the mine water sampling sites is not known, it is probable that the B concentrations of the rocks would not be drastically different than the estimated average for the continental crust, about 10 ppm (Chaussidon and Albared, 1992).

6.3.4 Controls on boron isotopes in fracture waters.

Adsorption of boron onto clays will result in the enrichment of ^{11}B in solution and ^{10}B

on clay surfaces. It would be expected that the progressive alteration of rock to clays would result in the increasing enrichment of ^{11}B in solution. However, alteration also will lead to the contribution of rock boron into solution. The change in an isotopic species can also be described mathematically using conservation of mass (equation 6.2). Instead of solving the equation for the molality of total boron, it is solved for the molality of boron - 11 , so that:

$$d(^{11}B) = \sum_{i=1}^{M} d\gamma_i - \sum_{i=1}^{N} d\theta_i \qquad \textit{eqn.}\ 6.4$$

where ^{11}B is the molality of boron - 11 in solution, $d\gamma_i$ is the molal input of boron- 11 and $d\theta_i$ is the molal incremental output of boron - 11. The small finite changes in the input and output of boron - 11 contribute to an incremental change in $d(^{11}B)$. Boron -10 can be included into equation so that:

$$d(R\,^{11}B) = \sum_{i=1}^{M} R_i^{*}\, d\gamma_i - \sum_{i=1}^{N} R_i^{\dagger}\, d\theta_i \qquad \textit{eqn.}\ 6.5$$

where R is the ratio of molalities of boron - 11 to boron - 10 ($^{11}B/^{10}B$) in solution, R^* is the input isotopic ratio and $R^{\dagger}$ the output isotopic ratio. It is assumed that isotopic equilibrium exists between all dissolved boron-bearing species in solution and that all outputs are in isotopic equilibrium with the parent solution, so that

$$R^{\dagger}_i = R\alpha \qquad \textit{eqn.}\ 6.6$$

where α is the equilibrium fractionation factor between the i-th output and the solution. With this assumption, the defining differential equation used to predict isotopic evolution becomes:

$$d(R^{11}B) = \sum_{i=1}^{M} R_i^* \, d\gamma_i - \sum_{i=1}^{N} R\alpha \, d\theta_i \qquad \textit{eqn. } 6.7$$

A solution to equation 6.7 is meaningful if, over a segment of reaction progress, the input isotopic composition, R^*_i, the output fractionation factors, α, and the relative rates of input to output remain constant. Equation 6.7 was solved for R using finite difference methods and a Personal Computer. The finite difference solution and the code is given in appendix 1.3.

The degree of isotopic fractionation between boron in solution and boron sorbed onto clay is expressed as a fractionation factor (α). Boron fractionation factors determined empirically, range from 0.957 to 0.975 (Schwarcz et al., 1969; Palmer et al., 1987). Progressive alteration of rock causes the $^{11}B/^{10}B$ ratio in solution to approach a asymptotic value (Fig. 6.10). This isotopic asymptotic value is closely approached when, 1) the amount of boron entering into solution is equal to the amount of boron leaving the solution and 2) the isotopic ratio of boron entering into solution is the same as the isotopic ratio of boron leaving the solution. Once these conditions are met then the isotopic ratio in solution is simply represented by the equation,

$$R = R^*/\alpha \qquad \textit{eqn. } 6.8$$

This limiting value is highly sensitive to the fractionation factor and the isotopic composition of the boron input (ie the $\delta^{11}B$ of the altering mineral). The difference between 0.957 and 0.975 results in a change of the asymptotic value from 35.7 to 16. 1 ‰, respectively, assuming the main contributor of boron to solution is plagioclase, having a isotopic value of -8.8‰. The highest $\delta^{11}B$ in the fracture waters are higher than the highest asymptotic value calculated for the model. This discrepancy may be a result of the accuracy

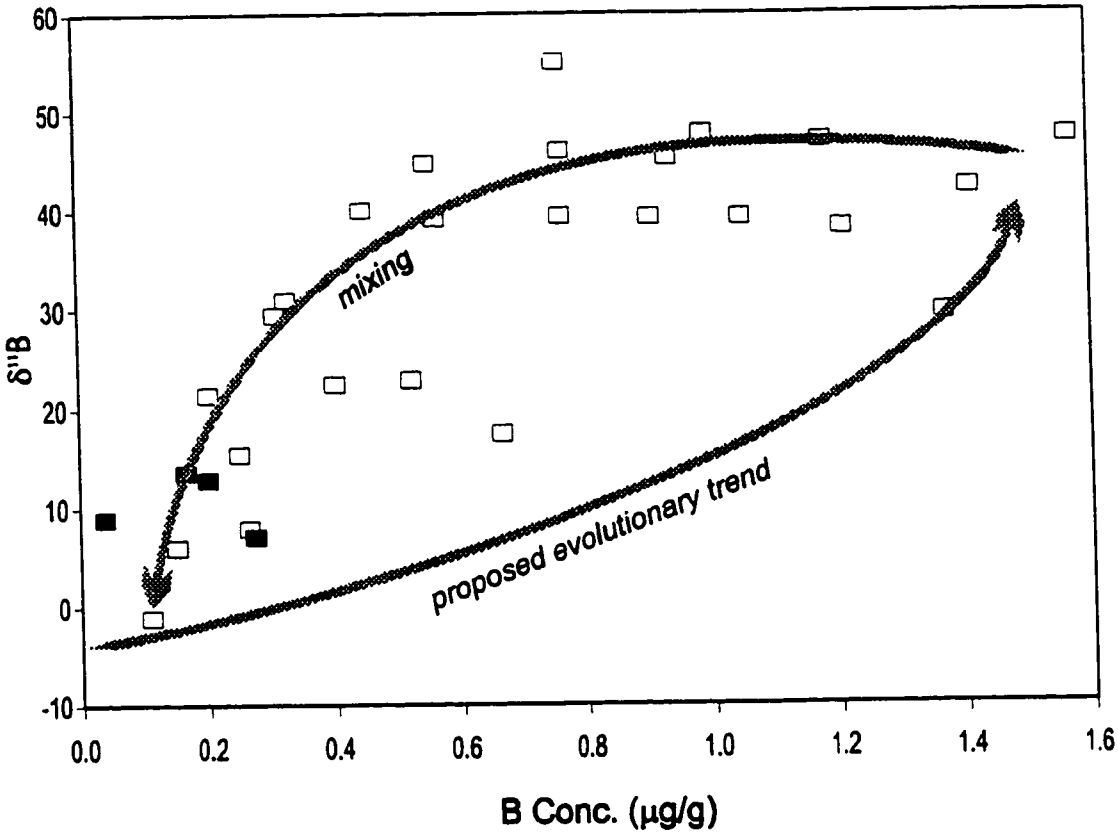

Figure 6.11. The proposed evolutionary trend of boron concentration and isotopic concentration based on a fractionation factor (α) of 0.960, a boron concentration in plagioclase [B]$_r$ of 3.7 µg/g, and a partition coefficient Kd of 2.5. The trend is superimposed onto groundwater data from the Lac du Bonnet Batholith. Although the model explains the formation of the fracture waters with the highest concentrations and ^{11}B, the distribution of groundwater data is more indicative of mixing. The presence of mixing is supported by other geochemical indicators such as TDS, Ca, and Sr (Li, 1989).

of the calculated average $^{11}B/^{10}B$ entering into solution. The average isotopic composition of plagioclase was calculated from only 3 plagioclase separates. If it is assumed that the boron isotopic composition is essentially uniform for all phases in the batholith then an average calculated from all analysis of whole rock and feldspar boron isotopic analyses (≈ -3.4) may be more representative of the $^{11}B/^{10}B$ entering into the fracture waters. This small increase in the calculated average would result in a new asymptotic value of 41.5 ‰, well within the region defined by the highest fracture water values.

If the boron chemistry in the fracture waters is solely dependent on the degree of water-rock interaction, that is, the integrated R/W, that each packet of water has experienced, then the $\delta^{11}B$ and [B] distribution of the fracture waters should correlate with the trend predicted by the model. As can be seen in Figure 6.11, the fracture waters, exhibit a greater degree of ^{11}B-enrichment for a given boron concentration, than is predicted by the model. This discrepancy may be due to mixing occurring within the fracture system of the batholith. Mixing between fracture zones is supported by correlations between TDS, Ca, Sr, HCO_3 and SO_4 (Li, 1989). Although the model does not explain the general trend in the data, it does explain the ^{11}B-enrichment and low boron concentrations in the fracture waters. In this respect, the fracture waters having the higher B concentrations and the highest ^{11}B-enrichment may represent older waters that have undergone a greater degree of water rock interaction than the fracture waters with lower B concentrations and lower $\delta^{11}B$ -values.

6.3.5 Controls on boron concentration and isotopes in pore fluids.

Due to the limited data on boron in the pore fluids and in minerals, one can only speculate on the origin of the low boron concentrations and isotopic composition of the pore fluids relative to the fracture waters. The low isotopic compositions indicate that a large component of the boron is terrestrial (ie. rock derived); this fits well with the strontium isotopic data that shows a whole rock isotopic signature (Fig. 6.12) , however, the boron

Figure 6.12. Boron and strontium isotopic composition of groundwaters in the Lac du Bonnet Batholith. Fracture waters (□) show a small increase in $^{87}Sr/^{86}Sr$ with increasing $^{11}B/^{10}B$. The pore fluids (■) distinct from the fracture waters by their enrichment in radiogenic ^{87}Sr. Shaded region represents the whole rock isotopic composition of the Lac du Bonnet granites.

Figure 6.13. $\delta\ ^{18}O$ vs. δ D plot of various fluids. URL pore fluids plot above the Global Mean Water Line (GMWL) and lie in the region defined by the extrapolation of the Canadian Shield mine waters (Sudbury and Yellowknife)(Fritz and Frape, 1982). Positioning of pore fluids (■)that isotopic equilibrium has been established between fluid and silicate minerals. All additional information is from Kerrich and Kamineni (1988). The WNRE groundwaters are from the WhiteShell Nuclear Research Site.

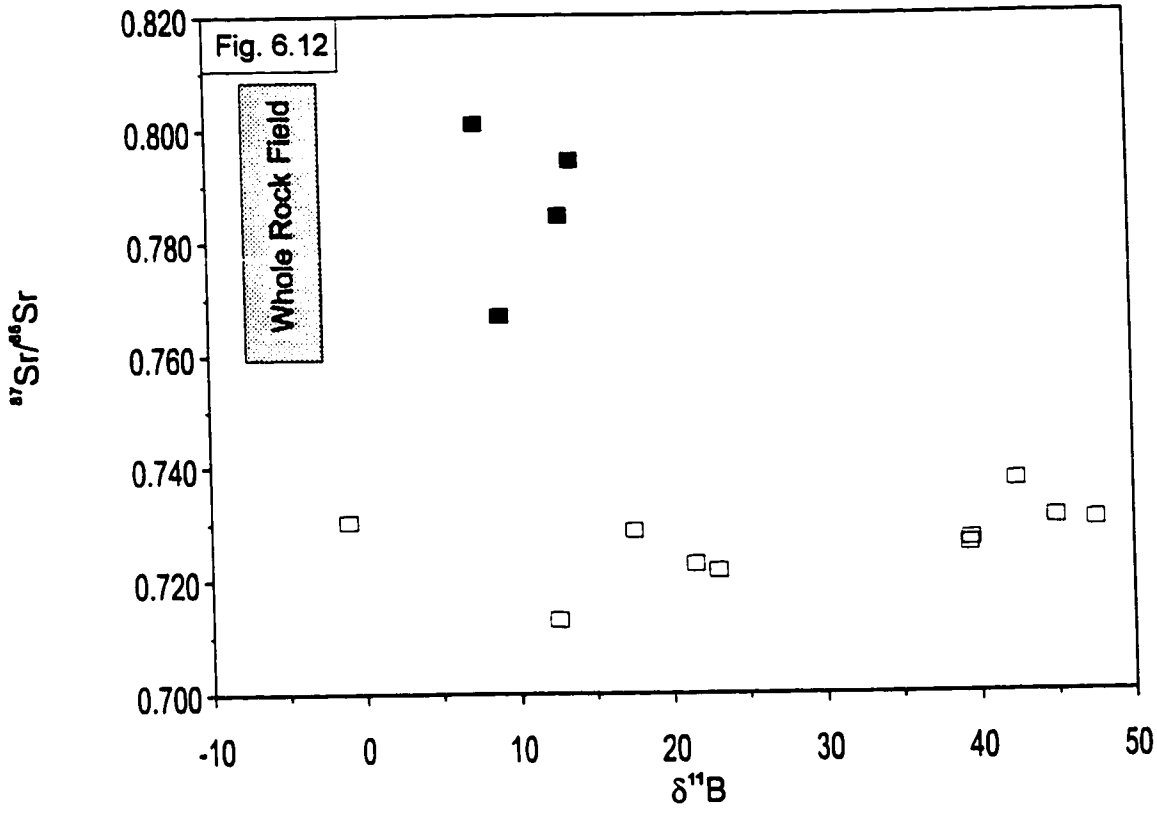
Fig. 6.12
Whole Rock Field
0.820
0.800
0.780
0.760
0.740
0.720
0.700
$^{87}Sr/^{86}Sr$
-10
0
10
20
30
40
50
$\delta^{11}B$

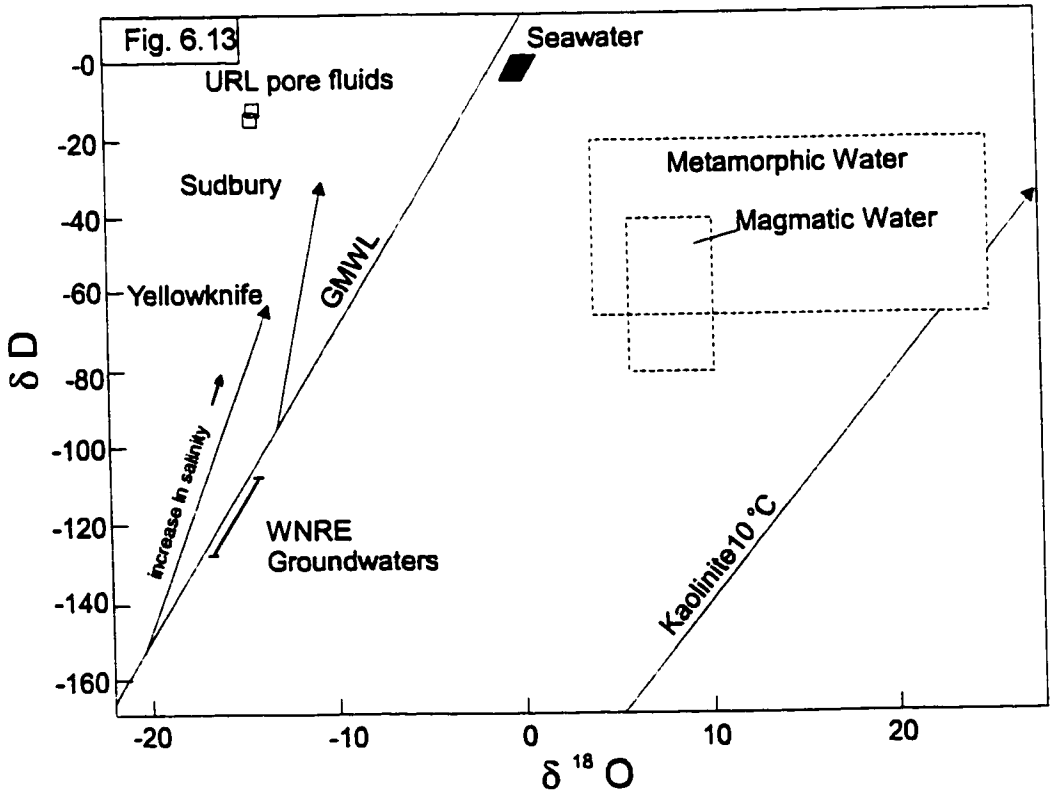
Fig. 6.13
Seawater
URL pore fluids
Sudbury
Yellowknife
GMWL
Metamorphic Water
Magmatic Water
increase in salinity
WNRE
Groundwaters
Kaolinite10 °C
-0
-20
-40
-60
-80
-100
-120
-140
-160
δ D
-20
-10
0
10
20
δ 18 O

isotopic composition of the pore fluids are still enriched ^{11}B relative to the whole rock. The *p*H has not been analysed in any of the pore fluid samples and therefore it can not be determined whether $B(OH)_3$ or $B(OH)_4^-$ is the dominant species. If the pore fluids do represent a closed system, the pore fluids are likely alkaline due to the hydrolysis of the feldspar minerals. At high *p*H (>9), $B(OH)_4^-$ would be the only species present in the fluid. From experiments of Palmer et al., (1987), the fractionation factor for $B(OH)_4^-$ is 0.996, close to unity. Accordingly, the pore fluids would be enriched in ^{11}B with respect to the altering plagioclase, but not to the extent seen in the more acidic fracture waters. Alkaline conditions may also explain the low [B] concentrations in the pore fluids due to the greater degree of $B(OH)_4^-$ sorption onto clay minerals compared to $B(OH)_3$.

Another possible sink for the boron in the pore fluids is the formation of neogenic albite. It has been suggested that albitization is an important control on the major cation chemistry in the pore fluids. Although plagioclase does not typically contain significant amounts of boron, plagioclase formed under low temperature conditions may have boron as a major component. For Instance, reedmergnerite ($NaBSi_3O_8$) which is isostructural with low albite, has been found in unmetamorphosed dolomitic oil shales (Applemen and Clark, 1965; Milton et al., 1960.).

6.3.6 Interpretation of other isotope systems

In addition to the boron and strontium isotopic systems, other systems may also indicate isotopic equilibrium between pore fluids and minerals has been achieved. Two water samples from 413-033- SM7-28 have $\delta^{18}O$-values of -14.73 and -14.60, and δD-values of -18.54 and -16.54 (pers. comm. M. Gascoyne) and plot above the Global Mean Water Line (GMWL). The only other groundwaters known, to plot above the GMWL are the Canadian Shield mine waters (Fritz and Frape, 1982). Mine waters sampled from different mine regions within the Shield form distinct mixing arrays between shallow and dilute meteoric

Figure 6.14. The 3 mixing end members as defined by Li (1989). Fracture Zone 3 waters (□) are meteoric in origin, while Fracture Zone 2 waters (+) are a mixture of ^{18}O-enriched meteoric waters and a depleted end member interpreted as glacial melt. Fracture Zone 1 waters (●) are derived from glacial melt and a 3rd end member enriched in ^{87}Sr and ^{18}O. The origin of the 3rd end member was unknown.

Figure 6.15. Reinterpretation of the 3 mixing end members of Li (1989). The unknown 3rd mixing end member is interpreted to be intergranular fluids in unfractured rock (pore fluids). Fracture Zone 1 waters are more enriched in ^{87}Sr relative to Fracture zone 2, indicating a greater contribution of pore fluids to the Fracture Zone 1.

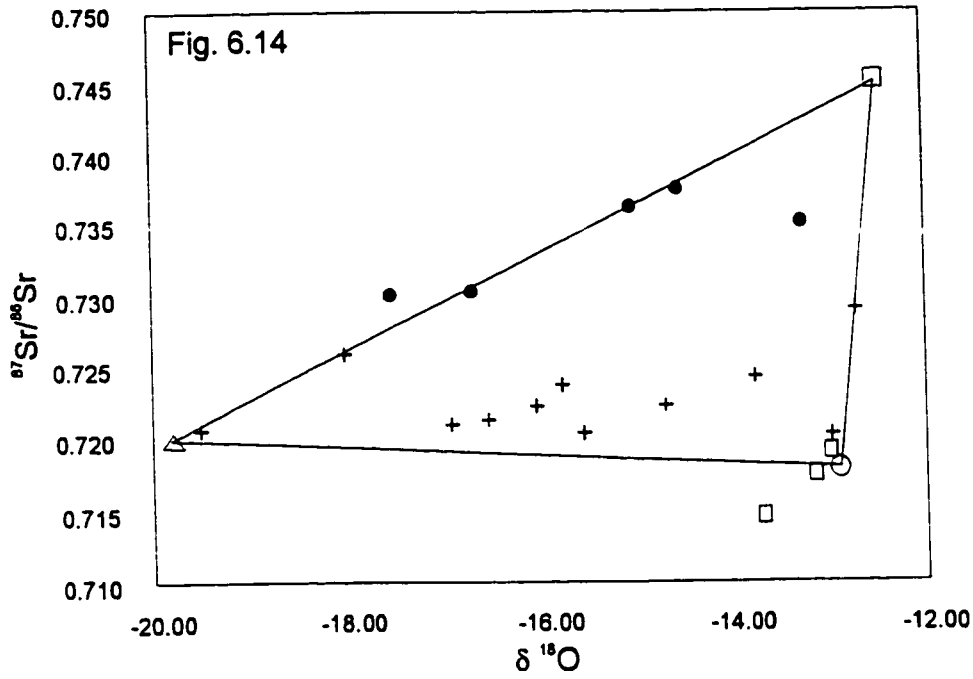
Fig. 6.14
0.750
0.745
0.740
0.735
0.730
0.725
0.720
0.715
0.710
$^{87}Sr/^{86}Sr$
-20.00
-18.00
-16.00
-14.00
-12.00
$\delta\ ^{18}O$

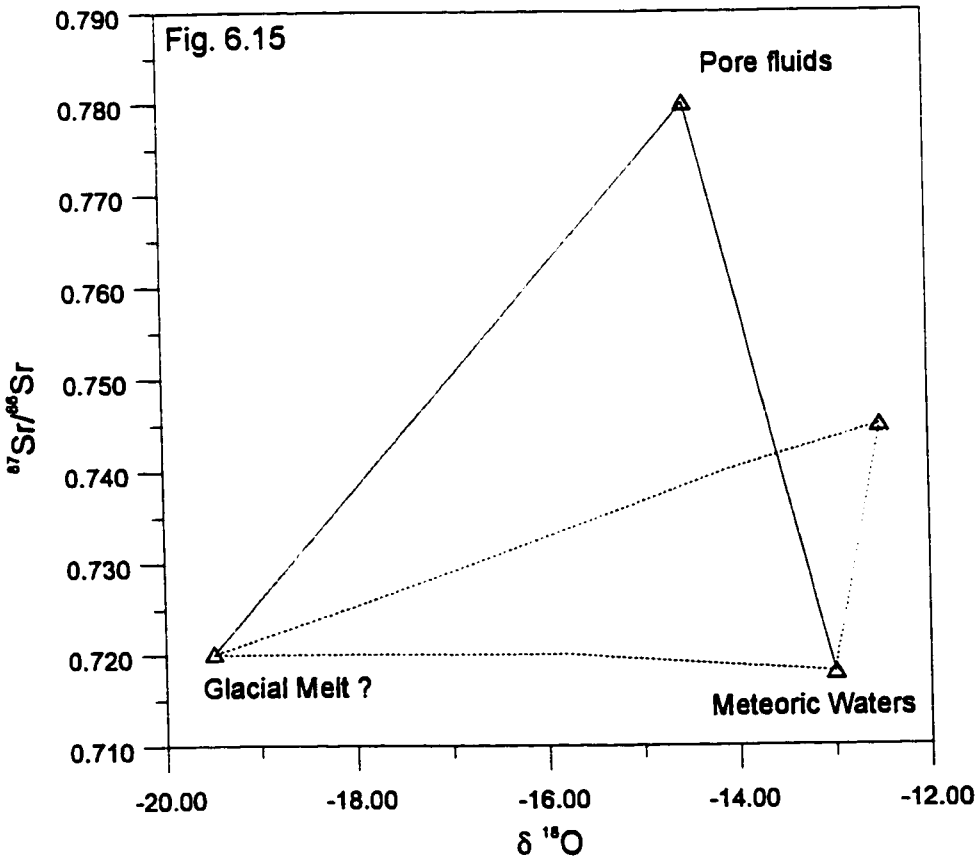
Fig. 6.15
Pore fluids
Glacial Melt ?
Meteoric Waters
0.790
0.780
0.770
0.760
0.750
0.740
0.730
0.720
0.710
$^{87}Sr/^{86}Sr$
-20.00
-18.00
-16.00
-14.00
-12.00
$\delta\ ^{18}O$

waters and deeper very saline brines. The trajectories of these trend converge towards a common brine which is depleted in ^{18}O and enriched in deuterium (Fig. 6.13). Although, the origin of this brine is unclear, it has been suggested that the isotopic signature of this brine is characteristic of a fluid that has reached low temperature isotopic equilibrium with the rocks of the Canadian Shield. The $\delta^{18}O$ and δD of the water samples from 413-033-SM7-28 plot near the region defined by the Shield's common brine and indicates that fluids located in the intergranular cavities surrounding this sampling location may have reached isotopic equilibrium. Additional information on oxygen and hydrogen isotopes is not available from other pore fluid samples, so whether isotopic equilibrium in these isotopic systems is a common attribute of the pore fluids is uncertain. Considering that strontium and boron do appear to be in isotopic equilibrium in pore fluids from different locations within the batholith, it is probable that isotopic equilibrium in $\delta^{18}O$ and δD isotopes may also be a constant feature of the pore fluids.

Due to the distinct isotopic composition of the pore fluids, contributions of pore fluids to fracture waters should be reflected in the fracture water's isotopic composition. Based on $^{87}Sr/^{86}Sr$ and ^{18}O composition of groundwaters from the URL, Li (1989) proposed that the groundwater (fracture waters) chemistries represented mixing between three end members, shallow local meteoric water; a deep fresh groundwater, which was interpreted to be glacial melt; and a deep saline groundwater of unknown origin. The three hypothetical end members were defined in $^{87}Sr/^{86}Sr$- ^{18}O space as (0.718, -13 ‰), (0.721,-20‰) and (0.745, -12.5‰), respectively (Fig 6.14). Due to the additional information collected in this study, the saline end member is now assumed to represent equilibrated intergranular fluids. The coordinates of the saline end member is therefore revised to (0.780,-14.6‰) (Fig. 6.15). The greater ^{87}Sr-enrichment in Fracture Zone 1 waters compared to Fracture Zone 2 indicates the greater proportion of pore fluid contributed to the deeper fracture zone.

CHAPTER SEVEN
FLUID INCLUSIONS AND POSSIBLE SOURCES OF SALINITY IN GROUNDWATERS

Evidence has been presented that groundwater salinity in the fracture zones has its' origin in the very saline fluids found in the intergranular cavities of the rock matrix. The primary origin of salinity in the pore fluids, however, is not known. This study has shown that geochemical tracers, such as cation ratios and isotopes, have been greatly modified by water-rock interaction, and that even at chemical equilibrium, exchange between solution and host rock continues to occur, modifying the isotopic composition of the pore fluids. Such intense water-rock interaction, precludes the use of these tracers in determining the origin of salinity in the pore fluids. What may remain relatively unchanged in the original solution is the total salinity.

Information on the paleohydrology of the granite can be obtained by investigating fluid inclusions trapped in mineral grains. By determining the salinities of the inclusions, a history of the different fluids that have been present in granite, can be developed. In unfractured rock, inclusions should be representative of fluids present in the effective porosity of the rock during entrapment of the inclusions. Successive migrations of fluid through the pore network may lead to the formation of multiple generations of inclusion salinities.

Microscopy of thin sections of grey granite reveal that aqueous inclusions are ubiquitous in quartz. Both one-phase (aqueous solution) and two-phase (aqueous solution and gas bubble) inclusions were observed, although one-phase inclusions dominate. Rarely, three-phase inclusions containing a daughter mineral were observed. Inclusions were typically 2 μ to 15 μ. The majority of the inclusions are found in healed fractures but inclusions were also observed as clusters or trails .

Final melting temperatures, Tm(ice), and homogenization temperatures, Th, were obtained for aqueous inclusions in quartz from 3 unfractured grey granite samples taken in

the depth range of 200-450 m. Melting temperatures range from 0 to -25.8 °C (Fig. 7.1). This distribution of temperature represents a wide range of salinities from essentially pure water (0 mg/L) to at least 23.3 eq. wt% NaCl as calculated from the equation of Bodnar (1993). Some of the final melting temperatures measured are lower than the $NaCl-H_2O$ eutectic temperature of -21.1°C. The presence of KCl , $CaCl_2$, or $MgCl_2$ in addition to NaCl in the inclusion fluid will depress the liquidus and eutectic temperatures below that of pure $NaCl-H_2O$. The presence of calcite daughter minerals (pers. comm. Alan Anderson) in several of the inclusions would suggest that $CaCl_2$ may be a constituent in the inclusions.

The wide range of salinities indicates that different circulating fluids have infiltrated into unfractured rock during the 2.6 Ga. history of the batholith, and that fluids in the present effective porosity have a complex history of fluid mixing. Due to the small number of rock samples taken, the possible source of the fluids, the number of fluid generations, and the extent of fluid circulation can only be speculated. Several generalizations can be made. Two-phase inclusions typically have moderate to high salinity and exhibit homogenization temperatures between 100-350 °C with a mode around 250°C (Fig. 7.2). These inclusions are interpreted to have been formed during the hydrothermal stage of the batholith's cooling from 2.0 to 0.5 Ga (Gascoyne and Cramer, 1987) . A better estimate of the time of formation using temperature of formation cannot be made due to the uncertainty of the pressure conditions during inclusion entrapment. The Lac du Bonnet batholith was emplaced at approximately 5 km depth (Gascoyne and Cramer, 1987). If the inclusions formed early on in the cooling history of the pluton, then a pressure correction of approximately 0.14 Ga is necessary to calculate the temperature of formation; assuming an average salinity of 15 eq. wt%, this is a temperature correction of 130°C, using the data from Potter (1977). This results in a temperature of formation of 380 °C (assuming T_h = 250°C). Fluid inclusions formed during the last stages of hydrothermal activity, when the pluton was near surface, may have homogenization temperatures close to the temperature of formation.

The most dilute fluid inclusions are found solely along healed fractures and typically

Figure 7.1 Frequency of Tm(ice) (melting temperatures of ice) from quartz fluid inclusions in unfractured rock sections.

Figure 7.2 Frequency of Th (homogenization temperatures) from quartz fluid inclusions in unfractured rock sections.

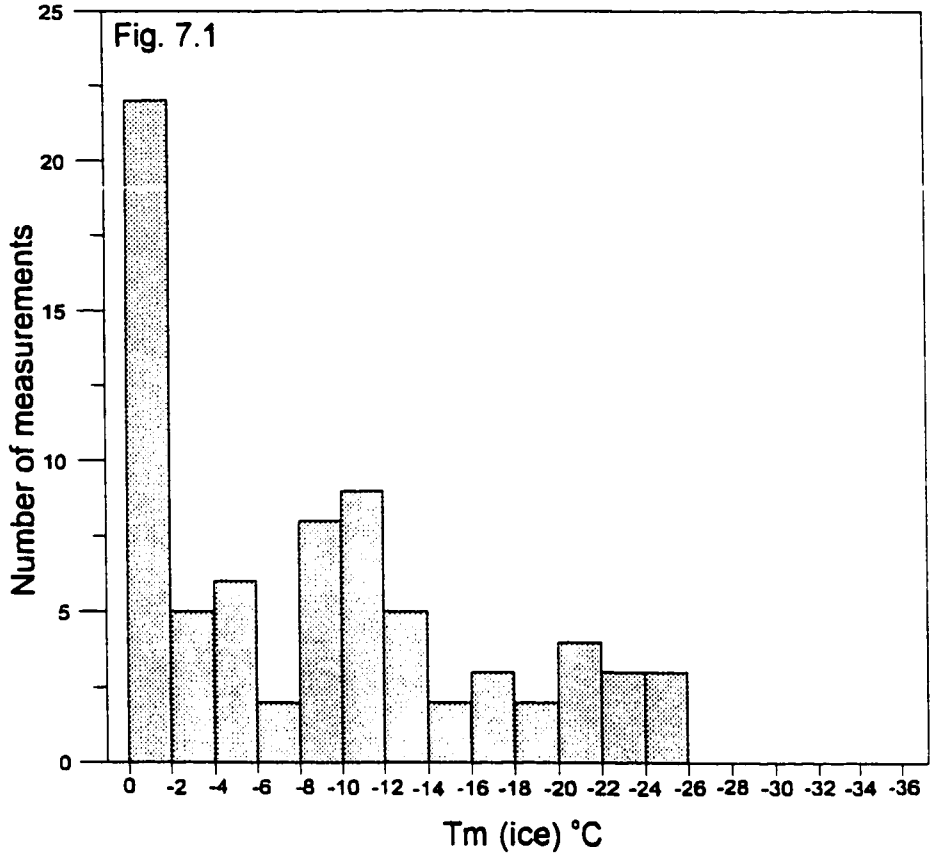
Fig. 7.1
Number of measurements
0
5
10
15
20
25
0 -2 -4 -6 -8 -10 -12 -14 -16 -18 -20 -22 -24 -26 -28 -30 -32 -34 -36
Tm (ice) °C

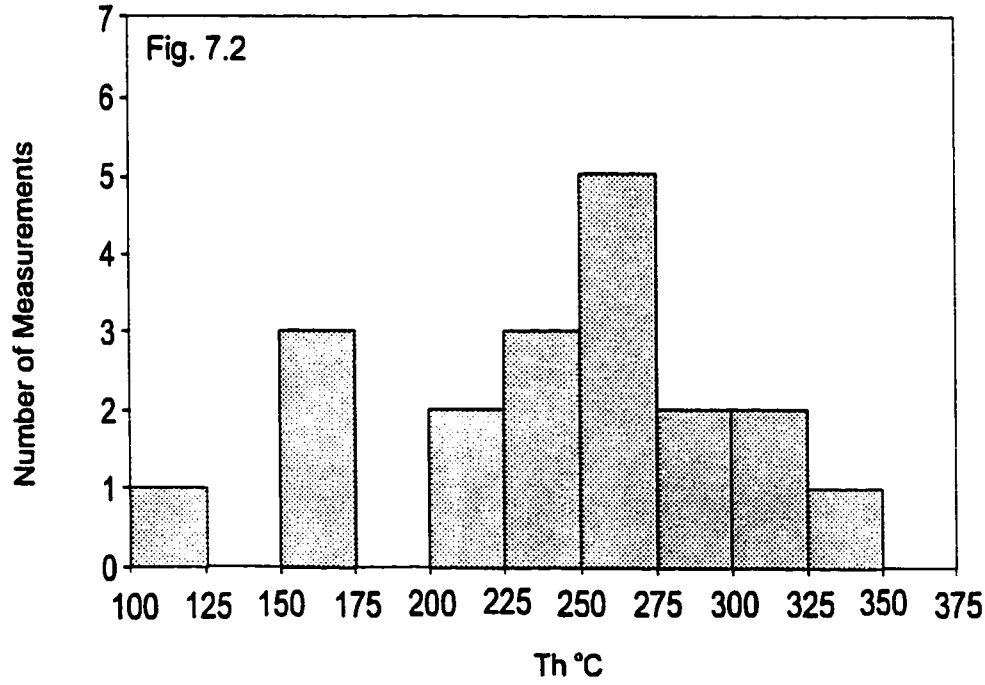
Fig. 7.2
Number of Measurements
0
1
2
3
4
5
6
7
100 125 150 175 200 225 250 275 300 325 350 375
Th °C

are only one-phase. The one-phase dilute inclusions are interpreted as low-temperature relicts that have formed in recent times (<450 Ma), however, it is still possible that the one-phase inclusions that have not nucleated a bubble at 20°C may have formed under pressure and reasonably high temperatures. In both cases, the pore network in the unfractured rock samples have experienced the influx of at least two types of fluids, an early saline fluid followed by a less saline fluid. In this regard, the pore fluids within the Lac du Bonnet at 200-450 m level are unlikely to be a product of a single precursor fluid.

It is interesting to note that, based on calculated hydraulic heads, the estimated pore fluid salinity in unfractured rock at > 1000 m in the Lac du Bonnet batholith is in excess of 200 g/L (Stevenson et al., 1996a). This value is very close to the salinities found in the most saline fluid inclusions. If such high pore fluid salinities can be confirmed by direct sampling, this may be evidence for the retention of these early formed fluids in the pore network and their isolation from later circulating meteoric water. Further evidence of the isolation of these pore fluids may be obtained by determining the salinity of fluid inclusions at depth. The absence of more recent influx of meteoric water should be reflected in the fluid inclusions by the absence of aqueous inclusions with low salinities and the predominance of salinities similar to that of the associated pore fluids. A strong correlation between pore fluids and fluid inclusion salinity would be evidence for 1) a fluid inclusion origin of the pore fluids in the deeper regions of the batholith 2) the isolation pore fluids from circulating low temperature meteoric water. Fluid inclusions have also been proposed as possible sources of salinity in the groundwaters of the Stripa granite in Sweden (Nordstrom and Olsson, 1987; Nordstrom et al., 1989).

This has implications for assessing the suitability of a body of rock as a site for a nuclear waste repository. There is a consensus that forecasting events over 10,000 years becomes very uncertain. One major factor for the uncertainty is the large environmental changes that may be brought about with the onset of ice ages which occur at 10,000-50,000 year intervals (Shemilt and Sheng, 1989). Applied stress during glaciation and the release of

stress due to isostatic rebound may cause fracturing in the rock body hosting the repository, allowing for the infiltration of dilute groundwater. Very saline pore fluids associated with very saline, mono-generational fluid inclusions may indicate a region within a pluton, where the hydrology has remained undisturbed during previous glacial events and would likely to remain so during future glaciations. A more extensive study, however, is necessary relating salinity in fluid inclusions and pore fluids before a genetic connection can be made between the two fluids.

CHAPTER EIGHT
CONCLUSIONS

Very saline fluids have been found in sparsely fractured and unfractured rock of the Lac du Bonnet batholith exhibiting chemical characteristics distinct from groundwater in the fracture zones of the batholith. They are 1) enriched in radiogenic ^{87}Sr; 2) depleted in Sr with respect to Ca; 3) depleted in Na, Sr, and Mg with respect to Cl. 4) have low $\delta^{11}B$-values and low boron concentrations. This dissimilarity in compositions between these fluids and fracture waters indicates that two distinct chemical environments are present in the Lac du Bonnet batholith. The fracture waters are strongly controlled by dissolution and alteration of minerals, in particular plagioclase. The dominance of plagioclase dissolution on fracture water chemistry is seen in the positive Na/Ca molar ratios, Ca/Sr molar ratios similar to that of oligoclase, and Sr isotopic composition of the fracture waters. Although it is probable that these groundwaters have reached partial equilibrium with the host rock (ie. equilibrium with K-feldspar) the continued dissolution of plagioclase indicates that the water-rock system has not reached chemical equilibrium. Disequilibrium would be expected in the more permeable fractured regions of the pluton, where advective transport of dissolved constituents would be relatively rapid and, in this respect, the fracture zones can be viewed as an open system.

Boron isotopes in the fracture waters exhibit a marine-like composition. Due to boron's low concentration and the relationship to other ions in solution, the source of the boron is *not* considered to be of marine origin. The low boron concentrations and boron isotopic composition are interpreted to represent an attainment of steady-state composition. Alteration of minerals, mainly plagioclase, in the fracture system releases boron into solution and forms clays which remove boron from solution. Continued removal of boron from solution increases the ^{11}B in solution as ^{10}B is preferentially sorbed onto the clay surfaces. Continued alteration will lead to steady-state concentration and isotopic composition similar to the isotopic compositions of fluids of marine origin. This model of boron exchange

between water and rock can reconcile the low boron concentrations and high $\delta^{11}B$ in the fracture waters of the Lac du Bonnet Batholith and may explain the same relationship in groundwaters of the Canadian Shield.

In contrast to the fracture waters, pore fluids are near to, or have reached, chemical equilibrium with the host rock. The evidence for this is the establishment of isotopic equilibrium between fluid and mineral surface. The differences in cation chemistry between pore fluids and fracture waters is attributed to the formation of low albite.

The nature of the pore network (ie. the narrow pore aperture, the low permeability of the granite, and the very high water volume/mineral surface ratio) makes intergranular pores a more favourable location for a fluid to attain chemical equilibrium than the fracture zones. Transport of dissolved solids is by the slow process of diffusion, the pore fluid - rock system is therefore, essentially a closed system. In addition, the time required to reach chemical equilibrium would be relatively short due to the extremely large water volume/mineral surface ratio.

Only when a rock and fluid are in chemical equilibrium can thermodynamic isotopic equilibrium be attained between fluid and mineral surfaces and so, isotopic equilibrium may be used as an indicator for chemical equilibrium. It must be noted that although a fluid having a whole rock isotopic signature signifies a fluid in isotopic equilibrium, as well as chemical equilibrium with its' host, the converse, is not necessarily true. That is, a fluid which is in chemical and isotopic equilibrium does not necessarily exhibit a whole rock signature. An affinity with the host rock is possible only when, for a given volume of fluid, the amount of Sr in the mineral surface layer available for exchange far exceeds the amount of Sr in the fluid. Therefore, the nature of a pore network makes it a more favourable environment for the attainment of a whole rock signature in a fluid than would be expected in a fracture zone.

It is probable that in the Lac du Bonnet batholith, other isotopic systems are also in isotopic equilibrium. A water sample having whole rock strontium signatures is known to have $\delta^{18}O$ and $\delta^{2}H$ values plotting above the meteoric waterline similar to mine waters of

the Canadian Shield. Fritz and Frape (1982) considered large-scale low-temperature equilibration between primary silicates and fluids as a possible cause for the unusual isotopic signature of the mine waters but favoured a exchange process involving the hydration of primary silicates formed at high temperature and argued that isotopic equilibrium with primary silicates was improbable at low temperatures. The argument against low temperature isotopic equilibrium is that it is dependent on the very slow process of diffusion.. However, with the discovery of the whole rock affinity of pore fluid Sr, a stronger case can be made for low temperature isotope exchange of oxygen and hydrogen between fluids and primary silicates in the mine waters of the Canadian Shield and in the Lac du Bonnet Batholith.

Because of the availability of relatively large volumes of water in fractured rock, investigations of the hydrogeochemistry of crystalline rocks has focussed mainly on more permeable regions. It has been shown in this study that fluids found in the unfractured regions exhibit a distinct ion and isotope signature from fluids in fractured regions. Furthermore, viewed on a regional scale, the volume of these fluids and the amount of dissolved load may far exceed that found in fracture zones. It is probable that ions are transferred between the rock matrix and fractures via diffusion and possibly by advection in newly formed fractures. Interpreting groundwater chemistry in crystalline rocks, in particular isotope chemistry, must take into consideration the pore fluid reservoir. Furthermore, pore fluids have been extensively altered so that little, if any, chemical characteristics of the original fluid remains, making identification of the original source of the fluids, based on isotopic or chemical signatures, difficult.

Due to the high salinity of the pore fluids and the presence of very saline fluid inclusions found in quartz grains, it is proposed that pore fluid salinity may be a result of breakage and leaching of fluid inclusions into the effective porosity of the granite. The presence of very dilute fluid inclusions in quartz grains between 200-450 m implies that at least two generations of fluids have circulated through the unfractured rock, most probably, an early saline fluid and a later dilute meteoric fluid. It is recommended that a more

comprehensive study of fluid inclusion and pore fluid salinity be done to determine a possible genetic link between the two fluids.

Modelling the migration of radionuclides from a nuclear waste repository requires a thorough understanding of the geochemistry of groundwaters surrounding the vault. This study has shown that saline fluids within the rock matrix of the Lac du Bonnet Batholith have a chemistry different from fluids found in fractured rock. The presence of two chemically and isotopically distinct fluid reservoirs within the same rock body is probably not unique to the Lac du Bonnet Batholith, but is a characteristic of most groundwater systems in crystalline rocks. This added complexity in the hydrogeology of a potential repository must be taken into consideration when modeling the behaviour of radionuclide migration and the interaction between vault materials and fluids after closure.

The geochemistry and isotopic composition of groundwater in the Lac du Bonnet batholith have been used to determine the source of groundwater salinity, from which is inferred the residence time of groundwaters within the batholith. The higher salinity of the pore fluids relative to the fracture waters and the similarity in Br/Cl ratio of the two water types suggests that much of the fracture water salinity is derived from pore fluids. Considering that intense water-rock interaction has modified the chemical and isotopic composition of the pore fluids, geochemical tracers are not useful as indicators of the source of salinity. Therefore, suggestions that groundwater salinity in the batholith is of marine origin, based on the chemistry of the waters, should be considered unproven.

REFERENCES

Acker J.P. and Bricker, O.P. (1992) The influence of pH on biotite dissolution and alteration kinetics at low temperature. *Geochim. Cosmochim. Acta* **56**, pp. 3075 - 3092.

Aggarwal J.K., Palmer M.R., Ragnarsdottir K.V. (1992) Boron isotopic composition of Icelandic hydrothermal systems. In *Proc. WRI-7* (eds Y.K. Kharaka and A.S. Maest), pp. 693-696. A. A. Balkema Publ.

Agyei E.K. and McMullen C.C. (1968) A study of the isotopic abundance of boron from various sources. *Can. J. Earth Sci.* **5**, pp. 921-927.

Appleman D.E. and Clark J.R. (1965) Crystal Structure of Reedmergnerite boron albite, and its relation to feldspar crystal chemistry. *Am. Miner.* **50**, pp 1827-1850.

Barth S. (1993) Boron isotope variations in nature: a synthesis. *Geol. Rundsch.* **82**, pp 640-651.

Barbier Y. and Rosset R. (1968) Étude de la fixation du bore sur une résine échangeuse d'anions, en présence de mannitol. *Bull. Soc. Chim. France* **12**, pp. 5072-5077.

Basset R.L. (1990) A critical evaluation of the available measurements for the stable isotopes of boron. *Appl. Geochim.* **85**, pp 541-554.

Blundy J.D. and Wood B.J. (1991) Crystal-chemical controls on the partitioning of strontium and Ba between plagioclase feldspar, silicate melts, and hydrothermal solutions. *Geochim. Cosmochim. Acta* **55**, pp. 193-209.

Bodnar R.J. (1993) Revised equation and table for determining the freezing point depression of H2O-NaCl solutions. Geochim. Cosmochim. Acta 57, pp. 683-684.

Bottomley D.J., Gascoyne M., Ross J.D. and Ruttan J.T. (1986) Hydrogeochemistry of the East Bull Lake pluton. *Atomic Energy of Canada Ltd. Tech. Record.* **TR-382**, p28.

Bottomley D.J., Gregoire D.C., Raven K.G. (1994) Saline groundwaters and brines in the Canadian shield; geochemical and isotopic evidence for a residual evaporite brine component. *Geochim. Cosmochim. Acta.* **58**, pp. 1483-1498.

Bowers T.S., Von Damm K.L. and Edmond J.M. (1985) Chemical evolution of mid-ocean ridge hot springs. *Geochim. Cosmochim. Acta* **49**, pp. 2239-2252.

Bowers T.S. and Taylor H.P. Jr. (1985) An integrated chemical and stable isotope model of the origin of mid ocean ridge hot spring systems. *J. Geophy. Res.* **90**, pp. 12583-12606.

Brown A. and Davison C. (1986) Geoscience research at Canada's Underground research laboratory, Lac du Bonnet, Manitoba. *Field Trip 10: Guidebook, GAC-MAC*, Ottawa. p 23.

Brown A. Soonswala N.M., Everitt R. A and Kamenini D.C. (1989) Geology and geophysics of the Underground research laboratory site Lac du Bonnet Batholith, Manitoba. Can. J. Earth Sci. **26**, pp. 404 - 425.

Bullen T.D., Krabbenhoft D.P., and Kendall C. (1996) Kinetic and mineralogic controls on the evolution of groundwater chemistry and $^{87}Sr/^{86}Sr$ in a sandy silicate aquifer, northern Wisconsin, USA., *Geochim. Cosmochim. Acta* **60**, pp. 1807 - 1821.

Catanzaro E.J., Champion C.E., Garner E.L., Marinenko G., Sappenfield K.M. and Shields W.R. (1970) Boric acid; isotopic, and assay standard reference materials. (U.S.) *Natl. Bur. Stand., Spec. Publ.* **260-17**, pp. 1-60.

Chaussidon M. and Albarede F. (1992) Secular boron isotope variations in the continental crust: and ion microprobe study. *Earth Planet. Sci. Lett.* **108**, pp 229-241.

Chernis P.J. and Robertson P.B (1987) Natural and stress-relief microcracks in the Lac du Bonnet Granite. In *Geotechnical Studies at Whiteshell Research Area (RA-3)*. Eds T.J. Katsube and J.P. Hume, pp. 21 - 32.

Christ C. and Harder H. (1978) Boron. In *Handbook of Geochemistry* Vol. II/1:5 Eds. K.H. Wedepohl.

Clayton R.N., Friedman I., Graf D.L., Mayeda T.K., Meents W.F. and Shimp N.F. (1966).The origin of saline formation waters: 1. isotopic composition. *J. Geophys. Res.* **71**, pp 3869-3882.

Couture R. A., and Seitz M. G., (1986) Movement of fossil pore fluids in granite basement, Illinois. *Geology* **14**, pp. 831 - 834.

Couture R.A., Seitz M.G., and Stemdler M. J. (1983) Sampling of brine in cores of Precambrian granite from northern Illinois. , *J. Geophys. Res.* **88 (B9)**, pp. 7331 - 7334.

Davisson M.L. and Criss R.E. (1996) Na-Ca-Cl relations in basinal fluids. *Geochim. Cosmochim. Acta* **60**, pp. 2743 - 2752.

Drew D.J. and Vandergraaf T.T. (1988). Construction and operation of a high pressure radionuclide migration apparatus. *Atomic Energy of Canada Ltd. Tech. Report*, TR-476.

Edmunds W.M., Andrews J.N., Burgess W.G., Kay R.L.F. and Lee D.J., (1984) The evolution of saline and thermal groundwaters in the Carnmenellis granite, *Mineral. Mag.* **48**, pp. 407-424

Edmunds W.M., Kay R.L.F. and McCartney R.A. (1985) Origin of saline groundwaters in the Carnmellis granite: natural processes and relation during hot dry rock reservoir circulation. *Chem. Geol.* **49**, p287 - 307.

Edmunds W.M., Kay R.L.F., Miles L. and Cook J.M. (1987) The origin of saline groundwaters in Carnmellis granite, Cornwall (U.K.): further evidence from minor and trace elements. in *Saline Water and Gases in Crystalline Rocks*, Eds P. Fritz and S.K. Frape Geol. Assoc. Canada Special Paper 33, eds P. Fritz and S.K. Frape, pp. 127 - 144.

Eggleston C.M., Hochella M.F., Hellmann R. and Crerar D.A. (1988) formation of leached layers during albite hydrolysis (abstr.) *Abstracts with Programs, Geol. Soc. Amer. 1988 Ann. Mtg.*, p A42.

Everitt R.A., Brown A., Davison C., Gascoyne M., and Martin C.D. (1990) Regional and local setting of the Underground Research Laboratory. In: *Information Package on AECL's Underground Research Laboratory.*

Faure G. (1994) *Principles and Applications of Inorganic Geochemistry*, MacMillan Publishing, New York, p 626.

Franklyn M. (1987) Sr isotopic composition of saline waters and host rock in the Eye-Dashwa lakes pluton, Atikokan, Ontario. Unpub. M.Sc.,Thesis p 108.

Franklyn M., McNutt R.H., Kamineni D.C., Gascoyne M., and Frape S.K. (1991) Groundwater $^{87}Sr/^{86}Sr$ values in the Eye-Dashwa Lakes pluton, Canada: Evidence for plagioclase-water reaction. *Chem. Geol. (Isot. Geosci. Sect.)* **86**, pp 111 - 122.

Frape S.K. and Fritz P. (1981) A preliminary report on the occurrence of saline groundwaters on the Canadian shield. Atomic Energy of Canada Limited Tech. Rep. **AECL -136**, p. 68.

Frape S.K., Fritz P., and McNutt R.H. (1984) Water-rock interaction and chemistry of groundwaters from Canadian shield. *Geochim. Cosmochim. Acta* **48**, pp. 1617 - 1627.

Frape S.K. and Fritz P. (1987) Geochemical trends from groundwaters from the Canadian shield. in *Saline Water and Gases in Crystalline Rocks*, Eds P. Fritz and S.K. Frape. Geol. Assoc. Canada Special Paper 33, pp. 127-144.

Fritz P. and Frape S.K., (1982) Saline groundwaters in the Canadian shield - a first overview. *Chem. Geol.* **36**, pp. 179 -190.

Fritz B. Clauer N., and Kam M.(1987) Strontium Isotopic data and geochemical calculation as indicators for the origin of saline waters in crystalline rocks. in *Saline Water and Gases in Crystalline Rocks*, Eds P. Fritz and S.K. Frape Geol. Assoc. Canada Special Paper 33, eds P. Fritz and S.K. Frape, pp. 121-126.

Garrels R.M. (1967) Genesis of some groundwaters from igneous rocks. in *Researches in Geochemistry VII*, eds P.H. Abelson, pp 405 - 420.

Gascoyne M. and Cramer, J.J. (1987) History of actinide and minor element mobility in an Archean granitic batholith in Manitoba, Canada. *Appl. Geochim.* 2, pp 37-54.

Gascoyne M., Davison C.C., Ross J.D. and Pearson R.(1987) Saline groundwaters and brines in plutons in the Canadian Shield; in *Saline Water and Gases in Crystalline Rocks*, Eds: P. Fritz and S.K. Frape. Geol. Assoc. of Canada Special Paper 33, pp. 53-68.

Gascoyne M., Ross J.D., Purdy A., Frape S.K. Drimmie R.J., Fritz P., and Betcher R.N. (1989a) Evidence for penetration of sedimentary basin brines into an Archean granite of the Canadian Shield. In: *6th International Symposium on Water-Rock Interaction WRI-6*, (ed.) D. C. Miles, Rotterdam (AA Balkema). pp 243 - 245.

Gascoyne M., Ross J.D., Watson R.L. and Kamenini D.C. (1989b) Soluble salts in a Canadian shield granite as contributors to ground water salinity. *Water-Rock Interaction*, pp. 247 -249.

Gascoyne M., Stoes-Gascoyne S., and Sargent F.P.(1995) Geochemical influences on the design construction and operation of a nuclear waste vault. *Appl. Geochim.* **10**, pp. 657-671.

Govindaraju K. (1984) Compilation of working values for 170 international reference samples of mainly silicate rocks and minerals. *Geostandards Newsletter* **8** (special issue).

Gregoire D.C. (1987) Determination of boron isotope ratios in geological materials by inductively coupled plasma mass spectrometry. *Anal. Chem.* **59**, pp. 2479-2484.

Gregoire D.C. (1990) Determination of boron in fresh and saline waters by inductively coupled plasma mass spectrometry. *Jour. Anal. Atom. Spec.* **5**, 623 -???.

Griffault L.Y., Gascoyne M., Kamineni C., Kerrich R. and Vandergraaf T.T. (1993) Actinide and rare earth element characteristics of deep fracture zones in the Lac du Bonnet granitic batholith, Manitoba, Canada. *Geochim. Cosmochim. Acta.* **57**, pp 1181-1202.

Grigsby C.O., Tester J.W., Trujillo P.E., Counce D.A., Abbot J., Holley C.E. and Blatz L.A. (1983) Rock-water interaction in hot dry geothermal system: field investigations of in situ geochemical behaviour. *J. Volcan. Geotherm. Res.* **15**, pp. 101 - 136.

Grimaud D., Beaucaire C., and Michard G. (1990) Modeling of the evolution of groundwaters in a granite system at low temperature: the Stripa granite, Sweden. *Appl. Geochim.* **5**, pp. 515-525.

Guha J. and Kanwar R. (1987) Vug brines-fluid Inclusions: a key to the understanding of secondary gold enrichment processes and the evolution of deep brines in the Canadian Shield. in *Saline Water and Gases in Crystalline Rocks*, eds: P. Fritz and S.K. Frape. Geol. Assoc. of Canada Special Paper 33, pp. 95-101.

Harriss R.C. (1969) Boron regulation in the oceans. *Nature* **223**, pp 290-291.

Helgelson H.C. Murphy W.M. and Aagaard P. (1984) Thermodynamic and kinetic constraints on reaction rates among minerals and aqueous solutions. II Rate constraints, effective surface area, and hydrolysis of feldspar. *Geochim. Cosmochim. Acta* **48**, pp. 2405 - 2432.

Hemming N.G. and Hanson G.N. (1992) Boron isotopic composition and concentration in modern marine carbonates. *Geochim. Cosmochim. Acta.* **56**: 537-543.

Hemming N.G. and Hanson G.N. (1994) A procedure for the isotopic analysis of boron by negative thermal ionization mass spectrometry. *Chem. Geol. (Isot. Geosci. Section)* **114**, 147-156.

Hershey J.P., Fernandez M., Milne P.J. and Millero F.J. (1986) The ionisation of boric acid in NaCl, Na-Ca-Cl and Na-Mg-Cl solution at 25°C. *Geochim. et Cosmochim. Acta* **50**, pp 143-148.

Heumann K.G. and Zeininger H. (1985). Boron trace determination in metals and alloys by isotope dilution mass spectrometry with negative thermal ionization. *Int. J. Mass Spectrom. Ion Processes* **67**, pp. 237-252.

Hitchon B., Levinson A.A., and Horn M.K. (1977) Bromide, iodide, and boron in Alberta formation waters. *Alberta Research Council Economic Geology*, **Report 5**, p 25.

Hochella M. F. (1990) Atomic structure, microtopology, composition and reactivity of mineral surfaces in mineral-water interface geochemistry: *Reviews in Mineralogy* **24**.

Ichikuni M. and Musha S. (1978) Partition of strontium between gypsum and solution. *Chem. Geol.* **21**, pp. 359 - 363.

Ishikawa, T. and Nakamura, E. (1990) Suppression of boron volatilization from a hydrofluoric acid solution using a boron-mannitol complex. *Anal. Chem.* **62**, pp. 2612-2616.

Kakihana H., Kotaka M., Sutoh S., Nomura M., and Okamoto M. (1977) Fundamental studies on the ion-exchange separation of boron isotopes. *Bull. Chem. Soc. Japan* **50**, pp 158-163.

Kamineni D.C. (1987) Halogen-bearing minerals in plutonic rocks: a possible source of chlorine in saline groundwater in the Canadian Shield. in *Saline Water and Gases in Crystalline Rocks*, eds: P. Fritz and S.K. Frape. Geol. Assoc. of Canada Special Paper 33, pp. 69-79.

Kamineni D.C., Gascoyne M., and Melnyk T.W. (1992) Cl and Br in mafic and ultramafic rocks: significance for the origin of salinity in groundwater. *Water-Rock Interaction WRI-7*. pp. 801-804.

Katsube T.J. and Hume J.P. (1987) Pore structure characteristics of granitic rock samples from the Whiteshell research area. In *Geotechnical Studies at Whiteshell Research Area (RA-3)*. Eds T.J. Katsube and J.P. Hume, pp. 113 - 154.

Katz A., Sass E., Stavinsky A., and Holland H. D. (1972) Strontium behaviour in the aragonite-calcite transformation: An experimental study at 40-98°C. *Geochim. Cosmochim. Acta* **36**, pp. 481 - 496.

Kelly W.C., Rye R.O., and Livnet A. (1986) Saline mine waters of the Keweenawan Peninsula, northern Michigan: their nature, origin, and relation to similar deep waters in Precambrian crystalline rocks of the Canadian Shield. *Amer. J. Sci.* **286**, pp. 281-308.

Keren R. and Mezuman V. (1981) Boron adsorption by clay minerals using a phenomenological equation. *Clays and Clay minerals* **29**, pp 198-204.

Kerrich R. and Kamineni D.C. (1988) Characteristics and chronology of fracture-fluid infiltration in the Archean, Eye Dashwa Lakes pluton, Superior Province: Evidence form H, C, O isotopes and fluid inclusions. *Contrib. Mineral. Petrol.* **99**, 430-445.

Klötzli U.S. (1992) Negative thermal ionisation mass spectrometry: a new approach to boron isotope geochemistry. *Chem. Geol. (Isot. Geosc. Sect.)* **101**, 111-122.

Knauth L.P., Kumar M.B., and Martinez J.D. (1980). Isotope geochemistry of water in Gulf Coast salt domes. *J. Geophys. Res.* **85**, pp. 4863-4871.

Krogh T.E, Davis G.L., Ermanovics I., and Harris N.B.W. (1976) U-Pb isotopic ages of zircons from the Berens Block and English River gneiss belt. *Proc. 1976 Geotraverse Conference*, **46**.

Lagache M. and Dujon S.C. (1987) Distribution of Strontium between plagioclase and 1 molar aqueous chloride solutions at 600 °C, 1.5 and 750 °C, 2 Kbar. *Bull. Mineral.* **110**, pp 551-61.

Lasaga A.C., Soler J.M., Ganor J., Burch T.E., and Nagy K.C. (1994) Chemical weathering rate laws and global geochemical cycles. *Geochim. Cosmochim. Acta* , **58**, pp. 2361 - 2386.

Leeman W.P., Vocke R.D., and McKibben M.A. (1990) Boron isotope studies of geothermal fluids. *Eos* **71**, pp 1686-1687.

Li W. (1989) Isotopic Studies of the Groundwaters and their host rocks and minerals from the Underground Research Laboratory (URL), Pinawa, Manitoba, Canada. Unpub M.Sc. Thesis, p 202.

Li W., Franklyn M.T., McNutt R.H., Schwarcz H.P., Gascoyne M., and Kamineni D.C., and Frape S.K. (1989) Sr isotopic study of the Eye-Dashwa Pluton, Ontario and the Lac du Bonnet Pluton, Manitoba: plagioclase/water reaction. In *Proc. WRI-6, Malvern U.K.*, eds. PL. Miles), pp. 441 - 444.

Longstaffe F.J. (1987) Stable isotope studies of diagenetic processes. In: *Short Course in Stable Isotope Geochemistry of Low Temperature Fluids.* (ed.) T.K. Kyser., pp 187-257.

Lorens, R.B. (1981) Sr, Cd, Mn, and Co distribution coefficients in calcite as a function of calcite precipitation rate. *Geochim. Cosmochim. Acta* **45**, pp. 553 - 561.

Madé B. (1991) Modelisation thermodynamique et cinetique des reactions geochimiques dans les interations eau-roche. Unpublished Ph.d. thesis, L'Universite Louis Pasteur. p. 308.

McCrank G.F.D. (1985) Results of a geological survey of the Lac du Bonnet Batholith, Manitoba. Atomic Energy of Canada Limited Rep. AECL-7816, p. 63

McNutt R.H., Frape S.K. and Fritz P. (1984) Strontium isotopic composition of some brines from the Precambrian shield of Canada. *Isot. Geosc.* **2**, pp. 205 - 215.

McNutt R.H. (1987) $^{87}Sr/^{86}Sr$ ratios as indicators of water/rock interactions: applications to brines found in Precambrian age rocks from Canada. in *Saline Water and Gases in Crystalline Rocks*, Eds P. Fritz and S.K. Frape : Geological Association of Canada Special Paper 33, pp. 81 - 88.

Michaud G. (1990) Behaviour of major elements and some trace elements (Li, Rb, Cs, Sr, Fe, Mn, W, F) in deep hot waters from granitic areas. *Chem. Geol.* **89**, pp. 117 -134.

Milton C. Chao E.C.T., Axelrod J.M., Grimaldi F.S.(1960)Reedmergnerite $NaBSi_3O_8$, the boron analogue of albite, from the Green River Formation, Utah. *Am. Miner.* **45**, pp 188-199.

Morse J.W. and Bender M. (1990) Partition coefficients in calcite: Examination of factors influencing the validity of experimental results and their application to natural systems. *Chem. Geol.*, **82**, pp. 265 - 277.

Mucci A. and Morse, J.W. (1983) The incorporation of Mg^{2+} and Sr^{2+} into calcite overgrowths: influences or growth rate and solution composition. *Geochim. Cosmochim. Acta* **47**, pp. 217 - 233.

Nakamura E., Ishikawa T., Birck J.L., and Allègre C.J. (1992) Precise boron isotopic analysis of natural rock samples using a boron-mannitol complex. *Chem. Geol. (Isot. Geosc. Sect.)* **94**, pp. 193-204.

Nomura M., Kanszki T., Ozawa T., Okamoto M., Kakihana H., (1982) Boron isotopic composition of fumarolic condensates from some volcanoes in Japanese island arcs. *Geochim. Cosmochim. Acta.* **46**: pp 2403-2406.

Nordstrom D.K., Andrews J., Carlson L., Fontes J.C., Fritz P., Moser H. and Olssen T. (1985) Hydrogeological and hydrogeochemical investigations in boreholes - final report of the phase I geochemical investigations of the Stripa groundwater: *SKB Stripa project. Swedish Nuclear Final and Waste Management Company*, Report 85-06, p. 250.

Nordstrom D.K. and Olssen T. (1987) Fluid inclusions as a source of dissolved salts in deep granitic groundwaters. in *Saline Water and Gases in Crystalline Rocks*, Eds P. Fritz and S.K. Frape Geol. Assoc. Canada Special Paper 33, eds P. Fritz and S.K. Frape, pp. 111 - 120.

Nordstrom D.K., Lindblom S., Donahoe R.J., and Barton C.C. (1989) Fluid inclusions in the Stripa granite and their possible influence on the groundwater chemistry. *Geochim. Cosmochim. Acta.* **53**, pp 1741-1755.

Oi T., Nomura M., Musashim M., Ossaka T., Okamoto M., and Kakihana H. (1989) boron isotopic compositions of some boron minerals. *Geochim. et Cosmochim. Acta* **53**, pp 3189-3195.

Palmer M.R., Spivak A.J. and Edmond J.M. (1987) Temperature and pH controls over isotopic fractionation during adsorption of boron on marine clays. *Geochim. et Cosmochim. Acta* **51**, pp 2319-2323.

Palmer M.R. and Sturchio N.C. (1989) Boron isotope systematics of the Yellowstone National Park (Wyoming)hydrothermal system: a reconnaissance. *Geochim. et Cosmochim. Acta* **54**, pp 2811-1815.

Pearson F.J. (1987) Models of mineral controls on the composition of saline groundwaters of the Canadian shield, in *Saline Water and Gases in Crystalline Rocks*, Eds P. Fritz and S.K. Frape : Geological Association of Canada Special Paper 33, pp. 39 -51.

Peters T. (1986) Structurally incorporated and water extractable chlorine in the Boettstein granite (N. Switzerland). *Contrib. Mineral. Petrol.* **94**, pp 272 - 275.

Petrović R., Berner R. A. and Goldhaber M.B. (1976) Rate control in dissolution of alkali-feldspars. I Study of residual feldspar grains by X-ray photoelectron spectroscopy. *Geochim. Cosmochim. Acta* **40**, pp. 537 - 548.

Pingitore N. E. and Eastman M. P. (1986) The coprecipitation of Sr^{2+} with calcite at 25°C and 1 atm. *Geochim. Cosmochim. Acta* **50**, pp. 2195 - 2203.

Potter R.W. (1977) Pressure corrections for fluid inclusions, homogenization temperatures based in the volumetric properties of the system, NaCl - H2O. U.S. Geol. Survey J. Res. 5, pp 603-607.

Richards H.G., Savage D., Andrews J.N. (1992) Granite-water reactions in an experimental Hot Dry Rock geothermal reservoir, Rosemanowes test site, Cornwall, U.K. *Appl. Geochim.* 7, pp 193-222.

Savin S.M. and Epstein (1970) The oxygen and hydrogen isotope geochemistry of clay minerals. *Geochim. Cosmochim. Acta* **34**, pp 25-42.

Schwarcz H.P., Agyei E.K., and McMullen C.C. (1969) Boron isotopic fractionation during adsorption from seawater. *Earth Planet. Sci. Let.* **6**, pp 1-5.

Seyfried W.E. Jr., Janecky D.R., and Mottl M.J. (1984) Alteration of the oceanic crust: implications for geochemical cycles of lithium and boron. *Geochim. Cosmochim. Acta* **48**, pp 557-569.

Shegina Y.P. and Kaminskaya A.B.(1967) Experimental simulation of the natural separation of boron isotopes. *Geochimiya* **10**, pp 1111-1115.

Shemilt L.W. and Sheng G. (1989) Evaluation of the Canadian high-level waste research grogram in an international context. in *High Level Radioactive Waste and Spent Fuel Management, Vol II*, Eds. S.C. State, R. Hohout, and A. Suzuki. pp 403-410.

Shivi P.N. and Mattigod (1992) Modeling boron adsorption of kaolinite. *Clays and Clay Min.* **40**, pp. 192-205.

Spencer R.J. (1987) Origin of Ca-Cl brines in Devonian formations, western Canada sedimentary basin, *Appl. Geochim.* **2**, pp. 374-384.

Spivak A.J. and Edmond J.M. (1986) Determination of boron isotope ratios by thermal ionization mass spectrometry of dicesium metaborate cation. *Anal. Chem.* **58**, pp. 31-55.

Spivak A.J. and Edmond J.M. (1987a) Boron isotope exchange between seawater and oceanic crust. *Geochim. et Cosmochim. Acta* **51**, pp 1033 - 1042.

Spivak A.J. and Edmond J.M (1987b) The sedimentary cycle of the boron isotopes. *Geochim. Cosmochim. Acta* **51**, 1939-1950.

Stevenson D.R., Kozak E.T., Davison C.C., Gascoyne M., Broadfoot R.A. (1996a) Hydrogeologic characteristics of Domains of Sparsely Fractured Rock in the Granitic Lac du Bonnet Batholith, south eastern Manitoba, Canada. *Tech. Report AECL - 11558*, p. 26.

Stevenson D.R., Brown A., Davison C.C., Gascoyne M., McGregor R.G., Ophori D.U., Scheier N.W., Stanchell F., Thorne G.A., and Tomsons D.K. (1996b) Revised Conceptual Hydrogeologic model of a crystalline rock environment, Whiteshell Research Area, southeastern Manitoba, Canada, *Tech. Report AECL-11331.*

Swihart G.H., Moore P.B. and Callis E.I. (1986) Boron isotopic composition of marine and non-marine evaporite borates. *Geochim. Cosmochim. Acta.* **50**, pp. 1297-1301.

Thode H.G., MacNamara J., Lossing F.P. and Collis C.B. (1948) Natural variations in isotopic content of Boron and its chemical atomic weight. *J. Am. Chem. Soc.* **70**, pp 3008-3001.

Thompson G., Melson W.G. (1970) Boron contents of serpentinites and metabasalts in the oceanic crust: implications for the boron cycle in the oceans. *Earth Planet. Sci. Lett.* **8**, pp 61 - 65.

Vengosh A. Chivas A.R. and McCulloch M.T. (1989) Direct determination of boron and chlorine isotopic compositions in geological materials by negative thermal - ionization mass spectrometry. *Chem. Geol. (Isot. Geosc. Sect.)* **79**, pp. 333-343.

Vengosh A., Chivas A.R., McCulloch M.T., Starinsky A. And Kolodny Y. (1991a) Boron isotope geochemistry of Australian salt lakes. *Geochim. et Cosmochim. Acta* **55**, pp 2591-2606.

Vengosh A., Kolodny Y., Starinsky A., Chivas A.R. and McCulloch M.T. (1991b) Coprecipitation and isotopic fractionation of boron in modern biogenic carbonates. *Geochim. et Cosmochim. Acta* **55**, pp 2901 - 2910.

Vengosh A., Starinsky A., Kolodny Y, and Chivas A.R. (1991c) Boron isotope geochemistry as a tracer for the evolution of brines and associated hot springs from the Dead Sea, Israel. *Geochim. et Cosmochim. Acta* **55**, pp 1689-1695.

Vengosh A., Starinsky A, Kolodny Y., Chivas A.R., and Raab M. (1992a) Boron isotope variations during fractional evaporation of sea water: new constraints on the marine vs. Nonmarine debate. *Geology* **20**, pp 799-802.

Vengosh A. (1992b) Boron isotope variations during brine evolution and water-rock interactions. In: *7th International Symposium on Water-Rock Interaction WRI-7*, Park City, Utah, USA, 13-18 July 1992, (eds) Y.K. Kharaka and A.S. Maest, Rotterdam (AA Balkema). Vol. 1, pp 693 - 696.

Wigley T.M.L., Plummer L.N., Pearson F.J. (1978) Mass transfer and carbon isotope evolution in natural water systems. *Geochim. Cosmochim. Acta* **42**, pp 1117 - 1139.

Xiao Y.K., Beary E.S. and Gasset J.D. (1988) An improved method for the high precision isotopic measurement of boron by thermal ionization mass spectrometry *Int. J. Mass. Spect. Ion. Processes*, **85**, pp. 203-213.

Yang W. A. and Kilpatrick R.J. (1989) Hydrothermal reaction of albite and a sodium aluminosilicate glass: A solid-state NMR study. *Geochim. Cosmochim. Acta* **53**, pp. 805-819.

Zeininger H. and Heumann K.G. (1983) Boron isotope ratio measurement by negative thermal ionization mass spectrometry. *Int. J. Mass Spectrom. Ion Phys.* **48**, pp. 377-380.

Zhai, M. (1996) *Boron Cosmochemistry*. Unpub. P.hd. thesis, McMaster University, p 109.

Appendix 1. Derivation of Boron Adsorption Model.

1.1 Determining Boron Concentration

The change in concentration of a chemical species in any aqueous environment is described mathematically by a conservation of mass equation (Wigley et al., 1978).

$$dB = \sum_{i=1}^{M} d\Gamma_i - \sum_{i=1}^{N} d\Theta_i \qquad eqn.\ 1.1$$

Where dB is the change in amount of boron in solution, $d\Gamma_i$ and $d\Theta_i$ are contributions to B from M sources (inputs) and N sinks (outputs). The model is simplified by assuming that there is only one source and one sink for boron in the system. The dissolution of the rock is the source of boron and is expressed as $M_r[B_r]$, where M_r is the mass of rock reacting with a mass of water W. The sink is the clay formed during alteration or the rock. The amount of boron adsorbed onto clay surfaces (B_c) for a given mass of clay (C) is related to the boron concentration in solution by a partition coefficient K_d such that,

$$K_d = \frac{\frac{B_c}{C}}{\frac{B}{W}} \qquad equ.\ 1.2$$

If it is assumed that mass is neither gained or lost during alteration, then $M_r = C$. Substituting for the inputs and outputs, equation 1.1 can be written as follows,

$$dB = d(M_r[B_r]) - d(\frac{M_r}{W}BK_d) \qquad eqn.\ 1.3$$

The boron amounts can be transformed to concentrations by multiplying both sides by W/W.

$$Wd[B] = [B_r]dM_r - [B]K_d dM_r \qquad eqn.\ 1.4$$

Equation 1.4 is rearranged to the form,

$$\frac{Wd[B]}{[B_r]-K_d[B]} = dM_r$$

$$-\frac{W}{K_d}\left\{\frac{-K_d d[B]}{[B_r]-K_d[B]}\right\} = dM_r$$

Integration gives the solution,

$$-\frac{W}{K_d}\ln([B_r] - K_d[B]) = M_r + C \qquad equ.\ 1.5$$

Because $[B] = 0$ when $M_r = 0$,

$$-\frac{W}{K_d}\ln[B_r] = C \qquad equ.\ 1.6$$

Substituting equation 1.6 back into equation 1.5,

$$-\frac{W}{K_d}\ \ln([B_r] - K_d[B]) = M_r - \frac{W}{K_d}\ \ln [B_r]$$

$$-\frac{W}{K_d}\ \ln([B_r] - K_d[B]) - \ln[B_r] = M_r$$

$$\ln\left\{\frac{[B_r] - K_d[B]}{[B_r]}\right\} = -K_d\left\{\frac{M_r}{W}\right\}$$

$$[B_r] - [B]K_d = [B_r]\ e^{-K_d\left(\frac{M_r}{W}\right)}$$

$$[B] = \frac{[B_r]}{K_d}\left\{1 - e^{-K_d\left(\frac{M_r}{W}\right)}\right\} \qquad \textit{equ.}\ 1.7$$

Equation 1.7 relates the concentration of boron in solution with rock/water ratio. As M_r/W increases the exponential term approaches 0, and the term $[B]$ approaches a limit defined by $[B_r]/K_d$.

1.2 Determining Boron Isotopic Composition

Equation 5.7 can be solved by finite difference methods on a computer. The solution is based on the finite difference solution used to model mass transfer and carbon isotope evolution in natural water systems (Wigley et al., 1978).

$$R\Delta(^{11}B) + (^{11}B)\Delta R = \sum_{i=1}^{M} R^{*}_{i}\,\Delta\gamma_i - \sum_{i=1}^{N} R\alpha\,\Delta\theta_i \qquad \textit{eqn.}\ 1.2.1$$

where the prefix Δ denotes a small but finite change. Given $\Delta\gamma$, $\Delta\theta$, and the values of R^{*}_{i}, R, and α at the beginning of an increment. $\Delta(^{11}B)$ can be determined from equation 5.2 by calculating the proportion of ^{11}B in total boron inputs and outputs, and the new value of R determined using

$$R + \Delta R = \frac{R\left\{^{11}B - \sum_{i=1}^{N} \alpha_i \Delta\theta_i\right\} + \sum_{i=1}^{M} R^{*}_{i}\,\Delta\gamma_i}{^{11}B + \Delta(^{11}B)} \qquad \textit{eqn}\ 1.2.2$$

$\Delta\gamma_i$, the input of boron -11 is determined by

$$\Delta\gamma_i = \frac{R^{*}_{i}}{R^{*}_{i}+1}\,\Delta\Gamma_i \qquad \textit{eqn}\ 1.2.3$$

$\Delta\theta_i$, the output of boron - 11 is determined by

$$\Delta\theta_i = \frac{R\alpha}{R\alpha+1}\,\Delta\Theta_i \qquad \textit{eqn.}\ 1.2.4$$

The following code is written in C++ to solve for R, the isotopic ratio in solution, with progressive alteration, (ie. increasing M/W). The code was compiled as a dynamic link library (DLL) and was accessed through a graphical user interface written in Visual Basic 3.0. All calculations and graphs plotting isotopic ratios were determined using a step,

ΔM_r = 0.00001 g.

1.3 Finite difference DLL.

```
// File : BORDLL.CPP

#include <windows.h>
#include <stdlib.h>
#include <stdio.h>
#include "bordll.h"
#include <float.h>

// Allow access of LoopFunc from Visual Basic Program Boron.exe
//NumIter is the number of iterations chosen by user
//RWincr is the step increase of rock/water ratios
//PartCoef is the partition coefficient of boron between solution and clay
//Sample is the sampling interval of the program
//BRConc is the boron Concentration in the rock/mineral

void FAR PASCAL _export LoopFunc(long NumIter, double RWincr,
        double PartCoef, long Sample,  double BRConc, double RIsotope,
        double FracFactor )
{
                long iter = 0;
                double RWsum = 0;
                double SolInitConc = 0;
                double SolFinalConc = 0;
                long TakeSample = Sample;
                double RConc = BRConc/1e+6;      // convert [B] rock from ppm to microg/g
                double InputB11;
                double OutputB11;
                double FinalSolB11;
                double InitSolB11 = 0;
                double FinalRatio =RIsotope;
                double InitRatio =RIsotope;

                FILE *file_ptr;      // create pointer to file 'data.fil'

                file_ptr =fopen("data.fil","w");      // open file 'data.fil' for writing
```

```
fprintf(file_ptr,"%s\n","InputB11,OutputB11,SolB11,RWsum,SolFinalConc,FinalRatio");

        do
    {
        iter ++;
                        //Determine the B concentration in solution
            SolFinalConc = (SolInitConc+ RWincr * RConc)/
                        (PartCoef * RWincr +1);

            SolInitConc = SolFinalConc;
            RWsum = RWsum + RWincr;

                        //Determine the B isotopic composition in solution

        InputB11 = RIsotope/(RIsotope + 1)*(RWincr*RConc);
        OutputB11 = FinalRatio*FracFactor/(FinalRatio*FracFactor +1)

*(RWincr*SolFinalConc*PartCoef);

        FinalSolB11 = FinalRatio/(FinalRatio+1) *SolFinalConc;

        FinalRatio = (InitRatio *(InitSolB11-FracFactor*OutputB11)+
                RIsotope*InputB11)/(FinalSolB11);

        InitRatio = FinalRatio;
        InitSolB11 = FinalSolB11;


            if (iter == 1)
            {

fprintf(file_ptr,"%e,%e,%e\n",RWsum,SolFinalConc,FinalRatio);
                    TakeSample = TakeSample+ Sample;
             };


            if (iter == TakeSample)

            {
                fprintf(file_ptr,"%e,%e,%e\n",
```

```
RWsum,SolFinalConc,FinalRatio);
                                TakeSample = TakeSample + Sample;
                        };

                } while (iter < NumIter);

        fclose(file_ptr);
}
#pragma argsused
int FAR PASCAL LibMain( HANDLE hInst, WORD wDS, WORD wHpSz, LPSTR
lpCmdLn )
{
        return 1;
}
```

Appendix 2.0. Tm and Th Temperatures of Fluid Inclusions in the Lac Du Bonnet Batholith.

Sample 403-A6

Inclusion #	Tm	Th L-V	Vol%	Salinities
1	-	250.0	0.9	-
2	-20.1	273.4	0.85	22.4
3	-	284.5	0.85	-
4	-13.3	-	0.85	17.2
5	-16.4	220.1	0.95	19.8
6	-16.3	210.1	0.90	19.7
7	-10.7	-	1.00	14.7
8	-14.2	165.8	0.90	18.0
9	-12.9	260.8	0.90	16.8
10	-20.2	-	0.95	22.5
11	-21.3	260.2	0.90	23.2
12	-13.4	-	1.00	17.3
13	-8.0	-	0.90	11.7
1a	-10.2	-	1.00	14.1
2a	-10.8	-	1.00	14.8
3a	-0.8	-	1.00	1.4
4a	-0.8	-	1.00	1.4
5a	-2.4	-	1.00	4.0
6a	-14.5	-	1.00	18.2
7a	0	-	1.00	0
8a	-2.6	-	1.00	4.3

Sample
403-A2

Inclusion #	Tm	Th L-V	Vol%	Salinities
1	-0.4	-	1.00	0.7
2	-0.6	-	1.00	1.1
3	-7.0	-	1.00	10.5
4	-5.5	-	1.00	8.5
5	-1.2	-	1.00	2.1
6	-10.4	-	1.00	14.4
7	-23.5	233.5	0.90	24.6
8	-5.6	-	1.00	8.7
9	-22.4	252.8	0.90	24.0
10	-23.3	-	0.90	24.5
11	-12.3	-	1.00	16.2
12	-13.1	-	0.95	17.0
13	-17.4	-	0.85	20.5
13a	-21.3	248.7	0.90	23.2
14	-2.1	-	1.00	3.5
14a	-4.6	-	1.00	7.3
15	-1.1	-	1.00	1.9
16	-2.0	-	1.00	3.4
17	-11.2	-	0.92	15.2
18	-3.1	-	1.00	5.1
19	-1.0	-	1.00	1.7
20	-1.4	-	1.00	2.4
21	-9.9	-	0.80	13.8

Sample 200-A

Inclusion #	Tm	Th L-V	Vol%	Salinities
1	-8.1	-	0.95	11.8
2	-8.8	-	1.00	12.6
3	-9.1	-	1.00	13.0
4	-0.6	-	0.30	1.1
5	-0.4	237.2	0.95	0.7
6	-24.2	-	1.00	25.1
7	-24.7	-	1.00	25.4
8	-10.5	163.0	0.95	14.5
9	-0.4	168.1	0.90	0.7
10	-10.6	-	0.98	14.6
11	-8.2	-	0.90	11.9
12	-1.3	-	1.00	2.2
13	-5.3	-	1.00	8.3
14	-9.4	-	1.00	13.3
15	-6.6	-	1.00	10.0
16	-0.6	325.4	0.90	1.1
17	-0.6	320.0	0.90	1.1
18	-18.2	-	1.00	21.1
19	-4.9	-	1.00	7.7
20	-5.4	-	1.00	8.4
21	-	117.5	0.98	0.0
22	-25.8	318.2	0.90	26.1
23	-10.2	-	1.00	14.1
24	-0.8	-	0.75	1.4
25	-19.1	-	0.80	21.8
26	-0.7	-	0.82	1.2
27	-8.2	-	1.00	11.9
28	-9.8	-	0.84	13.7
29	-0.7	-	0.75	1.2
30	-1.8	-	0.90	3.1
31	-2.6	-	1.00	4.3
32	-0.6	-	0.82	1.1
33	-0.9	-	0.60	1.6
34	-11.8	-	1.00	15.8
35	-1.2	242.7	0.70	2.1
36	-1.1	-	0.85	1.9

Appendix 3.0 Chemical data of Water Samples
Appendix3.1 Groundwaters.

Sample	$\delta^{11}B$	B (µg/g)	$^{87}Sr/^{86}Sr$	Sr (mg/L)	Na (mg/L)	Ca (mg/L)	K (mg/L)	Mg (mg/L)	Br (mg/L)	Cl (mg/L)
208-HC8-Z2	39.1	0.91	--	0.3	183	27.0	1.9	1.6	--	168
208-HC16-Z2	23.8	0.40	--	0.0	78	8.4	0.8	0.8	--	114
209-056-OC1-28	2.5	0.11	0.73032	0.2	543	11.2	1.2	0.1	2.1	687
B34-1-4	30.6	0.31	--	1.1	340	76.0	3.8	15.0	4.5	512
B37-1-2	22.8	0.20	0.72290	0.5	78	81.0	3.0	67.5	<0.03	1.1
B37-2-1	24.1	0.52	0.72174	1.0	177	88.6	2.7	40.4	<0.05	6.9
JE1-2	38	0.76	--	--	--	--	--	--	--	--
M1B-2-3	6.9	0.15	--	0.3	28	35.0	2.0	13.9	<0.03	2.8
M14-1-4	32.2	0.33	--	0.2	82	18.3	2.4	3.5	0.1	19
M4B-2-5	15.1	0.25	0.71320	1.7	218	5455	12.7	2.9	<1	9774
URL2-PZ15	7.4	0.27	0.80105	6.2	236	5140	3.2	6.1	58.7	10002
URL12-10-3	47.9	1.57	0.73039	2.3	690	169	2.6	3.5	3.5	1109
URL12-11-4	41.3	1.0	0.72619	0.2	101	22.0	2.5	2.0	0.3	73
URL12-12-2	46.9	0.94	0.73845	16	1324	1510	8.2	14.5	18.2	4276
URL13-5-1	22.9	0.67	0.72889	0.4	128	40.4	2.0	4.8	0.7	145
URL13-7-1	44.8	0.55	0.73076	9.5	1366	820	10.1	9.1	8.8	3350
URL13-9-1	13.5	0.16	0.79442	2.2	345	1295	6.3	12.7	7.5	2858
URL13-11-1	13	0.20	0.78467	4.5	124	2275	7.0	13.0	14.8	4330
URI14-8	46.4	0.99	--	5.4	1160	506	4.2	7.0	12.9	2449
413-033-SM7-28	9.5	0.04	0.76700	95	1328	29840	31.9	2.5	174.0	45981
WB2-13-4	47	0.77	0.72254	1.0	544	112	2.4	5.4	2.1	549
WB2-19-5	43.2	1.41	0.73749	69	3310	8315	13.4	35.1	154.0	19800
WB3-Pz3	39.3	0.56	0.72713	6.9	533	835	6.8	28.8	10.6	2316
WD3-895-10	52.7	0.76	--	--	--	--	--	--	--	--
WN4-6-8	38.8	1.21	--	13.8	1400	1370	9.0	60.8	11.9	3880
WN4-6-42	30.7	1.37	--	15.2	1530	1430	7.9	59.6	--	4500
WN4-6-7	47.3	1.18	--	13.6	1400	1350	9.0	63.8	13.7	3860
WRA1-4-SW10	40.1	0.45	--	23.1	5200	725	15.0	11.7	41.5	7990
WG2-2-8	6.7	0.26	--	0.2	70	27.0	2.6	2.7	<0.03	3.3

Appendix 3.2. Borehole Leach Test Experiment Water Samples.

403-014-MB2-Zone 1

Date	$^{87}Sr/^{86}Sr$	Sr (μg/g)	Na(mg/L)	Ca(mg/L)	K(mg/L)	Mg(mg/L)	Br(mg/L)	Cl(mg/L)
92/05/12	0.76693	1.2	23.4	468	1.6	0.5	2.2	843
92/09/09	0.76678	1.8	36.6	733	1.7	0.5	3.3	1419
93/01/04	0.76669	2.3	46.5	926	1.9	0.5	3.6	1707
93/03/18	0.76661	2.5	54.0	1055	2.4	0.8	--	1807
93/8/31	0.76681	3.4	67.1	1335	2.1	0.5	5.6	2746
94/2/23	0.76643	4.0	80.1	1630	2.1	0.5	0.8	2952
94/6/13	0.76653	4.1	86.5	1785	2.1	0.5	9.5	3400
94/11/23	0.76692	4.9	100.1	1990	2.2	0.5	9.6	3830

403-014-MB2-Zone2

Date	$^{87}Sr/^{86}Sr$	Sr (μg/g)	Na(mg/L)	Ca(mg/L)	K(mg/L)	Mg(mg/L)	Br(mg/L)	Cl(mg/L)
92/02/19	0.76775	0.6	10.5	230	0.8	0.4	1.0	409
92/05/12	0.76744	2.8	53.8	1168	1.3	0.7	5.5	2123
92/09/09	0.76743	4.8	90.3	2012	1.6	0.8	9.2	3822
93/01/04	0.76738	5.8	113.7	2425	1.7	0.6	10.2	4545
93/03/18	0.76709	6.1	129.1	2750	2.2	0.7	23.5	4627
93/8/31	0.76733	7.9	154.7	3170	2.0	0.6	17.5	5959
94/2/23	0.76726	7.4	144.9	2920	2.4	0.4	1.0	5684
94/6/13	0.76729	8.8	159.7	3365	2.2	0.4	3.0	9424
94/11/24	0.76723	9.0	181.1	3545	2.1	0.4	19.4	7873

404-017-GC1

Date	$^{87}Sr/^{86}Sr$	Sr (μg/g)	Na(mg/L)	Ca(mg/L)	K(mg/L)	Mg(mg/L)	Br(mg/L)	Cl(mg/L)
92/10/23	0.76333	1.0	58.6	525.0	1.8	0.1	1.8	940
92/12/02	0.76344	0.9	61.5	493.0	2.0	0.3	2.2	974
93/01/04	0.76311	1.0	66.4	546.0	1.9	0.1	2.3	1059
93/03/18	0.76308	0.4	27.7	214.0	1.3	0.2	5.5	974
93/8/31	0.76286	1.5	98.3	769.0	2.0	0.2	3.0	1460
93/11/24	0.76261	1.8	116.7	401.0	2.6	0.2	4.1	1904
94/2/23	0.76264	2.0	125.2	--	2.0	--	1.1	2070
94/6/13	0.76266	1.8	125.2	1060.0	2.1	0.2	5.2	2031
94/11/24	0.76275	3.2	196.0	1820.0	2.3	0.2	6.7	3601

406-033-GC2-Zone 1

Date	$^{87}Sr/^{86}Sr$	Sr (µg/g)	Na(mg/L)	Ca(mg/L)	K(mg/L)	Mg(mg/L)	Br(mg/L)	Cl(mg/L)
92/09/09	0.77295	1.0	20.5	395.0	1.8	0.1	1.6	726
92/10/23	0.77271	1.4	27.0	559.0	1.9	0.1	1.7	957
93/01/04	0.77254	1.9	40.6	785.0	2.2	0.1	3.1	1438
93/03/19	0.77232	-	1.6	11.4	0.6	0.0	0.4	74
94/2/24	0.77208	4.8	100.0	1890.0	2.8	0.1	1.0	3606
94/6/14	0.77204	5.0	112.4	2155.0	2.9	0.4	10.2	3963
94/11/25	0.77189	6.5	139.0	2470.0	3.0	0.1	10.9	4995

406-033-GC2-Zone 2

Date	$^{87}Sr/^{86}Sr$	Sr (µg/g)	Na(mg/L)	Ca(mg/L)	K(mg/L)	Mg(mg/L)	Br(mg/L)	Cl(mg/L)
92/06/11	0.77259	0.66	15.3	269.0	2.2	0.1	1.1	498
92/09/09	0.77184	1.44	32.4	571.0	2.7	0.1	3.0	1078
92/10/23	0.77147	1.81	39.3	742.0	2.9	0.1	2.2	1209
93/01/04	0.77119	2.10	50.3	863.0	3.1	0.1	3.3	1583
93/03/19	0.77126	2.34	59.5	988.0	3.4	0.2	10.0	1427
93/11/25	0.77082	2.62	64.6	1070.0	3.3	0.2	4.3	2011
94/2/24	0.77078	2.67	65.5	1065.0	3.2	0.2	8.0	1976
94/6/14	0.77073	2.56	69.2	1085.0	3.2	0.2	5.7	2017
94/11/24	0.77069	2.78	73.0	1140.0	3.2	0.2	0.5	2096

406-033-GC2-Zone 3

Date	$^{87}Sr/^{86}Sr$	Sr (µg/g)	Na(mg/L)	Ca(mg/L)	K(mg/L)	Mg(mg/L)	Br(mg/L)	Cl(mg/L)
92/06/11	0.76869	0.94	31.0	379.0	2.2	0.10	1.4	720
92/09/09	0.76825	1.76	56.0	666.0	2.7	0.2	2.7	1282
92/10/23	0.76798	1.98	64.8	771.0	2.8	0.2	2.4	1330
93/01/04	0.76781	1.99	69.9	775.0	2.9	0.1	3.1	1457
93/03/19	0.76786	2.23	75.6	844.0	3.0	0.1	–	–
93/8/31	0.76765	2.75	95.2	1030.0	3.1	0.1	4.0	2012
93/11/25	0.76754	2.79	95.4	1045.0	2.9	0.1	4.0	2057
94/2/24	0.76753	3.14	106.1	1170.0	3.0	0.1	17.7	2249
94/6/14	0.76749	3.06	115.7	1235.0	3.0	0.1	6.1	116
94/11/24	0.76742	3.38	129.4	1360.0	3.0	0.1	6.0	2497

Appendix 4. Location of Whole rock and Mineral Samples.

Name	Borehole	Location	Lithology
401-1	401-S11-PH1	38.05(depth)	grey granite
GC2-36	406-036-GC2	35.99 - 36.09 m	grey granite
GC2-10	406-036-GC2	9.91 - 10.02 m	granodiorite
GC2-15	406-036-GC2	14.95 - 15.05 m	granodiorite
URL2-791	URL2	781(depth)	grey granite
GC1-1	404-017-GC1	1.0 - 1.05 m	grey granite
MB2-1	403-014-MB2	0.93 - 1.0 m	grey granite
MB2-11	403-014-MB2	10.92 - 10.98 m	grey granite
403-A1	403-014-MB2	0.30 - 0.38 m	grey granite
403-A2	403-014-MB2	4.54 - 4.65 m	grey granite
403-A4	403-014-MB2	8.95 - 9.07 m	grey granite
403-A5	403-014-MB2	14.93 - 15.40 m	grey granite
403-A6	403-014-MB2	19.62 - 19.71 m	grey granite
HC11-31	208-016-HC11	30.96 - 31.05 m	pink granite
HC29-17	211-014-HC29	17.50 - 17.64 m	pink granite

Appendix 5.0 Methodology

Appendix 5.1 Sample Preparation

All whole rock specimens were sampled, by the author from drill cores stored at the Underground Research Laboratory. Fracture waters were supplied by Dr. Mel Gascoyne at AECL and were acidified with (8ml/L) HNO_3 and stored in 250 ml high density polyethylene (HDPE) bottles. Leach Test Experiment waters were also supplied by Dr. Gascoyne and were also acidified and stored in 20 ml HDPE bottles. The Pore Salt Extraction (PSE) waters were sampled by the author at AECL's Whiteshell Laboratories in Pinawa, Manitoba and were stored in 20 ml HDPE bottles and were not acidified.

Rock sample and mineral preparation followed the procedure outlined in Franklyn (1988) and Li (1989) with a few modifications. Mineral separates were obtained by hand crushing whole rock samples using a titanium mortar and pestle. A grain size of of +50 to -100 mesh was obtained by seiving the crushed sample through a nylon sieve. Prior to biotite-feldspar separation using a Franz Isodynamic Magnetic separator, magnetite from the crushed sample was removed by passing a hand held magnet over the rock powder. Following mineral separation using the magnetic separator, the feldspars were separated into plagioclase and K-feldspar fractions using a sodium polytungstate heavy liquid. Both feldspar and biotite separates were then hand picked to obtain a high degree of purity.

Procedures including sample dissolution of silicate samples, strontium column chemistry, and the determination of the isotopic composition and concentration of strontium in silicate samples are discussed in Franklyn (1988) and Li (1989) and are therefore, not described in detail here. A complete description of analytical procedures for the determination of the boron isotopic composition and concentration in water and silicate samples is given in Chapter 5.

Appendix 5.2 Isotopic Analysis of Strontium

Whole rock, mineral, and water samples isotopic composition were determined on a VG-354 mass-spectrometer using multiple Faraday detectors. For most water and silicate, samples a data collection procedure was used involving an aiming current of 5.0×10^{-11} amps on the ^{88}Sr peak and the collection of 15 blocks of data consisting of 10 measurements each. Due to the small amount of Sr in some of the PSE waters, isotopic ratios were determined using a Daly detector and a general peak jumping sequence. The reproducability of NBS 987 is 0.017% (2σ) and 0.15% using the Faraday and Daly detectors, respectively.

Appendix 5.3 Determination of Sr Concentration

Sr concentration in whole rock and mineral separates were determined by isotope dilution using an Elan ICP-MS. Silicate samples were prepared for analysis using the same procedure as that for isotopic analysis. A ^{86}Sr spike (97.6%) was used for Sr concentration analysis and was calibrated to a concentration of 1.68 μg/g. Accuracy and Precision of the method were determined by measuring the Sr concentration of two whole rock standards G-2 and GSP-1 (Table 1.1). The recommended Sr concentration of the standards are given in Govindaraju, 1984.

	G-2		GSP-1	
	Sr Conc.(μg/g)	Std (1σ)	Sr Conc. (μg/g)	Std(1σ)
	495	±13	246	±10
	478	±14	245	±6
	473	±13	235	±11
	476	±9	239	±8
	482	±12	233	±7
Mean:	481	±7	239	±5
Recommended:	480		240	

Table 1.1. Strontium Analysis of Rock Standards. Recommended values for rock standards are from Govindaraju, 1984.